The Department of Geodesy and Geoinformatics

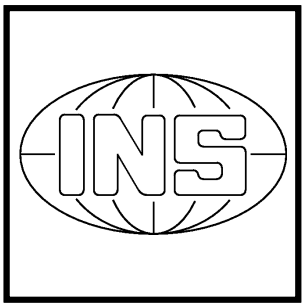

Stuttgart University

2013

editing and layout:
volker walter, friedhelm krumm, helga mehrbrodt, martin metzner

Dear friends and colleagues,

It is our great pleasure to present to you this annual report[1] on the 2013 activities and academic highlights of the Department of Geodesy & Geoinformatics of the University of Stuttgart. The Department consists of the four institutes:

- Institute of Geodesy (GIS),
- Institute of Photogrammetry (ifp),
- Institute of Navigation (INS),
- Institute of Engineering Geodesy (IIGS),

and is part of the Faculty of Aerospace Engineering and Geodesy.

Research

This annual report documents our research contributions in many diverse fields of Geodesy & Geoinformatics: from satellite and physical geodesy through navigation, remote sensing, engineering surveying and telematics to photogrammetry, geographical information systems and location based services. Detailed information on projects and research output can be found in the following individual institutes' sections.

Teaching

Our BSc program *Geodesy & Geoinformatics* is now fully operable. We were able to welcome 52 new BSc students in Winter Term 2013/2014. The first BSc students graduated at the end of 2013. The MSc program for Geodesy and Geoinformatik started with the winter-term 2012. Currently 18 students are taking part in this Master of Science program. The Diploma program is slowly being phased out. Total enrolment, in both the BSc and the Diploma programs, is stable at about 133 students. Please visit our website *www.geodaesie.uni-stuttgart.de* for additional information on the programs.

In its 8th year of existence, our international MSc program *Geomatics Engineering* (GEOENGINE) enjoys a gratifying demand. We register an enrolment of 32 students. We attract the GeoEngine student population from such diverse countries as China, Chile, Palestine, Iraq, Iran, Pakistan, Nigeria, India, Netherlands, Turkey, Greece, Egypt, Thailand and Bangladesh. Please visit *www.geoengine.uni-stuttgart.de* for more information.

[1] A version with colour graphics is downloadable from
http://www.ifp.uni-stuttgart.de/publications/jahresberichte/jahresbericht.html

Awards and scholarships

We want to express our gratitude to our friends and sponsors, most notably

- Verein Freunde des Studienganges Geodäsie und Geoinformatik an der Universität Stuttgart e.V. (F2GeoS),
- Microsoft company Vexcel Imaging GmbH,
- Ingenieur-Gesellschaft für Interfaces mbH (IGI),
- DVW Landesverein Baden-Württemberg,

who support our programs and our students with scholarships, awards and travel support.

Below is the list of the recipients of the 2012/13 awards and scholarships. The criterion for all prizes is academic performance; for some prizes GPA-based, for other prizes based on thesis work. Congratulations to all recipients!

Wolfgang Keller
Associate Dean (Academic)
wolfgang.keller@gis.uni-stuttgart.de

Award	Recipient	Sponsor	Program
Karl-Ramsayer Preis	Matthias Ellmer	Department of Geodesy & Geoinformatics	Geodesy & Geo-informatics
Diploma/MSc Thesis Award	Matthias Ellmer	F2GeoS	GEOENGINE
MS Photogrammetry / Vexcel Imaging Scholarship	Hailong FU Xiaoqian HAN	MS Photogrammetry / Vexcel Imaging	GEOENGINE
IGI Scholarship	Run SHI Ibrahim GHALWAINJI	IGI mbH	GEOENGINE
matching funds	Zelong LIAN Mahmoud HAERI NEJAD Farajh HAERI NEJAD Santoshkumar BURLA Ke GONG Jiny JOSE PULLAMTHARA Ji Jun DU Haochen LI Lili SHI Nahla M. A. MAHMOUD Yuanting LI Mohammed ABUSHARK	DAAD	GEOENGINE

Institute for Engineering Geodesy

Geschwister-Scholl-Str. 24D, D-70174 Stuttgart,
Tel.: +49 711 685 84041, Fax: +49 711 685 84044
e-mail: Sekretariat@ingeo.uni-stuttgart.de or
firstname.secondname@ingeo.uni-stuttgart.de
url: http://www.uni-stuttgart.de/ingeo/

Head of Institute

Prof. Dr.-Ing. habil. Volker Schwieger

Secretary

Elke Rawe

Emeritus

Prof. Dr.-Ing. Dr.sc.techn.h.c. Dr.h.c. Klaus Linkwitz

Scientific Staff

Ashraf Abdallah, M.Sc.	GNSS Positioning
Bara' Al-Mistarehi, M.Sc.	Construction Process
Dr.-Ing. Alexander Beetz (until 30.11.2013)	Machine Guidance
Shenghua Chen, M.Sc.	Kinematic Positioning
Dipl.-Ing. Otto Lerke (since 01.10.2013)	Machine Guidance
Xiaojing Lin, M.Sc.	Machine Guidance
Dr.-Ing. Martin Metzner	Engineering Geodesy
Dipl.-Ing. Annette Scheider	Kinematic Positioning
Annette Schmitt, M.Sc. (since 01.04.2013)	Multi-Sensor-Systems
Rainer Schützle, M.Sc.	Location Referencing
Dipl.-Ing. Li Zhang	Monitoring
Dipl.-Ing. Bimin Zheng	Monitoring

Technical Staff

Martin Knihs
Lars Plate
Mathias Stange

External teaching staff

Dipl.-Ing. Christian Helfert	Fachdienstleiter Flurneuordnung im Landkreis Biberach
Dipl.-Ing. Thomas Meyer	Landratsamt Ludwigsburg - Fachbereich Vermessung
Dipl.-Math. Ulrich Völter	Geschäftsführer intermetric Gesellschaft für Ingenieurmessung und raumbezogene Informationssysteme mbH
Dr.-Ing. Thomas Wiltschko	Entwicklungsingenieur Daimler Benz AG

General View

The Institute of Engineering Geodesy (IIGS) is directed by Prof. Dr.-Ing. habil. Volker Schwieger. It is part of the Faculty 6 „Aerospace Engineering and Geodesy“ within the University of Stuttgart. Prof. Schwieger holds the chair in „Engineering Geodesy and Geodetic Measurements“. In 2012 he was elected as Vice Dean of the Faculty 6.

In addition to being a member of Faculty 6, Prof. Schwieger is co-opted to the Faculty 2 „Civil and Environmental Engineering“. Furthermore, IIGS is involved in the Center for Transportation Research of the University of Stuttgart (FOVUS). Prof. Schwieger presently acts as speaker of FOVUS. So, IIGS actively continues the close collaboration with all institutes of the transportation field, especially with those belonging to Faculty 2.

Since 2011 he is full member of the German Geodetic Commission (Deutsche Geodätische Kommission - DGK). Furthermore, Prof. Schwieger is a member of the section „Engineering Geodesy“ within the DGK. He is head of the DVW working group 3 „Measurement Techniques and Systems“ and chairman of the FIG working group 5.4 „Kinematic Measurements“.

The institute’s main tasks in education focus on geodetic and industrial measurement techniques, kinematic positioning and multi-sensor systems, statistics and error theory, engineering geodesy and monitoring, GIS-based data acquisition, and transport telematics. Here, the institute is responsible for the above-mentioned fields within the curricula of „Geodesy and Geoinformatics“ (currently Diploma, Master and Bachelor courses of study) as well as for „GEOENGINE“ (Master for Geomatics Engineering in English language). In addition, the IIGS provides several courses in German language for the curricula of „Aerospace Engineering“ (Master), „Civil Engineering“ (Bachelor and Master), „Transport Engineering“ (Bachelor) and „Technique and Economy of Real Estate“ (Bachelor). Furthermore, lectures are given in English to students within the master course „Infrastructure Planning“. Finally, eLearning modules are applied in different curricula. Also during the year 2013, teaching was still characterized by the conversion of courses from Diploma to Bachelor and Master degree, now with the focus on the Master degree. This is going to continue within the next year.

The current research and project work of the institute is expressed in the course contents, thus always presenting the actual state-of-the-art to the students. As a benefit of this, student research projects and theses are often effected in close cooperation with the industry and external research

partners. The main research focuses on kinematic and static positioning, analysis of engineering surveying processes and construction processes, machine guidance, monitoring, transport and aviation telematics, process and quality modeling. The daily work is characterized by intensive co-operation with other engineering disciplines, especially with traffic engineering, civil engineering, archotecture and aerospace engineering.

Research and Development

Center for Transportation Research University of Stuttgart (FOVUS)

In 2013, the main activity within FOVUS was to prepare and submit research proposals on a national and an international level. A cooperation between German Rail (Deutsche Bahn AG) and University of Stuttgart was prepared mainly by the members of FOVUS.

With respect to education, the re-organization of the transportation-related study programs at the University of Stuttgart has been successfully completed. In the winter term 2013/2014, the second set of students enrolled for the new study program „Transportation Engineering“, in which also the IIGS is involved.

Location Referencing

Today, a number of devices, applications, and services gather, receive, share, visualize, or generally speaking, process information that somehow has a location-component. In many applications, this location-based information is referenced to objects in an electronic map (e.g. roads, buildings, etc.). The application areas range from smartphone apps to find the next restaurant or cash machine to safety-relevant vehicle-based systems with high requirements to reliability and robustness.

Two kinds of such map-based applications can be distinguish. The first category uses only one map base and all exchanged objects are referenced to this map. This can be achieved, with mobile clients (e.g. Smartphones, vehicle-based systems) using the same application, which is connected to a central map server. The objects are denominated by their object ID and can be uniquely identified within that closed system. A second kind of applications is open to be used with different types of clients with different maps in use. Such systems have the chance to reach a higher dissemination as client systems are not restricted to specific applications and vendors. One drawback, however, needs to be dealt with: map objects cannot be uniquely identified among different maps. A different and more generalized way to express the location of an information object is needed. Such systems are called „Location Referencing“ systems and enable the exchange of information objects between different systems using different maps.

A location must be defined on the source map as a set of line elements on that map. The encoder then collects all required information about this location from the source map and wraps it altogether into the „location reference“. This location reference is being transmitted to the receiving

system using a (probably) different kind of road map. In this system, a decoder unwraps the received location reference and searches its map for the corresponding lines that cover the same route as the original location on the source map (Figure 1).

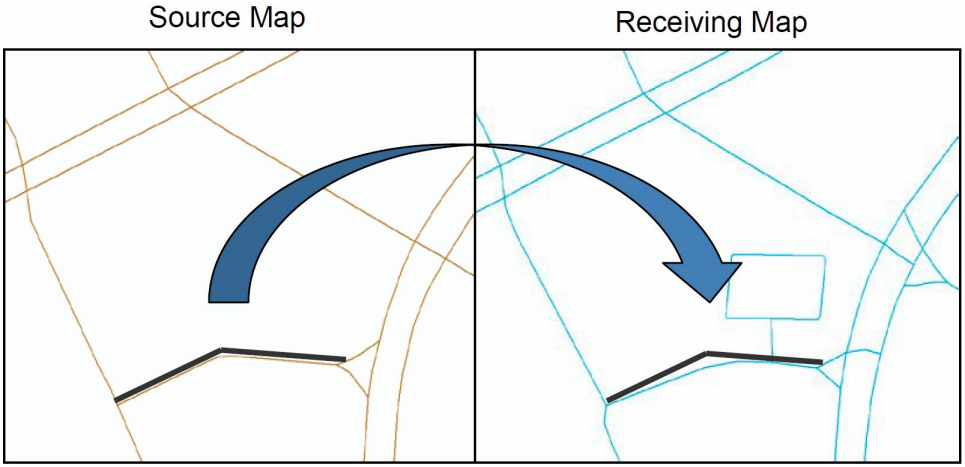

Fig. 1: Transferring a location reference

The location reference contains information about the geometric, topologic and semantic (i.e. attributes like road names and road class) properties of the original location. The transmitted information, however, has to satisfy a number of constraints: The bandwidth of the communication carrier (normally mobile internet connection) is limited. Furthermore, especially the transmitted semantic information cannot be matched without having a proper attribute mapping due to different attribute schemas at the different maps.

Available methods, like AGORA-C or OpenLR, have been used in different research projects in the past, however only reached moderate or even poor results. For some recent commercial applications of location referencing methods, the systems were restricted to specific maps which also were optimized for this particular use-case. Moreover, the location referencing data exchange format had to be adapted to the special circumstances. Altogether, the final system worked quite well but was restricted to a specific use-case, specific clients, and was not an open and flexible system anymore.

For the purpose of testing the possibilities of enhancing the success rate of such dynamic and map-agnostic location referencing systems, the IIGS sets up a location referencing test bed. During the reporting period, this test bed has reached a first intermediate functional level. It is capable of en- and decoding locations on different maps provided in shape file format. Maps that do not satisfy the format specifications directly, as for example from OpenStreetMap, can be converted using a specifically developed map converter. Batches of locations can be processed at once, the result sets are stored in a defined way and can be visualized for manual inspection together with

their underlying maps in ArcGIS quite handily using a newly developed Python-tool. Automatic evaluation procedures are capable to identify locations that might not have passed the transfer from one map to the other without fault. These locations can be inspected manually to identify possible possibilities for improvement in the location referencing procedures.

Time-Spatial Analysis for Low-Cost GPS Time Series

Multipath effects are the dominating errors for short baselines in monitoring applications. The time and spatial correlation can be analyzed by applying closely-spaced antennas. Three low-cost antennas with low-cost receivers have measured on the roof of the IIGS building. The three antennas were arranged in two positions: orthogonal (position 1) and parallel (position 2) to the wall (compare fig 2). It is expected that the multipath effect changes much more in position 1 than that in position 2.

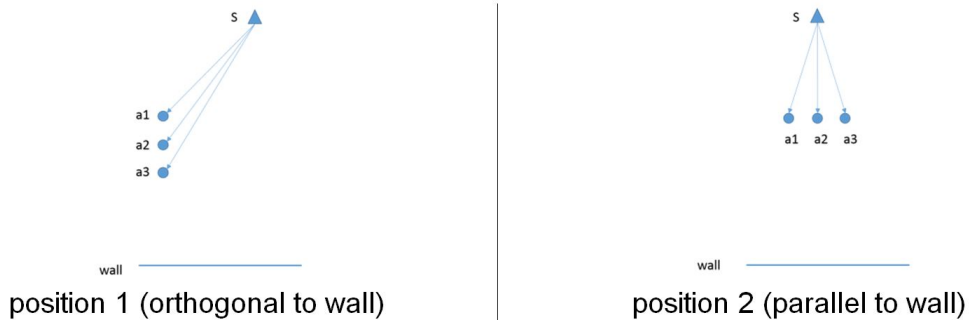

Fig. 2: Two test constellations (not scaled)

The distance between two adjoining antennas is 50 centimeters, the three antennas are numbered as a1, a2 and a3. The distance between the a2 (the middle one) and the wall is about 4.2 meters in position 1 and about 5.1 meters in position 2 and the antenna heights are all about 1.2 meters. The SAPOS station in about 500 meters away was taken as reference station and the three low-cost antennas as rover stations for the baselines. The GPS raw data (UBX-format) were stored directly from u-blox EVK-6T receivers with 1 Hz sampling rate. The receivers were measured in each position for several days.

The processing results are baselines (coordinates' differences) in UTM for every second. The time series of the coordinates were analyzed, about 5% outliers were detected and interpolated. There are no significant linear and short periodic trends (besides the period of one sidereal day) which can be found.

The cross-correlation between the baselines can be calculated. One simple approach was applied to improve the accuracies by using these spatial cross-correlations. It is assumed that the error influences are similar for each antenna; they change linear in space. For example, the coordinate

of antenna 2 can be corrected by the coordinates of antenna 1 and 3 by considering the cross-correlation. It can be calculated as blow:

$$x_{2\_cor}(t) = x_2(t) - \frac{K_{12}}{K_{12}+K_{23}} \cdot x_1(t) - \frac{K_{23}}{K_{12}+K_{23}} \cdot x_3(t)$$

The $x_1(t)$ to $x_3(t)$ on the right side are the original coordinates' residuals in east, north and height components. K_{12} and K_{23} are the correlation between the baselines s-a1 and s-a2, and between s-a2 and s-a3. They depend on the duration of the observations and on the positions. For testing this approach, one day solutions and four hour solutions were taken for each position.

Table 1 and 2 show the original and improved standard deviations of baseline s-a2 by applying the approach. Generally, almost all the standard deviations were improved (only one exception marked in table 2). The percentage of improvement is very different (maximum is 46%), on average about 21% for position 1 and 25% for position 2.

Position 1	Original standard deviation [mm]			Improved standard deviation [mm]		
s-a2	E	N	h	E	N	h
One Day solution	3.3	6.2	9.4	3.0	5.4	8.2
1. hour	1.9	4.1	5.4	1.7	2.5	5.1
2. hour	3.7	16.6	10.0	2.8	13.2	7.5
3. hour	2.7	5.3	16.6	1.5	3.5	10.6
4. hour	4.0	5.5	8.4	3.6	4.1	7.3

Table 1: Original and Improved Standard Deviation of Baseline s-a2 (Position 1)

Position 2	Original standard deviation [mm]			Improved standard deviation [mm]		
s-a2	E	N	h	E	N	h
One Day solution	3.3	5.7	9.5	2.3	4.1	7.0
1. hour	2.0	3.2	5.8	1.4	1.9	5.9
2. hour	2.5	3.1	5.8	2.2	2.0	5.6
3. hour	2.1	3.0	5.9	1.5	1.7	4.3
4. hour	2.4	3.3	10.7	2.0	2.1	7.3

Table 2: Original and Improved Standard Deviation of Baseline s-a2 (Position 2)

From these first test results, it can be seen that the approach that takes the spatial correlations into account can improve the accuracies of the results. The linear combination of correction is the simplest assumption. In the future, the spatial correction should be analyzed in more detail and another better and more reliable approaches can be developed.

Precise Point Positioning (PPP) using Bernese Software

The Bernese GNSS software Version 5.2 (BSW5.2) is scientific, high-precision processing software which was developed by the Astronomical Institute of the University of Bern (AIUB). Using Bernese software In PPP processing, the satellite orbits and clock data are available from the Center for Orbit Determination in Europe. The satellite and receiver phase center data is provided by IGS ANTEX standard data. For tropospheric modelling there are many models available in the software for dry and wet tropospheric parts. Moreover, the gradient models and mapping functions are also offered. The second order of ionospheric delay and high ionospheric orders are estimated in the PPP processing. Additionally, there are many other highly accurate models in the algorithms (e.g. ocean loading, atmospheric tidal loading).

To evaluate the PPP processing technique using Bernese software, four SAPOS stations (Stuttgart, Tübingen2, Geislingen and Heilbronn) with 24 hours observation time and 30 seconds sample interval were processed for static and kinematic techniques, (see Figure 3, left). The antenna type is TRM59800.00 SCIS and receiver type is TRIMBLE NETR5. Figure 3 (right) shows the processing procedure in static and kinematic technique. Bernese software provides the possibility to detect the session time or the observation time. The data is checked using teqc software before processing. In this processing, the observation time of the four stations were divided from 1 hour up to 24 hours. The error values are computed between the reference solution and the PPP solution.

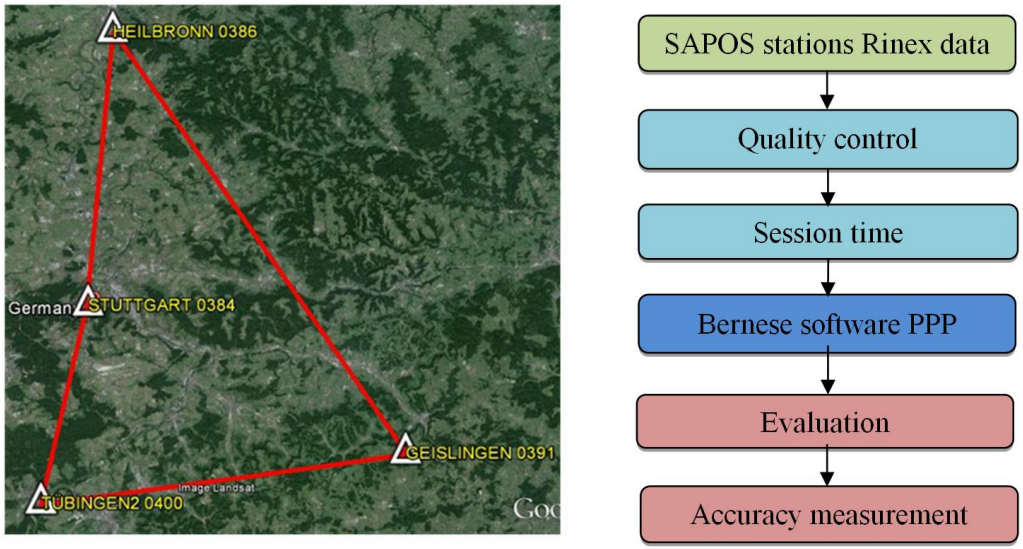

Fig. 3: SAPOS's Stations layout (left) - Processing procedure for PPP solution (right)

In case of static-PPP technique; Figure 4a illustrates the error in horizontal direction (position) for the four stations with different convergence times. The position error after 4 hours is around 1 cm and reaches mm after 12 hours. Figure 4b shows the error in height direction for the four stations in cm. The height error after 4 hours is around 2 cm and reaches 1 cm after 12 hours of convergence time for three of the four stations.

In case of kinematic-PPP technique; Figure 5a shows the RMS error in position for the different stations. For stations 0384, 0386 and 0400; the RMS error value reaches the level of 2 cm for 4 hours observation time. This error value is nearly stable to the end of this processing. Another side; station 0391 provides an RMS error in 2D of more than 2 cm for some observations times. The height RMS error is depicted in Figure 5b. The RMS error value is in between 2 to 5 cm after 4 hours. This error value reaches 2 to 3 cm after 12 hours.

The processing using Bernese software will be continued for the real kinematic tracks to assess the accuracy of PPP technique.

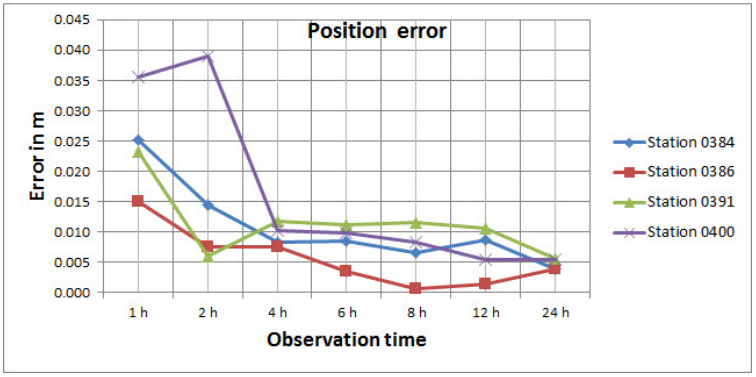

Figure 4a: Position error values for all stations in m for static-PPP

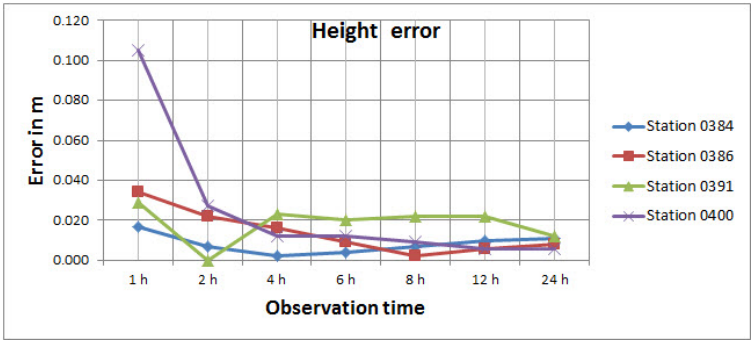

Figure 4b: Height error values for all stations in m for static-PPP

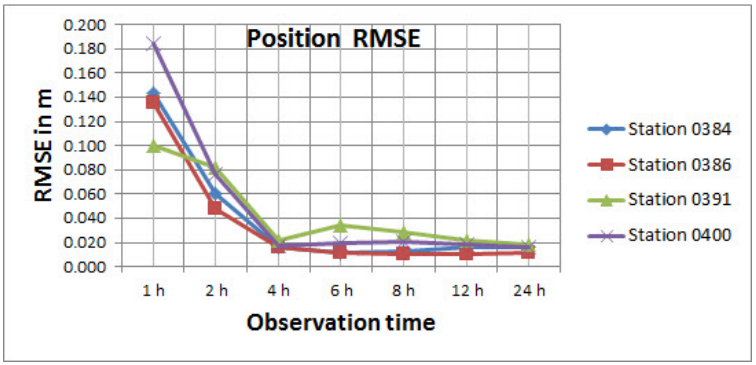

Figure 5a: Position RMSE values for all stations in m for kinematic-PPP

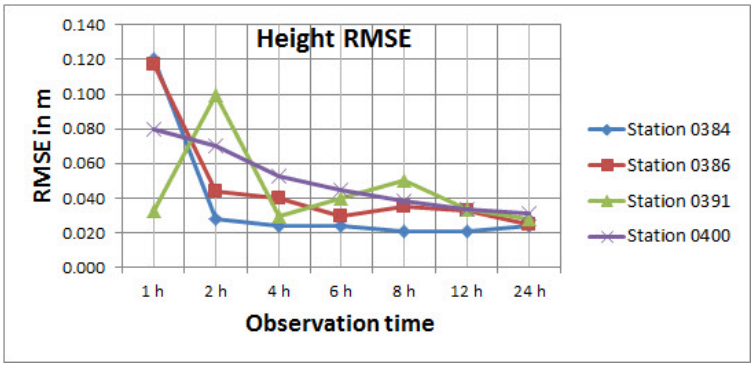

Figure 5b: Height RMSE values for all stations in m for kinematic-PPP

Further Development of the Construction Machine Simulator

The institute spent several years in developing a construction machine simulator. Now, GNSS-RTK solutions are integrated for the out-door simulator. A concrete plate was constructed for carrying out the outdoor simulator tests on Vaihingen Campus, University of Stuttgart. It is shown in the Figure 6. There are four pillars around the plate as a control network and the coordinates of the pillars are determined with GNSS static observation data and terrestrial measurements. According to the stake out data from the engineering construction map, the reference trajectory is generated on this plate. Different drive tests are carried out to investigate the control quality of the RTK solution.

The RTK-solution is computed using GNSS-Receivers of Leica Geosystems combined with SAPOS. The hardware components for the guidance system and their interactions are shown in Figure 7. The GNSS antenna is installed in the geometric center of the model truck. The model truck is composed of a steering servo-motor, a velocity motor and a receiver to obtain voltage from

the remote controller. The Leica GNSS receiver provides real-time 3D positions to the computer using radio modems. The control program which is developed with the programming language Labview computes the lateral deviation between the measurements and the reference trajectory. The digital-analogue converter converts the steering angle to voltage and sends it to the remote control.

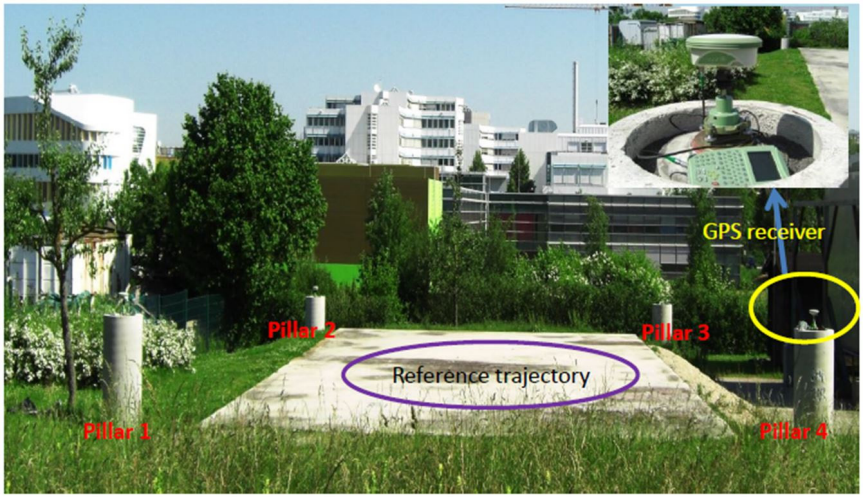

Fig. 6: Test field of the out-door simulator

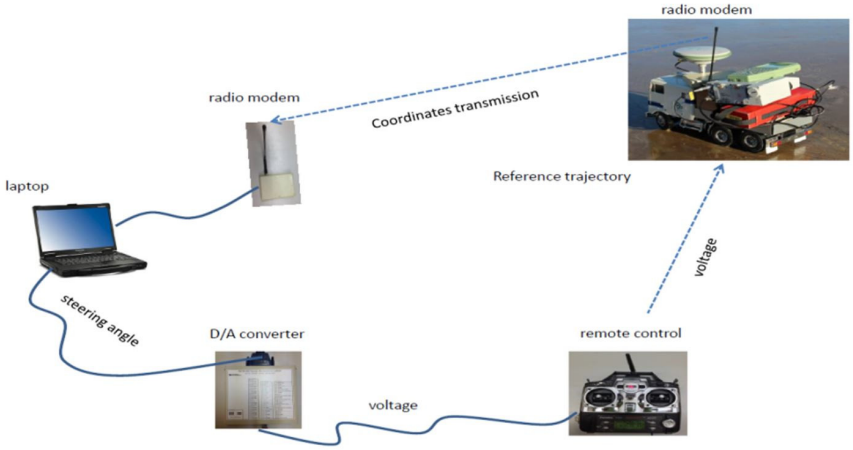

Fig. 7: Hardware components of the simulator

The experimental results show that the RMS of the lateral deviation is about 8-12 mm for a velocity of 7 cm/s with the 5 Hz real-time RTK solution. If the observation data is 20Hz, the RMS of the lateral deviation is about 5-8 mm for a velocity of 7 cm/s and 14 cm/s. The PID controller works better than the P, PI and PD controllers with different velocities and different observation data rates. The impact of the Kalman filter on the RMS of the lateral deviation is not significant when the velocity of the truck is about 7 cm/s and 14 cm/s. However, when the truck drives with a velocity of 30 cm/s, the control quality is improved by 1.6 mm by the implementation of the Kalman filter.

HydrOs - Optimization of Positioning in Areas of GNSS Shadowing along Inland Waterways

German inland waterways are surveyed by surveying vessels e.g. with multibeam depth sounders. The measured profiles of the river bed must be georeferenced, so the position of the vessel and the depth sounder respectively must be known. Currently many surveying vessels are equipped with GNSS antennas to determine their position. But positions in GNSS shadowed areas, e.g. under bridges or close to riparian vegetation, cannot be determined. Currently, these positions are calculated with a linear interpolation between known positions in post-processing mode.

The project HydrOs aims to developing an integrated hydrographic positioning system in cooperation with the German Federal Institute of Hydrology (BfG) to avoid cost-effective post-processing procedures. A multi-sensor system is designed, so multiple sensors can be used to determine the position of the vessel, if it is not possible to receive the GNSS signals. Next to GNSS, a GNSS-INS coupled system is already available on the vessels used for the HydrOs project. Additionally a Doppler Velocity Log (DVL), barometer, wind sensor and ampere meters to obtain the propeller directions and their revolution speed are integrated into the system. The HydrOs software already records the measured data. Besides, a filter module to process the data in real-time mode is currently developed.

Because of the non-linear model and observation equations an Extended Kalman Filter (EKF) is used for the evaluation of the measurements.

The developed motion models predict the following state variables in three dimensions: Angular rates, velocity components, orientation angles and coordinates. The angular rates and the orientation angles are always predicted with the same algorithm, but there are different approaches for the velocity components and the coordinates (Fig. 8). One model approach predicts the position change between epoch *k* and epoch *k+1* linearly referred to the coordinate axes of the local ship coordinate system. The spherical approach describes the coordinate changes on a great circle with curve radius R. To adapt the prediction quickly to driving manoeuvres, regulating variables are inserted into the model. For that purpose, also two approaches are evaluated: The resulting propeller direction as single regulating variable or a vector of regulating variables containing direction and rotation frequency of the propellers, flow velocity components, speed and direction changes caused by wind influence.

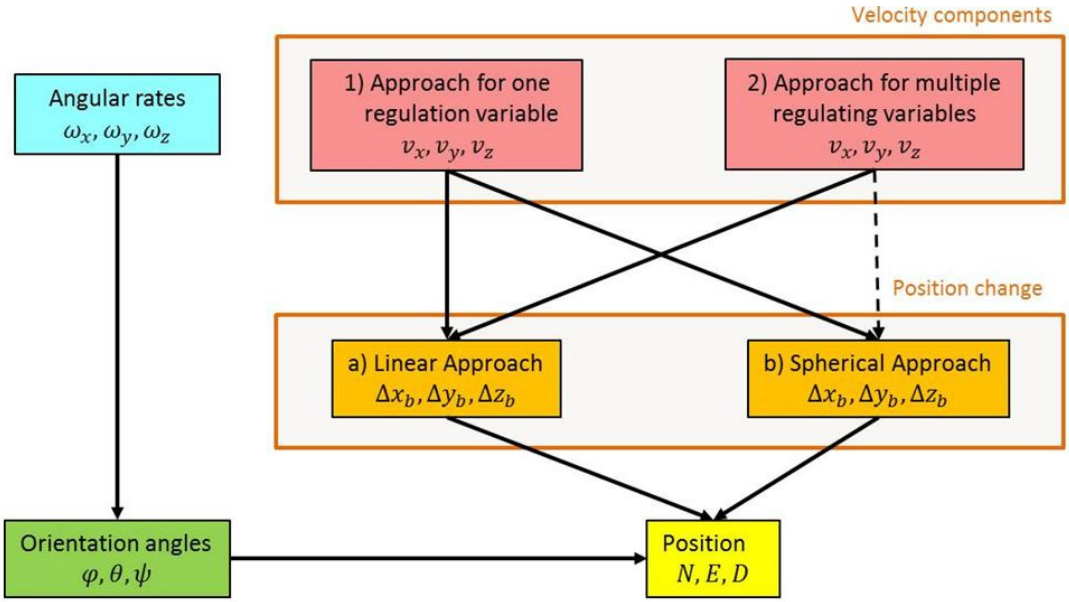

Fig. 8: Simulation scenarios

A performance test of the developed models was conducted using the Monte Carlo method. Therefore, measurement signals were simulated for a straight drive and a drive along a curve. For full observations availability it is shown that the described models reach an adequate accuracy level within the EKF. Because the regulating variables caused by wind are assumed to reach only a medium accuracy level, the approach for one resulting variable seems to be more promising. If a GNSS signal gap of 60s is simulated, the requirements are fulfilled for more than 90% of all cases provided that the linear approach with one regulating variable is used. But this means that the models must be improved furthermore to increase the reliability of the system.

For this reason, it is also important to detect GNSS measurements within regions of restricted GNSS signal reception. If they do not fulfill the requirements concerning position accuracy, those observations must not be integrated to the EKF. Therefore investigations have been conducted with multiple GNSS antennas on a platform. Some criteria were determined which might be used to detect inaccurate GNSS observations. The most promising solution combines several parameters like DOP values and the difference of measured velocities for different GNSS antennas.

Another sensor which was investigated concerning its ability of being integrated into the multisensor system was barometer. The measured air pressure was transferred to absolute and relative heights, so that the deviations could be considered. Only short-time height differences can reach an accuracy level of a few decimeters, other kinds of barometric height determinations are not accurate enough.

Detection of Hydrothermal Deformations of Sandstone using Laser Scanning

The damage documentation of cultural heritage, like buildings or sculptures, poses a great challenge to conventional measuring techniques. The main building of the University of Applied Sciences Stuttgart (HfT) was built from 1867 to 1873. The façade consists of sandstone, which is the most popular construction material for the historical city architecture in Baden-Württemberg. For our research two areas of the façade were chosen, in which there are at least 4 different types of damage like alveolarisation, crack, detachment, graffiti and algae. Each area is around 2x2 m^2 (Figure 9).

Fig. 9: Two areas on the façade (Area 1: left, Area 2: right)

It was planned to scan both areas in 6 different epochs. The first measurement took place on 22nd Feb. 2013. Epoch 2 was chosen as reference for the deformation analysis. For the deformation analysis of area 2, only the measurements from epoch 2,3,4,5 were used. Area 2 was not scanned in Epoch 6 because of a tree showing leaves for the first time in front of the façade.

Before carrying out the deformation analysis, the point clouds must be pre-processed in several steps (Figure 10). In Leica Cyclone all point clouds were georeferenced in the local coordinate system. For deformation analysis the exact border and the sizes of all epoch scans were defined and calculated in Matlab. In order to calculate and describe the deformation between two different epochs, the local normal vectors and the local volume changes were chosen for the comparison. After „façade cutting“ the changes of the local normal vectors and of the volume were also calculated in Matlab. Then the classifications of both comparisons were visualized. Finally the statistical tests were carried out for the deformation analysis.

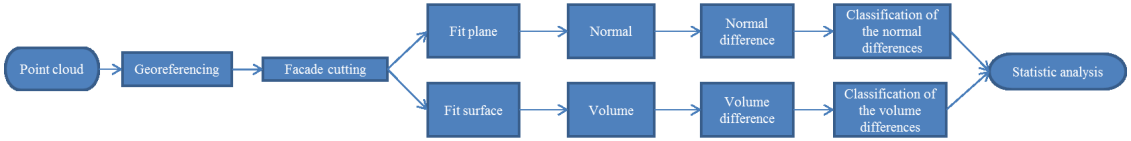

Fig. 10: Flow diagram of the data analysis

The difference vectors and their absolute values were calculated. With respect to the angle in radiant between normal vector n_{i_epoch2} of grid i in epoch 2 and the normal vector n_{i_epochj} of grid i in epoch 2 and the normal vector of grid i in epoch j the grids were colourised. With respectof grid i in epoch j the grids were colourised. With respect to the change of the volume, the grids were colourised, too (Figure 11). The change of the volumes is strongly correlated with changes in air temperature.

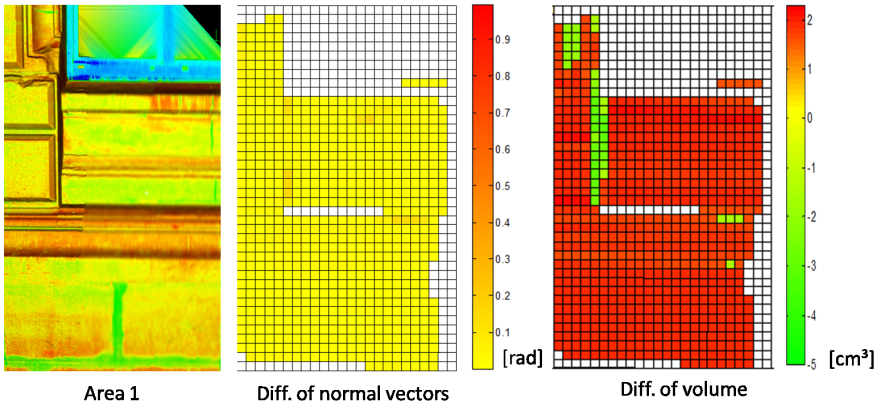

Fig. 11: Comparisons of area 1 between epoch 2 and epoch 3

The maximum angle difference of 0.95 rad between two normal vectors is calculated for the comparison of epochs 2 and 5 in area 1. Particularly with regard to the change in temperature it can be seen that the normal vectors with big differences are concentrated in the edge-area near the window. One possible supposition is that the air exchange may have an influence on this area, if the connection area between façade and window is not well isolated. Besides, the grids with big angle differences are located mainly at edge structures. In such areas the noise of the point clouds is strong and the number of points is reduced. The second reduces the redundancy of the plane estimation. Most of the angles are in intervals between 0 rad and 0.3 rad. The maximum volume difference -5.1 cm^3 can be found in area 1 between epoch 2 and 5.

The volume differences as well as the angle differences of the normal vectors have to be tested with respect to their significance. For both cases normal distributed values and a significance level of α=0.05 were assumed. Not all differences are significant. A typical pattern cannot be recognized from the data.

If figure 12 is observed, patterns are visible that cannot be explained. At the present it is not possible to give a complete explanation. It can be stated, however, that the standard deviation of the volume is strongly correlated with the standard deviation of the surface parameters. Take the grid 421 and 422 from area 1 in epoch 3 as an example (Figure 13).

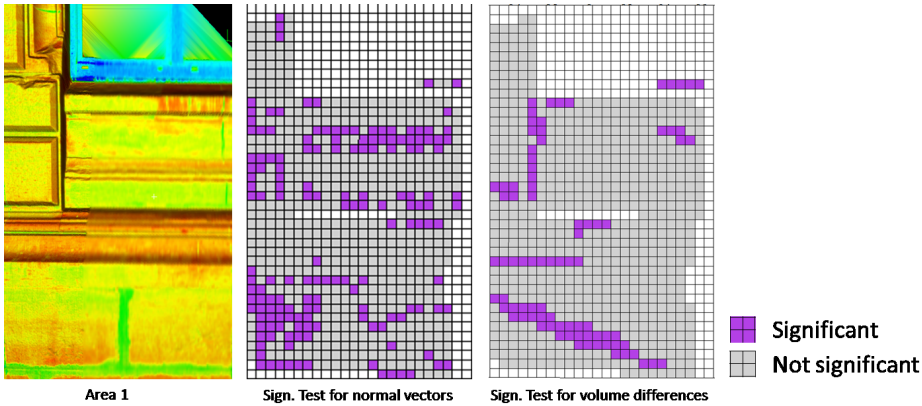

Fig. 12: Significance tests for nomal vector and volume changes of area 1

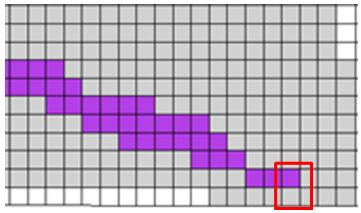

Fig. 13: Example for the significance test

Grid 422 has a volume difference of -5.7 cm^3, which has the same magnitude like the volume difference of -5.3 cm^3 of grid 421. The volume difference of grid 421 is significant, unlike the one of grid 422 (Table 3). This is caused by the respective standard deviations and finally by the standard deviations of the polynomial parameters: 0.002 in grid 422 is worse than 0.0005 in grid 421. This means that the surface fitting function has to be investigated in more detail in the future.

Grid	ΔV [cm³]	σ_ΔV [cm³]	σ_P
421	-5.3	2.6	0.0005
422	-5.7	5.9	0.002

Table 3: Accuracy of volume difference

In the next step the correlation between the surface parameters and the volume accuracy must be analysed. In the future, continuous temperature and huminity measurements nearby the façade have to be realized to overcome the deficiency. One approach to be considered in the modelling of the temperature and humidity influences by a finite element model (FEM) of the sandstone façade or in any case a part of it. In the best case the calibration of this model using geodetic measurements can be the target.

Automated Detection for Cracks Detection

Crack detection is considered as one of the most important issues in transportation and highway engineering. In the past, conventional visual and manual pavement distress analysis approaches were very costly. Also the measuring of linear cracks is consuming a lot of time, it is dangerous, labor-intensive, tedious, and subjective. For these reasons several image processing methods for crack detection algorithms have been developed. But many of them which depend on approximation algorithms, face some obstacles and problems. The work of this year provides an automated image processing crack detection algorithm. The goal is to extract automatically the linear cracks from sequence pavement images of different streets in Germany. The sequence pavement images (mobile mapping data) were observed by two Germany companies as follows: *LEHMANN + PARTNER GmbH* company using S.T.I.E.R mobile mapper system and *3D Mapping Solutions GmbH* company using MoSES mobile road mapping system.

Different case studies with different lighting conditions were analysed to evaluate the proposed automated image processing crack detection algorithm technique. Figure 14 illustrates the processing and evaluation methodology for crack detection. The proposed automated crack detection algorithm provides the possibility to detect the linear cracks from sequence pavement images (mobile mapping data) with different lighting conditions. Also the speed up factor shows a significant improvement.

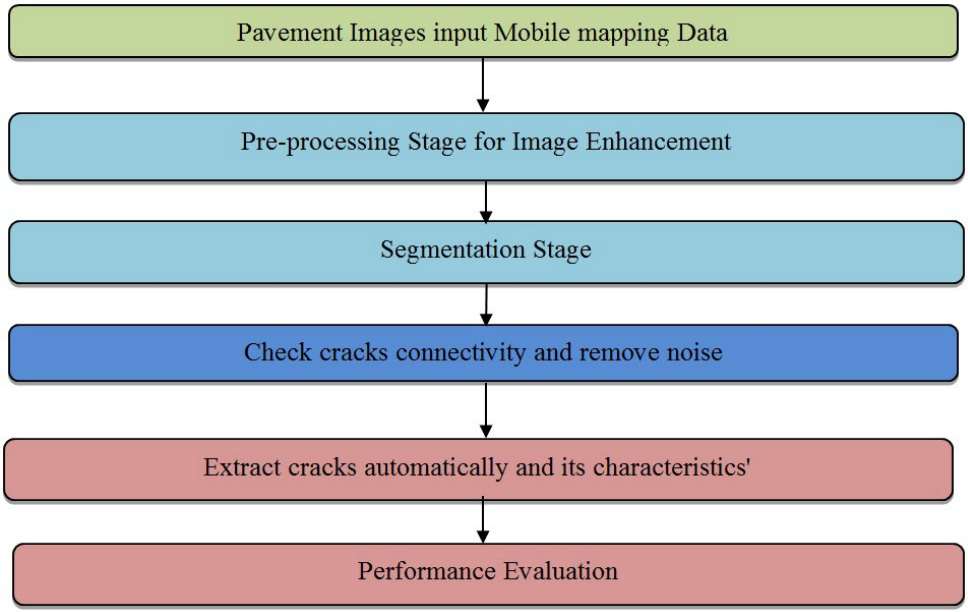

Fig. 14: The processing and evaluation methodology for crack detection

Robotics in Timber Construction

The project *Robotic Fabrication in Timber Construction* is realized in co-operation with the Institute for Computional Design, the Institute of Building Structures and Structural Design, industrial partners and partners from the state Baden-Württemberg. The goal of this project is to combine robotic fabrication with computational design, simulation processes, and 3D-surveying.

The result of this project will be a demonstrator pavilion, shown in Figure 15, for the state horticultural show *Landesgartenschau 2014* in Schwäbisch Gmünd. The pavilion will be constructed of 243 wooden elements which will have been produced by industrial robots. The elements, which consist of plywood with a thickness of 50 millimeters, are preformatted by a CNC-machine and afterwards processed by the robots.

Fig. 15: Pavilion

The surveyor's part in this project is the quality control of the elements and, after having built up the pavilion, the deformation analysis using laser scanning data. The quality control is effected by the laser tracker. The results of the laser tracker measurements are compared to the given design model.

For the quality control of the elements, a laser tracker API Radian is used together with the API IntelliProbe360™. The quality control is carried out by a control sample, this means that out of 243 elements 24 are measured. To measure the edges of the element a special adapter for the IntelliProbe360™ is developed by IIGS. As shown in Figure 16, each has at least five edges with minimum one box joint.

Fig. 16: Wooden Element

On each element of the box joint at least five points were measured. These point-wise measurings are compared with the CAD model. This comparison is effected by Spatial Analyzer's function „*Relationships*", which calculates the minimum distance between the measured point and the edges of the CAD model. The average aberration is 0.97 mm for all measured elements.

Wood is a vital basic material, for that reason four elements will be measure three times. So the change between the moment after production, shortly before transportation and after one night at the building site can be shown.

The next step will be the deformation analysis of the pavilion, which will be performed by a laser scanner. There will be a detailed investigation of the four elements which were measured three times by the laser tracker.

Publications

Beetz, A, Schwieger, V.: Automatic lateral control of a model dozer. Journal of Applied Geodesy, Heft 4, de Gruyter, 2013

Cramer, M., Schwieger, V., Fritsch, D., Keller, W., Kleusberg, A., Sneeuw, N.: Geoengine - the university of Stuttgart International master program with more than 6 years of experience. FIG Working Week, Abuja, Nigeria, 06.-10.05.2013 and Interexpo Geo-Siberia, Novosibirsk, Russia, 24.-26.04.2013.

Kealy, A., Retscher, G., Schwieger, V.: Preface to the Special Edition of the JAG on Ubiquitous Positioning and Navigation Systems. Journal of Applied Geodesy, Heft 4, de Gruyter, 2013.

Kuhlmann, H., Schwieger, V., Wieser, A., Niemeier, W.: Ingenieurgeodäsie - Definition, Kernkompetenzen und Alleinstellungsmerkmale. Zeitschrift für Vermessungswesen, Heft 6, Wißner Verlag, 2013.

Scheider, A., Schwieger, V.: Entwicklung von Verfahren zur Verbesserung der Ortung mit Global Navigation Satellite Systems (GNSS). BfG-Kolloquium: Neue Entwicklungen in der Gewässervermessung, Koblenz, 20./21.11.2012.

Schwieger, V., Lilje, M.: Innovative and Cost-effective spatial positioning. FIG Working Week, Abuja, Nigeria, 06.-10.05.2013 and Interexpo Geo-Siberia, Novosibirsk, Russia, 24.-26.04.2013.

Schwieger, V., Schweitzer, J., Zhang, L.: Ingenieurgeodästische Qualitätsmodllierung im Bauprozess. In: 125. DVW-Seminar: Qualitätssicherung geodätischer Mess- und Auswerteverfahren. Hannover, 24.-25.06.2013.

Zhang, L., Schwieger, V.: Investigation regarding different antennas combined with low-Cost receiver. FIG Working Week, Abuja, Nigeria, 06.-10.05.2013.

Zhang, L., Schwieger, V.: Monitoring mit Low-Cost GPS Empfängern - Chancen und Grenzen. In: 124. DVW-Seminar: GNSS 2013 - Schneller, Genauer, Effizienter. Karlsruhe, 14.-15.03.2013.

Zheng, B., Schwieger, V., Grassegger-Schön, G.: Detection of hydrothermal deformations of sandstone using laser scanning. 2nd Joint Symposium on Deformation Monitoring, Nottingham, UK, 09.-10.09.2013.

Presentations

Schwieger, V.: Construction Machine Guidance. Technical University of Construction Bucharest, Rumania, 18.-22.11.2013.

Schwieger, V.: Low Cost GNSS. Technical University of Construction Bucharest, Rumania, 18.-22.11.2013.

Schwieger, V.: Multi Sensor Systems. Technical University of Construction Bucharest, Rumania, 18.-22.11.2013.

Schwieger, V.: Trajektorienbestimmung mittels Kalman Filter. 10. Jenaer GeoMessdiskurs. 01.07.2013.

Zhang, L.: Monitoring mit Low-Cost GPS Empfängern - Chancen und Grenzen. In GNSS 2013 - Schneller. Genauer. Effizienter. 124. DVW-Seminar am 14. und 15. März 2013 in Karlsruhe.

Diploma Theses and Master Theses

Alhessi, Mohammed: Development and Implementation of an OpenLR Map Interface for Shape-Files.

Anisia, Vlad-Daniel: Comparison of two Software Products for the Object Modelling with Respect to Deformation Analysis using FARO Focus 3D Data.

Fitz, Daniel: Bestimmung von Referenz-Positionen für die photogrammetrische Auswertung von UAV-Bildflügen mittels einer automatischen Totalstation.

Ren, Zhenjie: Design, Implementation and Evaluation of Sensor Concepts for Robot Localization in the Indoor Area.

Wei, Xingyu: Analysis of Damage Dynamics on the North-East Facade of the HFT Stuttgart using Leica Laser- Scanner HDS7000.

Wen, Xinda: Development of Evaluation Functions for a Collosion Measuring Stand

Study Theses and Bachelor Theses

Bosch, Jascha: Untersuchung der Positionsgenauigkeit kinematischer GNSS Messungen in teilabgeschatteten Bereichen.

Diemer, Luis: Entwicklung eines formbasierten Location Referencing Verfahrens.

Alexander Grenz: Aufbau eines Referenzfestpunktfeldes zum Betrieb eines Outdoor-Baumaschinensimulators.

Kauker, Stephanie: Untersuchung verschiedener Laserscanner-Zielzeichen für die Registrierung von Punktwolken.

Scatturin, Raphael: Barometrische Höhenbestimmungen in einem Hydrographischen Ortungssystem (HydrOs).

Schaal, Carolin: Untersuchung des Auflösungsvermögens eines Laserscanners bei der Aufnahme feiner Strukturen.

Tao, Qin: Genauigkeitsuntersuchung der Low-cost IMU 3DM-GX2 von Microstrain.

Wang, Jinyue: Neuvermessung des Pfeilernetzes Vaihingen und Vergleich mit Low-Cost GPS Ergebnissen.

Wilhelm, Johannes: Untersuchungen zur Modellierung und der Datenmigration von kommunalen Daten im Rahmen des Abwassergebührensplittings.

Yang, Jiawei: Erfassung von Spannungs- und Meteorologiedaten für das Low-Cost GPS Monitoring System.

Ye, Zican: Untersuchung der inneren und äußeren Genauigkeit des Faro Focus 3D.

Yue, Fang: Einsatz von koordinatenbasierten Verfahren zum Location Referencing.

Education

Bachelor Geodesy and Geoinformatics

Basic Geodetic Field Work (Schmitt, Stange) 5 days
Engineering Geodesy in Construction Processes (Schwieger, Zheng) 3 Lecture/1 Lab
Geodetic Measurement Techniques I (Metzner, Schmitt) 3/1
Geodetic Measurement Techniques II (Schmitt) 0/1
Integrated Field Work (Metzner, Zheng) 10 days
Measurement Methods and Estimation Methods in Engineering Geodesy (Schwieger, Zheng) 2/2
Reorganisation of Rural Regions (Helfert) 1/0
Statistics and Error Theory (Schwieger, Zhang) 2/2

Master Geodesy and Geoinformatics

Industrial Metrology (Schwieger, Stange, Schmitt) 1/1
Land Development (Meyer) 1/0/0/0
Monitoring Measurements (Schwieger, Lerke) 1/1
Transport Telematics (German) (Metzner, Scheider) 2/2
Thematic Cartography (German) (Beetz, Metzner, Schützle) 1/1
Terrestrial Multisensor Data Acquisition (German) (Beetz, Schmitt) 1/1
Measurement Techniques within Closed Loops (Beetz) 2/0
Project Management in Engineering Geodesy (Wiltschko, Völter) 2/0

Master GeoEngine

Integrated Field Work (Metzner, Zheng) 10 days
Kinematic Measurements and Positioning (Schwieger, Beetz) 2/1
Thematic Cartography (Schützle) 1/1
Transport Telematics (Metzner, Scheider) 2/1
Monitoring (Schwieger, Lerke) 1/1

Bachelor Civil Engineering

Geodesy in Civil Engineering (Beetz, Scheider) 2/2

Master Civil Engineering

Geoinformation Systems (Metzner, Zheng) 2/1
Transport Telematics (Metzner, Scheider) 1/1

Bachelor Technique and Economy of Real Estate

Acquisition and Management of Planning Data (Metzner, Stange) 2/2

Master Infrastructure Planning

GIS-based Data Acquisition (Beetz, Schmitt) 1/1

Bachelor Transport Engineering

Statistics (Metzner, Stange) 0.5/0.5
Seminar Introduction in Transport Engineering (Metzner, Schmitt) 0.5/0.5

Institute of Geodesy

Geschwister-Scholl-Str. 24D, D-70174 Stuttgart,
Tel.: +49 711 685 83390, Fax: +49 711 685 83285
e-mail: gis@gis.uni-stuttgart.de or firstname.secondname@gis.uni-stuttgart.de
url: http://www.uni-stuttgart.de/gi

Head of Institute

SNEEUW NICO, Prof. Dr.-Ing.

Emeritus

GRAFAREND ERIK W, em. Prof. Dr.-Ing. habil. Dr.tech.h.c.mult. Dr.-Ing.E.h.mult.

Academic Staff

ANTONI MARKUS, Dr.-Ing.
KELLER WOLFGANG, Prof. Dr. sc. techn.
KRUMM FRIEDRICH, Dr.-Ing.
REUBELT TILO, Dr.-Ing.
ROTH MATTHIAS, Dipl.-Ing.

Research Associates

ABEDINI ABBAS, M.Sc.
CHEN QIANG, M.Sc.
DEVARAJU BALAJI, M.Sc.
ELMI OMID, M.Sc.
GOSWAMI SUJATA (since 15.10.)
IRAN POUR SIAVASH, M.Sc.
JAVAID MUHAMMAD ATHAR, M.Sc. (since 15.4.)
LI HUISHU (since 5.9.)
ROOHI SHIRZAD, M.Sc.
TOURIAN MOHAMMAD, M.Sc.
VISHWAKARMA BRAMHA DUTT, M.Sc. (since 1.10.)
WU GELI, M.Sc.

YE ZHOURUN, M.Sc.
ZHANG JINWEI, M.Sc. (since 1.10.)
ZHAO WEI, M.Sc. (until 20.9.)

Administrative/Technical Staff

GÖTZ THOMAS, Dipl.-Ing. (FH) (since 1.3.)
SCHLESINGER RON, Dipl.-Ing. (FH)
VOLLMER ANITA, Secretary

External Lecturers

BOLENZ S, Dipl.-Ing., Stadtmessungsamt, Stuttgart
ENGELS J, PD Dr.-Ing. habil., Stuttgart
HEß D, Dipl.-Ing., Ministerium für Ländlichen Raum und Verbraucherschutz Baden-Württemberg, Stuttgart
STEUDLE G, Dipl.-Ing., Ministerium für Ländlichen Raum und Verbraucherschutz Baden-Württemberg, Stuttgart

Guests

BORKOWSKI A, Prof., Wroclaw/Poland (1.-10.7.)
BRITCHI A, Bukarest/Romania (11.-24.6.)
GHITAU D, Prof., Bucharest/Rumania (16.7.-26.8.)
ISSAWY E, Prof. Dr., Cairo/Egypt (14.-26.6.)
TENZER R, Prof., Wuhan/China (10.-19.7.)
VARGA P, Prof. Dr., Budapest/Hungary (2.10.-29.11.)
WANG L, Luxembourg/Luxembourg (1.-31.10.)
YOU RJ, Prof. Dr., Tainan/Taiwan (5.8.-12.9.)

Research

Monitoring the water cycle using remote sensing approaches

In recent decades, remote sensing techniques have successfully been deployed to monitor the temporal variation of earth related phenomena. To understand the impact of climate change and human activities on earth water resources, monitoring the variation of water storage over long periods is a primary issue. On the other hand, this variation is a fundamental key to estimate the hydroelectric power generation variation and fresh water recreation.

Among the spaceborne sensors, satellite altimetry can provide surface water height with repeat periods of 10 and 35 days. Optical and SAR (Synthetic Aperture Radar) satellite imagery provide the opportunity to monitor the spatial change in coastline, which can serve as a way to determine the water extent repeatedly in an appropriate time interval.

The inland delta of the Niger river is one of the most fragile ecosystems of Sub-Saharan Africa. Patterns of land cover and land use vary extremely due to the pre-flood and post-flood hydrographical conditions of the Niger river and its tributaries. Spaceborne sensors provide a number of novel ways to monitor the hydrological cycle and its interannual and interseasonal changes.

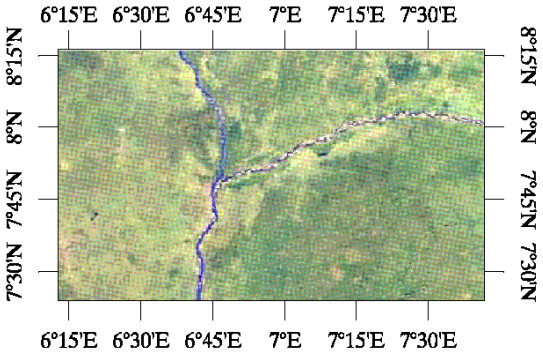

Figure 1: Part of Niger river

Daily snapshots of MODIS (Moderate Resolution Imaging Spectroradiometer) images in Terra and Aqua mode are appropriate for water cycle monitoring because of the availability in different bands and their time interval. While the difference between water and soil in infrared bands is remarkable, the water body is easily identified by applying k-means clustering in infrared bands. Here, MODIS level 3, 16-day vegetation indices (MOD13Q1) data sets with 250 m spatial resolution are used to determine the variation of width in two selected sections of Niger river.

To monitor the water area, all cloud free MODIS images are collected. Each of them are separately classified in two classes (water and land) applying k-means clustering. Finally, the water area is computed in each snapshot.

To evaluate the relationship between the variation of water level and water area, the variation of river width at an in situ gauge is compared with daily runoff during six years. Figure 3 demonstrates that there is a good agreement between water level and water area variations.

Water area together with water level are two fundamental parameters of the hydrological water cycle. Spaceborne geodetic sensors provide valuable information for monitoring the hydrological behaviour of lakes and rivers. Accurate estimation of these parameters gives us a promising sign to obtain the runoff without in situ data.

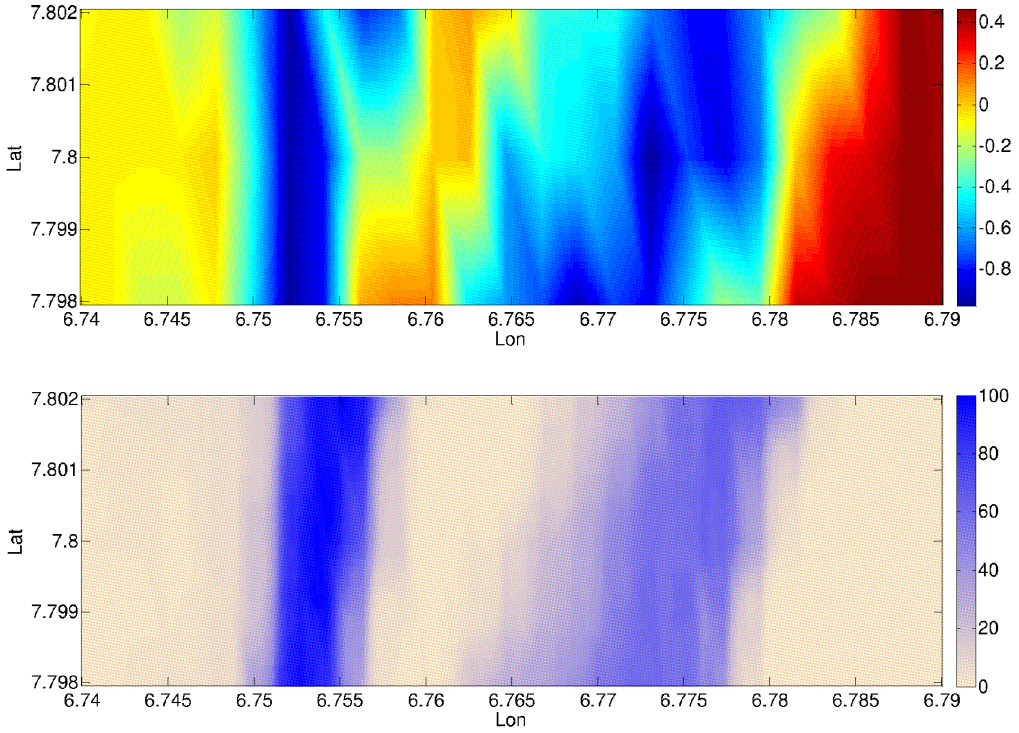

Figure 2: A NDVI image of the river near the in situ gage (top). Percentage of water coverage over 12 years (bottom)

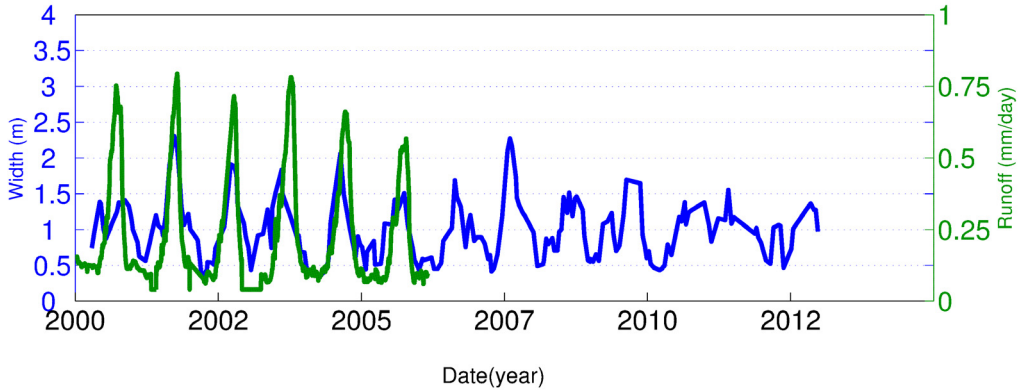

Figure 3: Relationship between daily runoff and river width near the in-situ gauge

Monitoring the water cycle using spaceborne geodetic sensors

Spaceborne sensors provide a number of novel ways to monitor the hydrological cycle and its inter-annual changes. The use of GRACE gravity data allows to determine continental water storage changes and to close the water budget on short time scales. Satellite altimetry can be used as a tool for monitoring inland water surface elevations. Optical satellite imagery provides the opportunity to monitor the spatial change in coastline, which can serve as a way to determine the water extent repeatedly in an appropriate time interval (Figure 4).

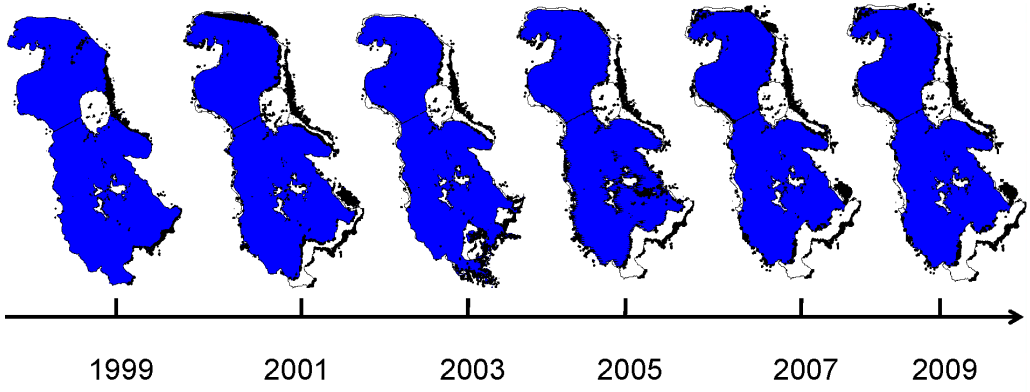

Figure 4: Surface water extent of Lake Urmia, Iran, obtained from MODIS imagery from 1999 to 2009

Assimilation of data sets from different sensors enables a better understanding of the hydrological cycle. The assimilation, for instance, allows us to monitor the desiccation of Lake Urmia in Iran. The Urmia Lake, a hypersaline lake in northwestern Iran is under the threat of drying up. The high importance of the lake's watershed for agricultural purposes demands a comprehensive monitoring of the watershed's behaviour.

The water storage change data from GRACE, surface water level over different parts of the lake from satellite altimetry, surface water extent estimation from optical imagery and in situ in situ observation of precipitation are assimilated to monitor the Urmia lake hydrological cycle (Figure 5).

A linear dynamic system consisting of a stochastic process model and observation equations is developed to assimilate the data from different sources. The dynamic system is solved by a Kalman filter to achieve an unbiased estimation with minimum variance. The assimilation results highlight an extra desiccation after 2009 in contrast to the increase of GRACE mass storage and precipitation.

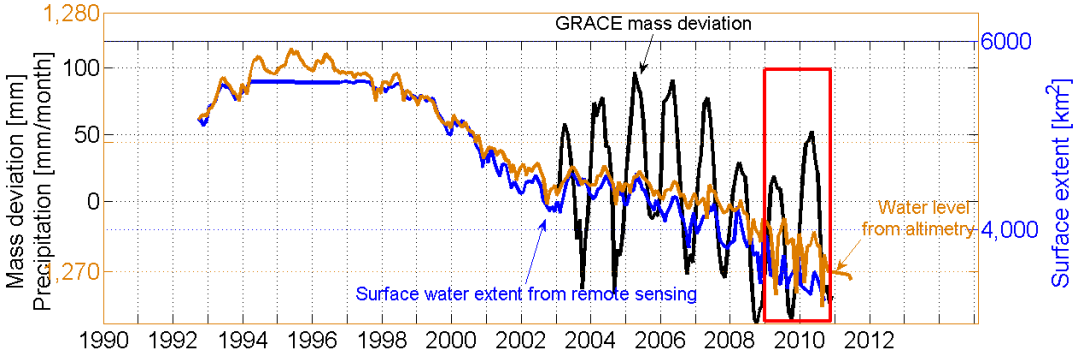

Figure 5: All in one: Time series of mass deviation from GRACE, precipitation from GPCC, precipitation of Nazchoolay station, surface water extent from remote sensing approach and water level from satellite alti-metry

CryoSat-2 for hydrological purposes: data processing, visualization and analysis

The publicly available global river discharge database is limited in spatial and temporal coverage. Although regional exceptions exist, the population of the database has declined over the past several years. As discharge is one of the most important parameters for modeling hydrological interactions, alternative measuring techniques must be sought. Our ultimate goal is to develop an algorithm to derive river discharge estimation without the need of current or past in situ data. For that purpose, only water level data is not sufficient and other types of hydrological data like slope, channel width, etc. are needed. Therefore the capability of the CryoSat-2 satellite for hydrological studies of rivers, more precisely of their water level, extent and slope is investigated. CryoSat-2 is a remote sensing satellite of ESA, which is originally designed for the monitoring of sea and land ice surfaces. It provides global radar altimetry data that can also be used for other areas of application.

A GUI based on MATLAB, called CryoTrack, has been developed, which allows the end user to comprehend the tracks of the CryoSat-2 satellite on a global grid and to access their measurements for selected area and period (Figure 6). With the help of this software, CryoSat-2 data was used to determine water height, extent and slope of rivers, by combining the information of several radar altimetry quantities. Analyzing several intersections between the satellite tracks and the Niger River as a case study revealed that slope and river water height can be estimated from CryoSat-2 data with acceptable accuracies. Our analysis shows that the transitions between water and land surfaces can be identified for wide rivers, for which their distance allows estimation the river width.

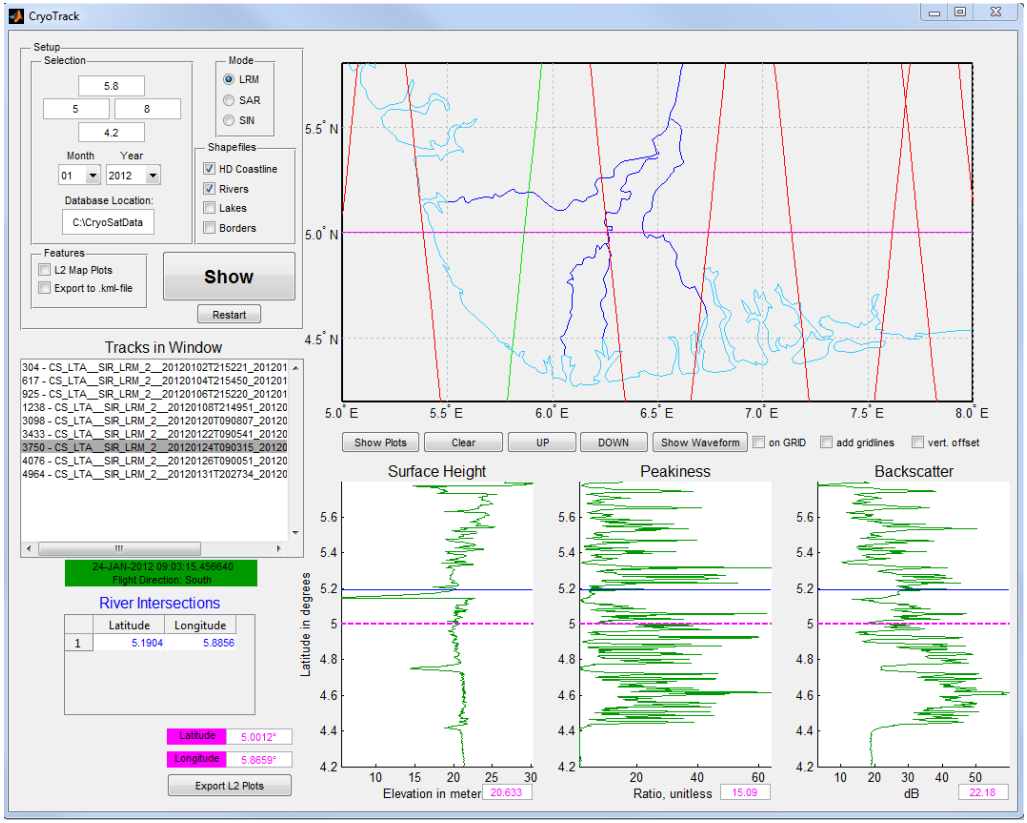

Figure 6: CryoTrack graphical user interface based on MATLAB

With the help of this software, CryoSat-2 data was used to determine water extent and slope of rivers, by combining the information of several radar altimetry quantities. Analyzing several intersections between the satellite tracks and the Niger River as a case study revealed that slope and river water height can be estimated from CryoSat-2 data with acceptable accuracies. Our analysis shows that the transitions between water and land surfaces can be identified for wide rivers, for which their distance allows estimation the river width.

Least squares prediction of discharge

In response to the limitations of the existing in situ discharge database, we estimate river discharge of ungauged basins by least squares prediction. In this method, discharge is predicted by mapping the discharge characteristics of gauged basins into ungauged ones through statistical correlations of past data (Figure 7).

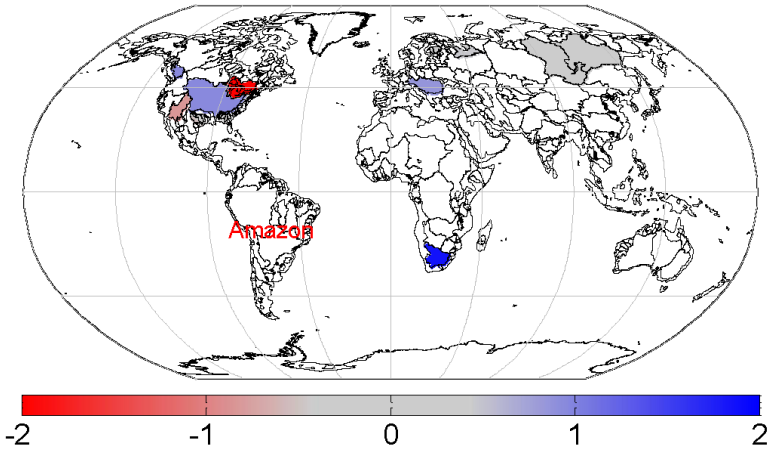

Figure 7: Contribution of 24 catchments to map the discharge characteristics into Amazon. The discharge characteristics generated through available past data between 1980-1990. For validation purposes, Amazon is considered to be ungauged here.

We follow two scenarios to form the covariance matrices out of available past in situ river discharge: (1) at the signal level, and (2) at the residual level after subtracting monthly mean values. Our validation shows that both scenarios are able to capture discharge values with relative errors less than 15% for 80% of the 25 catchments under study. We obtain Nash-Sutcliffe coefficients of over 0.4 for about 90% and of over 0.75 for about 50% of the catchments under study. We are thus able to avoid the complexity of hydrological modeling and the challenges (e.g. uncertainty) of spaceborne approaches for discharge estimation over ungauged basins.

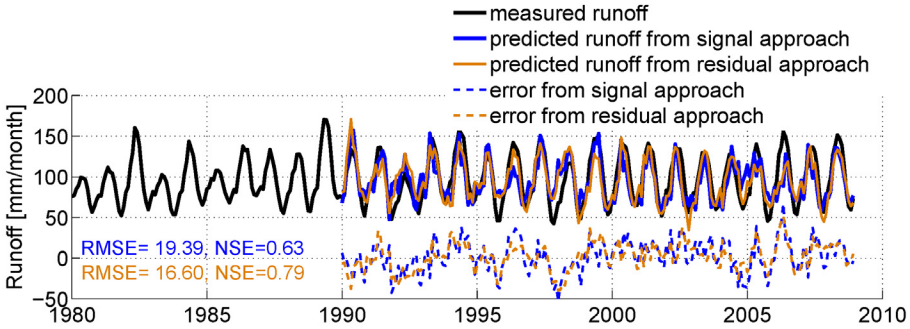

Figure 8: Prediction of discharge for the Amazon catchment with covariance matrices from a training period between 1980 and 1990.

Assessment the ability of pulse-limited altimetry in monitoring the water level of inland water body by full and sub-waveform retracking

Pulse-limited satellite altimetry was originally designed for oceanographic observations but they are able to monitor inland water bodies as well. So far, studying water level variations of inland water bodies, e.g. lakes, has been a challenge for this type of altimetry in terms of data quality. The returned altimetry waveforms can be seriously contaminated by topography and environmental error sources. Retracking is an efficacious method against this contamination to improve the accuracy of the range measurement and, consequently, to determine the water level. In addition, the choice of an optimal retracking algorithm appropriate for the specific regional water bodies is very important in this respect.

In this study we processed 18 Hz Envisat RA2 altimetry data, i.e. Sensor Geophysical Data records (SGDR), with different retrackers and 1 Hz Geophysical Data Records (GDRs) of this mission by on-board retrackers. First, for a given waveform the whole waveform, called full-waveform, was processed to estimate retracked water level variation using OCOG, Threshold and ?-parameter retrackers. In the next step we assumed that the reflecting surface inside the radar foot print is a complex surface with different responses. Therefore a given waveform is considered as a combination of a number of small waveforms, called sub-waveforms. Each sub-waveform was processed by all of the mentioned retrackers to determine water level variations. Finally the result of different retracked heights were compared with on-board retrackers, and with available in-situ gauge data.

Figure 9: Envisat ground track for cycle 92

The largest salt lake in the middle east, Urmia lake, has been selected as a testing area in this study. This lake is drying up due to climate change and human activities, e.g. irrigation and dam construction. Our retracking analysis shows that sub-waveform retracking outperforms full-waveform retracking. The minimum RMS, i.e. 18 cm, was obtained by retracking sub-waveform with threshold 50% algorithm.

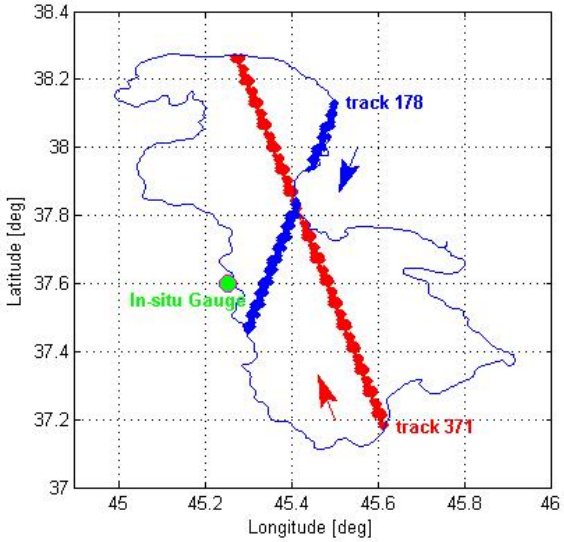

Figure 10: Envisat sub-satellite point over Urmia Lake

A general comparison of Figures 11 and 12 discloses the advantages of waveform retracking. By waveform retracking we can keep all of the measurements, even close to the shoreline, and have a qualified water level time series. We validated the water level obtained from satellite altimetry internally and externally. The internal validation shows that there is no bias and systematic error between ascending and descending track observations. The internal validation relates to the residual and precision of water level. It indicates that threshold retracking algorithm with different threshold values decreases the residual of the water level. The water level residual from ice-1 retacker is 27 cm while the residual from threshold 20% is 15 cm if we retrack the full-waveforms. But if we retrack the sub-waveforms with threshold 10% retracker the water level residual is 10 cm which is a significant improvement. The residual would be 13 cm if threshold 50% is used retrack the first detected sub-waveforms.

For the external validation we use available in-situ gauge data. To avoid elevation datum shift between in-situ gauge and satellite data the mean water level was removed from both time series. For full-waveform retracking there is improvement only by threshold retracker. The maximum improvement is 4 cm which is achieved by threshold 50%. For the β-5 parameter retracker the

accuracy before retracking is much better than that after retracking. It shows that for the full-waveforms β-5 parameter is not a proper retracker in the case of Urmia lake. However, for the sub-waveforms β-5 parameter retracker shows good performance. It obtained an accuracy of 22 cm when we use the first sub-waveforms detected in the full-waveforms.

Generally we have improvement by all retrackers when the first sub-waveforms are retracked. The minimum RMS, i.e. 18 cm, has been estimated by threshold 50% retracker. That means we have 8 cm improvement with respect to on-board retracker ice-1. Therefore, the first sub-waveform retracked by threshold 50% is the most robust estimator to monitor the water level variations of Urmia lake.

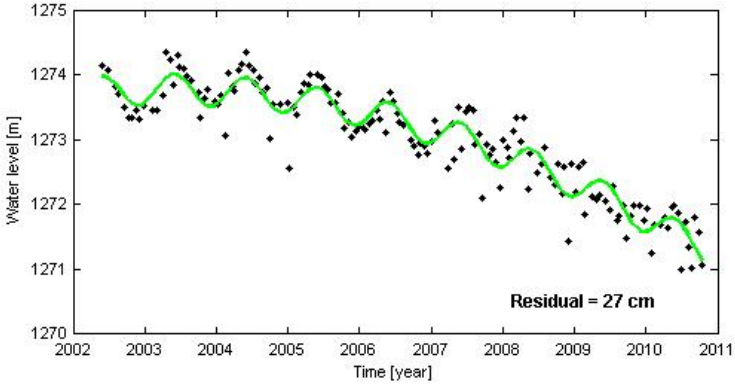

Figure 11: Water level of Urmia lake from standard on-board retracker, ice-1. It outperforms other on-board retrackers.

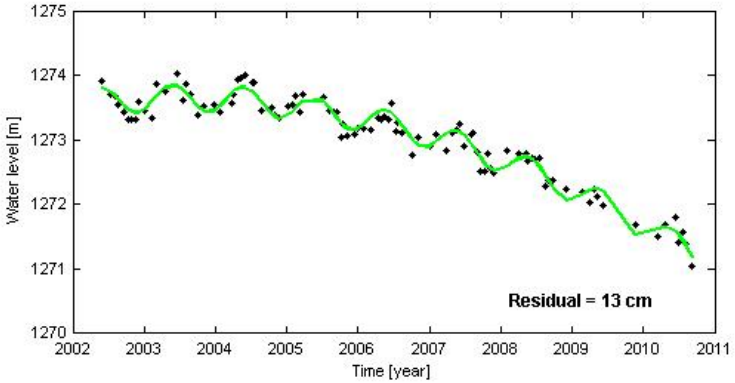

Figure 12: Water level of Urmia lake after waveform retracking using the first detected sub-waveform retracked by threshold 50% retracker.

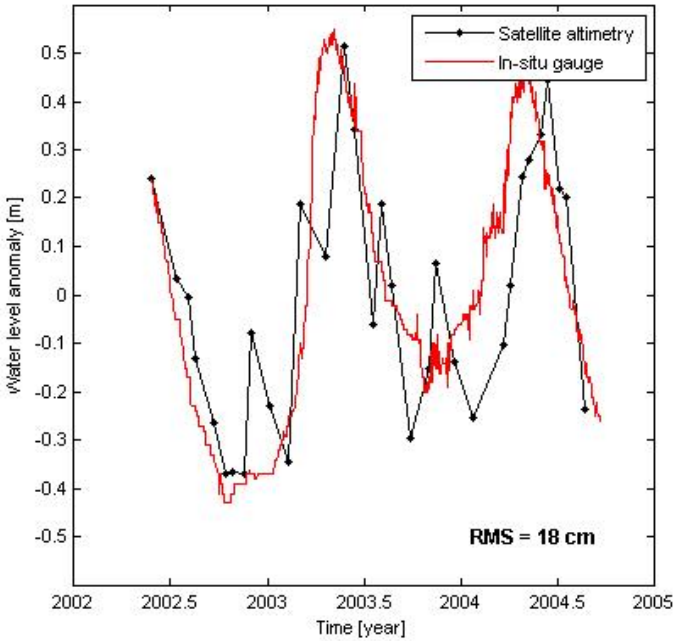

Figure 13: Validation of satellite derived water level against in-situ gauge water level time series

Comparison of GOCE-GPS hl-SST static gravity fields derived by different kinematic orbit analysis approaches

Several techniques have been proposed to exploit GPS-hl-SST (high-low satellite-to-satellite tracking) derived kinematic orbit information for the determination of long-wavelength gravity field features. These methods include the (i) energy balance approach, (ii) celestial mechanics approach, (iii) short-arc approach, (iv) point-wise acceleration approach, and (v) averaged acceleration approach. Although there is a general consensus that - except for energy balance - these methods theoretically provide equivalent results, real data gravity field solutions from kinematic orbit analysis have never been evaluated against each other within a consistent data processing environment. This research strives to close this gap. Within a joint project with the Space Research Institute of the Austrian Academy of Sciences GOCE gravity field estimates based on the aforementioned approaches have been compared. The individual solutions have been computed at the Institute of Navigation and Satellite Geodesy (energy balance approach, EBA) and the Institute of Theoretical Geodesy and Satellite Geodesy (short-arc approach, SAA) of Graz University of Technology, the Astronomical Institute of the University of Bern (celestial mechanics approach, CMA), the Department of Remote Sensing and Geoscience of the Delft University of Technology (averaged acceleration approach, AAA), and the Institute of Geodesy of the Univer-

sity of Stuttgart (point wise acceleration approach, PAA). Consistency concerns the input data sets, period of investigation, spherical harmonic resolution, a priori gravity field information and background models. The performance measures include formal errors, differences with respect to a state-of-the-art GRACE gravity field, (cumulative) geoid height differences, and SLR residuals from precise orbit determination of geodetic satellites (here: LAGEOS-1, Starlette). From the investigations (e.g. degree-RMS in Figure 14) it is concluded that real data analysis results are in agreement with the theoretical considerations concerning the (relative) performance of the different approaches: (i) the energy balance approach performs worse by approximately a factor of $\sqrt{3}$ and (ii) the other approaches perform similar. It was found that it is important (i) to consider the provided orbit covariances in the stochastic model, (ii) to account for the residual air-drag by common-mode accelerations as observed by the gradiometer (accelerometer) in the very low orbit height of GOCE and (iii) to exploit the full 1s-sampled GOCE kinematic orbit set.

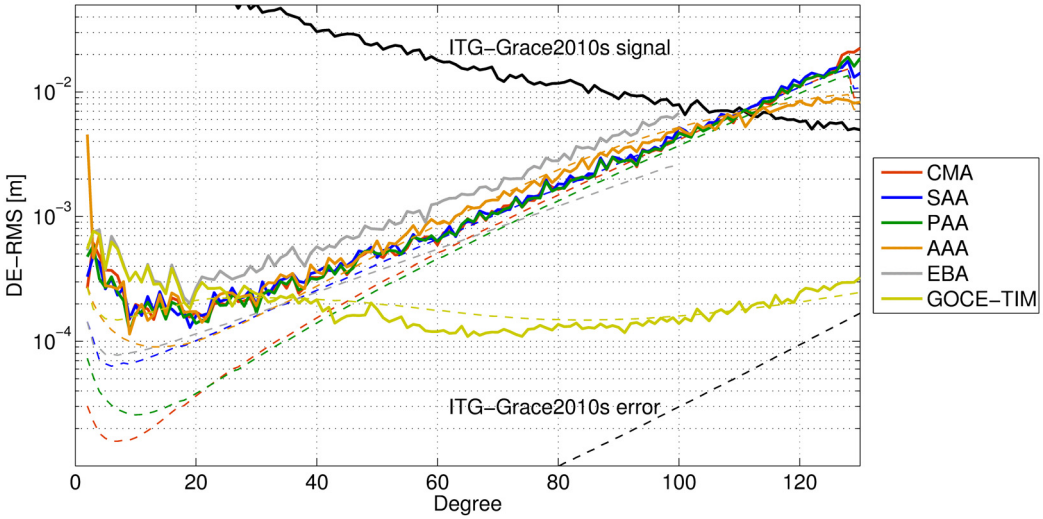

Figure 14: Results for the GOCE-R1 period. Black solid graph: ITG-Grace2010s signal; solid color graphs: DE-RMS of recovered spherical harmonic coefficients w.r.t. ITG-Grace2010s; dashed graphs: formal errors; near-zonal coefficients affected by the polar gap are omitted.

Comparison of mass trend and annual amplitude estimates from different time variable GOCE-GPS hl-SST gravity field recoveries

Recently it has been demonstrated from real data analysis of CHAMP that the detection of annual gravity signals and gravity trends from hl-SST (high-low satellite-to-satellite tracking) is possible for long-wavelength features, although the accuracy of a low-low SST mission like GRACE cannot be reached. This demonstrates the capability of hl-SST based time variable gravity recovery from ESA's magnetic field mission Swarm for bridging a possible gap between GRACE

and GRACE-FO. As a continuation of the comparison of static GOCE-SST solutions, a comparison campaign for time variable GOCE-SST gravity field solutions from different research groups was established. The aim was the evaluation of the different orbit processing algorithms, different gravity recovery procedures and dedicated post-processing strategies which have been adopted, as a second aim the results from CHAMP should be confirmed and third it was of interest if a higher spatial resolution can be reached due to the much lower GOCE orbit. The investigated time-variable solutions comprise (i) monthly gravity fields produced by the Institute of Geodesy of the University of Stuttgart (GIS) using the GOCE standard kinematic orbit product, the acceleration approach and polar gap regularization (REG), (ii) 20-day solution from the Department of Astronomics and Space Mission (DEOS) of the Delft University of Technology using a simple standard dynamic approach but accounting for daily variations by means of the Wiese approach and using the GOCE orbit subcycle (20 days) as recovery period and (iii) monthly GOCE and GRACE (and the combined result) hl-SST solutions generated by the Theoretical Geodesy and Satellite Geodesy (ITSG) of Graz University of Technology using a sophistic orbit determination method with improved ionosphere modeling and the short arc approach. The different solutions have been evaluated by the Space Research Institute of the Austrian Academy of Sciences by means of trend and annual amplitude estimates for important basins, as displayed in Figure 15. The results show that (i) a sophisticated orbit determination approach with advanced ionosphere modeling together with careful stochastic modeling within the gravity recovery approach is of great benefit, (ii) the quality of CHAMP is not completely met, probably because problems involved with the inclined sun synchronous orbit and (iii) the combination of measurements from several satellites, here GRACE and GOCE, leads to big improvements (which demonstrates the potential of Swarm for gap-bridging).

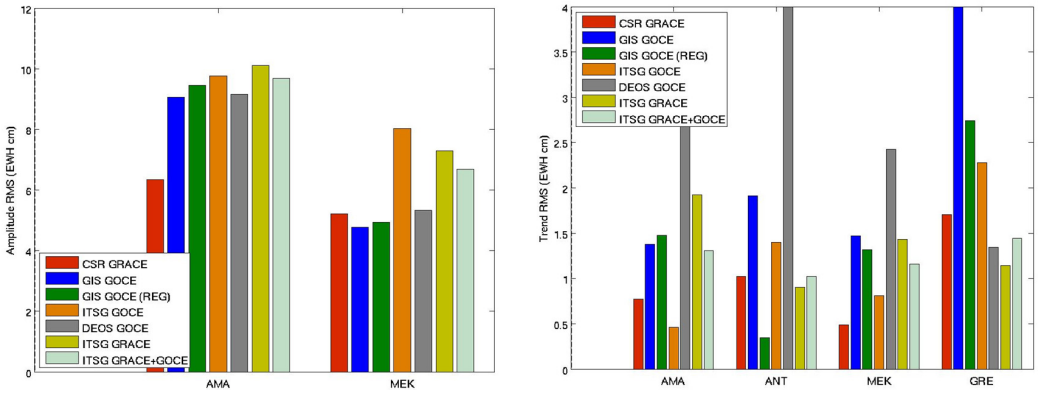

Figure 15: Estimates of annual amplitudes (left) and mass trends (right) for important basins from various time variable GOCE-GPS hl-SST gravity field recoveries (Gaussian smoothing of R = 1500 km applied) in comparison to CSR GRACE ll-SST solution; basins: Greenland (GRE), Amazonas (AMA), Mekong (MEK), Antarctica (ANT)

Investigations on the capability of Swarm as a gap-filling mission for estimating time-variable gravity fields and mass variations

Recently, the implementation of the GRACE Follow-On mission has been approved. However, this successor of GRACE is planned to become operational in 2017 at the earliest. In order to fill a potential gap of 3-4 years between GRACE and GRACE-FO, the capability of the magnetic field mission Swarm, which was launched in November 2013, as a gap filler for time-variable gravity field determination has to be investigated. Since the three Swarm satellites, two of which fly on a pendulum formation, are equipped with high-quality GPS receivers and accelerometers, orbit analysis from high-low Satellite-to-Satellite Tracking (hl-SST) can be applied for geopotential recovery. As data analysis from CHAMP and GRACE has shown, the detection of annual gravity signals and gravity trends from hl-SST is possible for long-wavelength features corresponding to a Gaussian radius of 1000 km, although the accuracy of a low-low SST mission like GRACE cannot be reached. However, since Swarm is a three-satellite constellation and might provide GPS data of higher quality compared to previous missions, improved gravity field recovery can be expected.

One of the most important scientific results of GRACE is the estimation of mass trends such as the ice mass loss on Greenland or water accumulation in the Amazon Basin. The potential of Swarm for the continuation of such mass trend time series is investigated. By means of reduced-scale simulations using the acceleration approach and taking into account time-variable background models of atmosphere, ocean, hydrology, ice, solid Earth and ocean tides as well as measurement noise a first simulation cycle based on monthly solutions (up to degree 60) was investigated.

In order to improve the data quality and extract the time variable signals, a Kalman-based filter approach is employed. The prediction model is derived directly from the time series of each coefficient separately and consists of the mean, a trend and a sine/cosine function with the main frequency at 1 cycles per year. The Kalman-filtered time series show a clear improvement in both the temporal and spectral domain without smoothing the signals of interest significantly, although the effect on detected basin mass trends was quite negligible in the simulations.

In a second step, mass trends are estimated by ?tting a regression line together with annual/semi-annual signals to (residual) mass-variation time-series. Figure 16 displays the mass trends for smoothing radii of R = 1000 km. Although the spatial map of mass trends looks quite noisy compared to the input signals the major trend signals, e.g. Greenland are clearly visible. The trend estimates for such dominant basins with stable spatial patterns can be determined quite accurate (deviations within 10-30%) while for basins with smaller trend signals the spatial patterns appear unstable and the errors are much larger. The results show the possible capability of Swarm for long-wavelength time-variable gravity recovery and mass trend estimation for basins with large signals (this holds also for the estimation of annual amplitudes) and motivates further investigations.

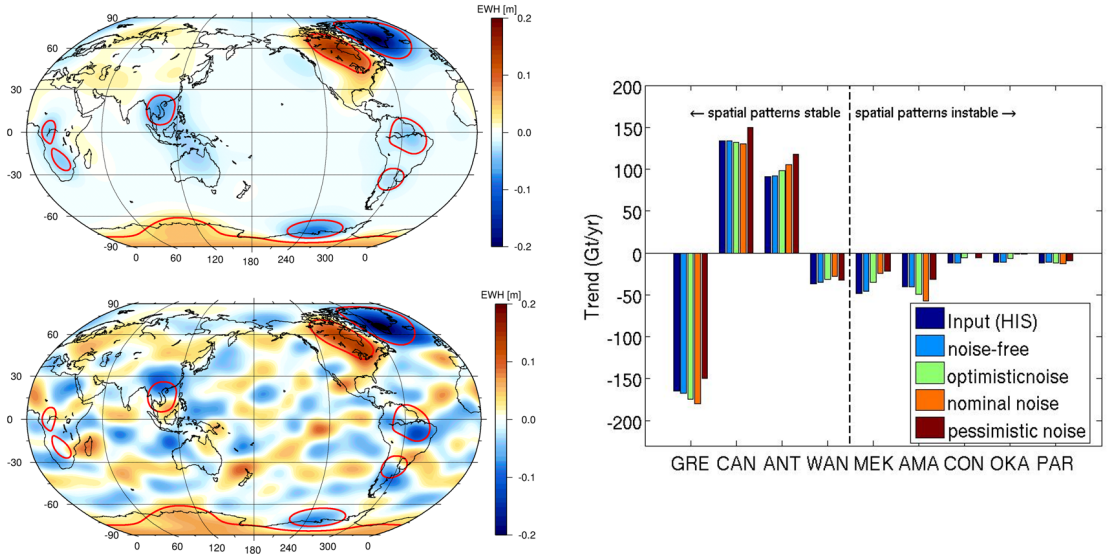

Figure 16: Mass trend estimates from simulated 5 years SWARM time series using Gaussian smoothing of R = 1000 km; top left: spatial map of trends from input models; bottom left: spatial map of estimated trends from simulated SWARM mission with pessimistic noise assumptions; right: estimated trends for major basins (different noise assumptions); basins: Greenland (GRE), Canada (CAN), Antarctica (ANT), West Antarctica (WAN), Mekong (MEK), Amazonas (AMA), Congo (CON), Okavango (OKA), Parana (PAR)

Influence of ground-track pattern distribution of double inline satellite pair missions on quality of the gravity solutions

The quality of recovery of time-variable gravity field is improved by employing two pairs of inline satellites. Iran Pour et al. (2013) showed that gravity solutions from two pairs of satellites significantly improve quality compared to the twice larger time-interval of the single pair scenarios with the same altitude. As an example, it has been shown that the 3-day gravity solutions of SH maximum degree 90 by two pair missions have quality improvement by approximately 5 times compared to the 6-day solutions of the single pair scenarios with the same altitude. That is indeed because of using an inclined satellite mission together with the near-polar mission where we simply add East-West measurement component to the North-South component of the near-polar satellite mission. It is also important to remember that 3-day gravity solutions also benefit from higher time resolutions compared to 6-day solutions. However, among the dual scenarios, it can be seen that the scenarios with slow ground-track gap evolution have the lowest quality. That is for example the scenario 2.5 of Table 1 (compared to the other scenarios of the table) where the repeat modes of the satellite pairs are drifting (β/α = 95/6) and slow skipping (β/α = 338/25) orbits.

That means the gap evolution of the ground-track affects the solutions' quality. The influence of the missions' altitudes on the quality of gravity solution, on the other hand, can be clearly seen for 3-day solutions of the first four scenarios of Table 1.

scenario	β/α [rev./day]	inclination [deg]	altitude [km]	error rms [mm]		
				3 d	6 d	32 d
1	503/32 503/32	89.5 72	333.8 305.0	0.8	0.4	0.2
2	125/8 503/32	89.5 72	360.7 305.0	0.9	0.4	0.2
3	503/32 125/8	89.5 72	333.8 332.1	1.1	0.4	0.2
4	125/8 125/8	89.5 72	360.7 332.1	1.2	0.4	0.2
5	95/6 338/25	89.5 72	301.3 362.9	1.3	0.7	0.3

Table 1: Global geoid height error rms for 3-day, 6-day and 32-day recoveries of different dual inline formation mission scenarios (L_{max} = 90)

The impact of ascending node angle difference of two pair mission scenarios ($\Delta\Omega$) has been investigated for the scenario 2.5 (Table 2). No significant influence of the different $\Delta\Omega$ has been seen for the long time-intervals solutions. However, for short-time gravity recovery of the sub-Nyquist solution (3-day recovery for SH maximum degree 90), one can see the effect of the ascending node angle difference, where $\Delta\Omega$ = 180° gives the smallest error. This means that for the short-time solutions, the ground-track pattern distribution gets more important.

ΔΩ [deg]	error [mm]		
	3 d	6 d	32 d
0	1.7	0.7	0.3
90	1.7	0.6	0.3
180	1.3	0.7	0.3

Table 2: Recovery errors of 3, 6 and 32-days of scenarios 5; Different $\Delta\Omega$ [deg]

Comparison of surface loading-induced deformations from GPS and GRACE

Mass transport and mass redistribution within the Earth system induce surface mass loading variation. Thus, it consequently leads to the surface deformation of the solid Earth.

The surface deformations can either be derived from GRACE through time-variable gravity field or be observed by IGS stations in 3D GPS coordinates. The surface deformations derived from GRACE are spatially smoothed with about 350 km spatial resolution. However, the deformations of IGS stations observed by GPS are discrete point measurements on the globe. Therefore, the consistency between the deformations from GRACE and GPS needs to be validated.

To investigate the level of agreement between GPS and GRACE, a number of IGS stations in three regions are selected (Tibetan plateau, Danube basin and Great Lakes area) with period of 8 years (2003-2011). The loading induced deformations occur primarily in vertical direction. As a result, the deformations in vertical direction from GRACE have quite consistent periodical patterns with ones from GPS as shown in Figure 17.

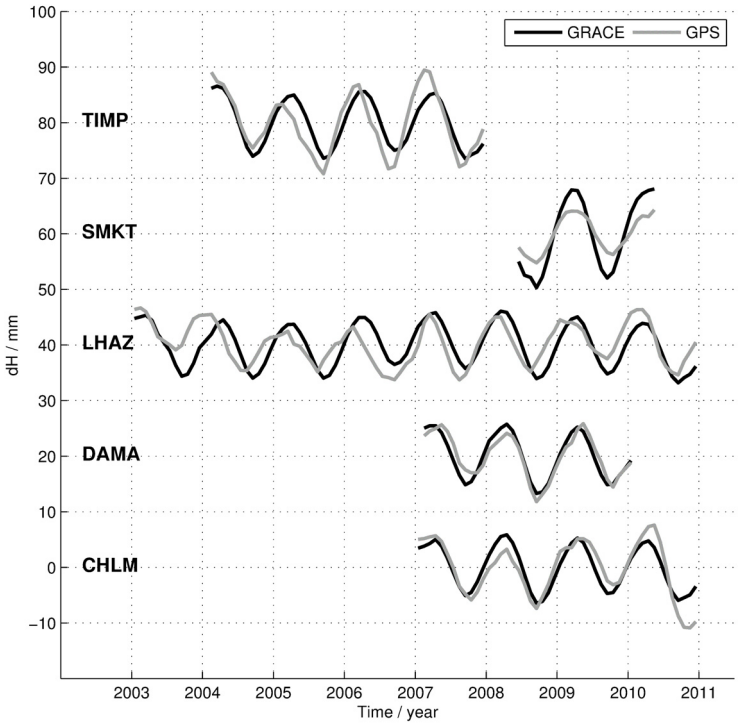

Figure 17: Comparisons of height displacements time series from GRACE and GPS of five IGS stations on Tibetan plateau

Many factors cause the disagreement between GPS and GRACE. The choice of optimal filter for GRACE solutions is among one of them. Isotropic Gaussian filter, anisotropic Gaussian filter, destriping filter and stochastic filter are compared to search for the best option. After investigation of the GPS sites located in Europe, we find that the destriping filter can significantly improve the consistencies. The optimum radius for the isotropic Gaussian filter combined with the destriping filter is around 350 km. For anisotropic Gaussian smoothing, there is no distinct difference with or without destriping filter. The optimum radius for the anisotropic Gaussian filter is around 300 km.

Compared with the deterministic filters, the stochastic filter does not show improvements over all the GPS sites located in Europe. However, the stochastic filter does provide higher spatial resolutions and performs better at GPS sites where significant mass variation happens, see Figure 18. This motivates us to do further comparison over other regions, e.g. Amazon and Greenland.

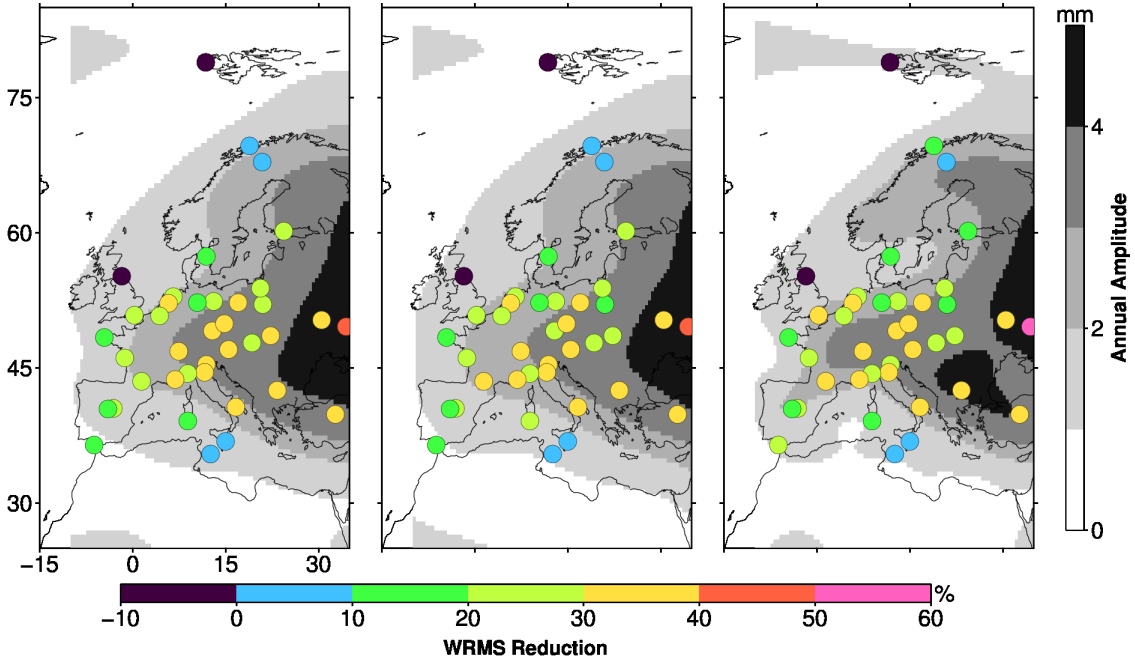

Figure 18: Background of each subplot illustrates grid amplitudes of annual height deformations from GRACE data filtered by the isotropic Gaussian filter of a radius at 350 km combining with the destriping filter IGD (left), the anisotropic Gaussian filter with a radius of 300 km (middle) and the stochastic filter (right), respectively. Circles indicate the weighted root mean squares (WRMS) reduction in the GPS signals after removing GRACE from GPS.

Modelling of the Earth's gravity field by boundary elements

The recovery of the Earth's gravity field is usually performed by spherical harmonics. This set of base functions is the natural choice for spherical bodies and has several advantages, but the resolution is limited by the sub area with the worst data distribution. In case of inhomogeneous data distribution (polar gaps and convergence of tracks in satellite observations), areas with different behavior of the field (e.g. ocean vs. land) or additional terrestrial data, the recovery of the gravity field is separated in two parts. The global behavior is determined via spherical harmonics and the effect of this smoothed field is removed from the signal. The residual signal is analyzed by localizing base functions like wavelets, radial basis functions or boundary elements, to recover the remaining structures.

In the concept of boundary elements, the residual field is assumed to be the result of a single layer on a reference figure, either the sphere or ellipsoid, or even the topography of the Earth. The residual potential of a single layer at position $\overline{x}$ is given by

$$T(\overline{\boldsymbol{x}}) = G \iint_S \frac{\sigma(\overline{\boldsymbol{y}})}{|\overline{\boldsymbol{x}} - \overline{\boldsymbol{y}}|} d\overline{\boldsymbol{y}},$$

where σ denotes the density and $\overline{y}$ the location in the layer (G: gravitational constant, S surface).

The single layer is subdivided into I simpler geometries s_i. Triangles are the most common patches, as they enable a flexible representation of any surface (Figure 19). Each triangle is defined by nodes located at the corners (k = 1,2,3), where the density values $\sigma_{i,k}$ are estimated in the adjustment. Then the single layer potential is approximated by

$$T(\overline{\boldsymbol{x}}) = G \sum_{i=1}^{I} \iint_{s_i} \frac{\sigma(\overline{\boldsymbol{y}})}{|\overline{\boldsymbol{x}} - \overline{\boldsymbol{y}}|} d\overline{\boldsymbol{y}},$$

where the density $\sigma(\overline{\mathbf{y}})$ is a linear interpolation of the density values $\sigma_{i,k}$ in the nodes into the interior of the element s_i.

In a first study, only the signal of the boundary elements themselves is considered. The simulation consists of 120 boundary elements in two distinct areas of the globe. The boundary elements form a network of almost 200 triangles with a mean lateral length of 480 km. The potential along the orbit is computed via a simplified energy balance approach (cf. Figure 20). Using the same triangles in the analysis, the residuals in the orbit are more than 12 orders of magnitudes smaller than the simulated signal (cf. Figure 21), whereas the approximation on ground still achieve 10 orders of magnitudes.

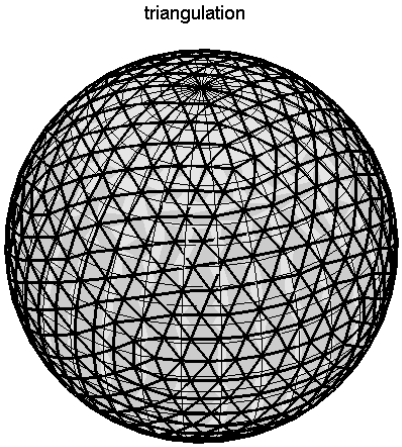

Figure 19: Triangulation of a sphere

The gravity field recovery from (simulated) potential values looks promising, but for real data the more accurate satellite observations - in particular relative range and rate-rates - has to be developed and implemented for the boundary element method. In addition, the adequate combination of spherical harmonics and the boundary elements and the combination of observation types require further investigations.

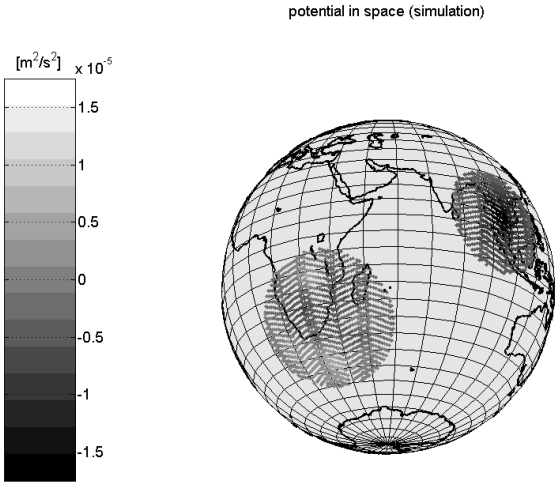

Figure 20: Potential in the orbit generated by 120 triangular boundary elements.

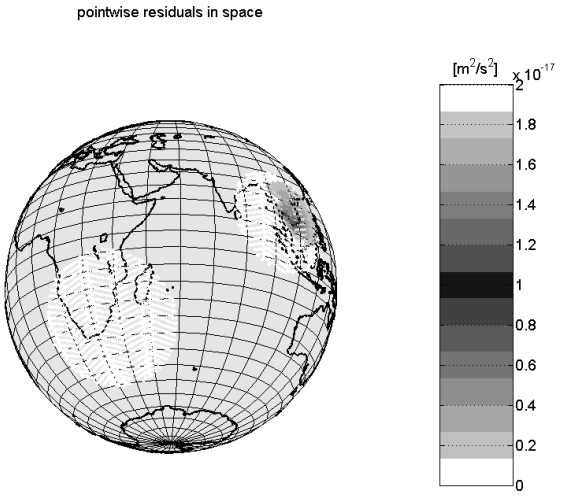

Figure 21: Point wise residuals in the orbit

Theses

Doctoral Theses

(http://www.uni-stuttgart.de/gi/research/dissertations.en.html)

IRAN POUR S: Sampling the Earth's Time-Variable Gravity Field from Satellite Orbit - Design of Future Gravity Satellite Missions

TOURIAN MJ: Application of spaceborne geodetic sensors for hydrology

Diploma/Master Theses

(http://www.uni-stuttgart.de/gi/education/dipl/diploma_theses.en.html)

CAO W: Change detection using SAR data

CHEN J: Precise positioning with low-cost GNSS receivers

REINHOLD A: Basislinienbestimmung mit GPS-Daten an Bord TerraSAR-X und TanDEM-X im Hinblick auf die Modellierung der Bahnmanöver (Baseline determination with GPS data on board TerraSAR-X and TanDEM-X with respect to maneuver modeling)

ZHANG Y: Coherency Analysis between SGs at BFO and Strasbourg

Bachelor Theses

(http://www.uni-stuttgart.de/gi/education/dipl/study_reports.en.html)

MAYER V: CryoSat-2 for hydrological purposes: Data processing, visualization and analysis
THOR R: Least-squares prediction of runoff

Awards

TOURIAN MJ: Winner of Outstanding Student Paper Award in AGU fall meeting 2013

Publications

(http://www.uni-stuttgart.de/gi/research/index.en.html)

Refereed Journal Publications

ANTONI M AND W KELLER: Closed solution of the Hill differential equation for short arcs and a local mass anomaly in the central body. Celestial Mechanics and Dynamical Astronomy 115, pp 107-121, DOI: 10.1007/s10569-012-9454-7

CHEN Q, T VAN DAM, N SNEEUW, X COLLILIEUX, M WEIGELT AND P REBISCHUNG: Singular spectrum analysis for modeling seasonal signals from GPS time series. Journal of Geodynamics 72, pp 25-35, DOI: 10.1016/j.jog.2013.05.005

IRAN POUR S, T REUBELT AND N SNEEUW: Quality assessment of sub-Nyquist recovery from future gravity satellite missions. Journal of Advances in Space Research 52, pp 916-929, DOI:10.1016/j.asr.2013.05.026

KRAWINKEL T, D HÜCKER, C SCHIKSCHNEIT, K BEERMANN, J FLURY, S VEY, M ANTONI AND U FELDMANN-WESTENDORFF: Sub-cm-Konsistenz von nivellierten Normalhöhen, GNSS-Positionen und Quasigeoid im Testgebiet Harz. Zeitschrift für Geodäsie, Geoinformation und Landmanagement 138, pp 201-209

NAJIBI N, A ABEDINI AND H NAJIBI: Analysis of Sea Ice Leads in Baffin Island Sea Using Spaced Based Infrared Remote Sensing Data and Mathematical Hydrological Models. International Journal of Geosciences Research 1, pp 1-11

NAJIBI N, A ABEDINI AND RA SHEIBANI: Harmonic Decomposition Tidal Analysis and Prediction Based on Astronomical Arguments and Nodal Corrections in Persian Gulf, Iran. Research Journal of Environmental and Earth Sciences 5, pp 381-392

SAHAMI SHIRAZI A, J CLAWSON, Y HASSANPOUR, MJ TOURIAN, A SCHMIDT, EH CHI, M BORAZIO AND K VAN LAERHOVEN: Already Up? Using Mobile Phones to Track and Share Sleep Behavior. International Journal of Human-Computer Studies 71, pp 878-888, DOI: 10.1016/j.ijhcs.2013.03.001

TOURIAN MJ, N SNEEUW and A BÁRDOSSY: A quantile function approach to discharge estimation from satellite altimetry (ENVISAT). Water Resources Research 49, pp 1-13, DOI: 10.1002/wrcr.20348

VISHWAKARAMA BD, K JAIN, N SNEEUW AND B DEVARAJU: Mumbai 2005, Bihar 2008 Flood Reflected in Mass Changes Seen by GRACE Satellites. Journal of the Indian Society of Remote Sensing 41, pp 687-695, DOI: 10.1007/s12524-012-0256-x

WEIGELT M, N SNEEUW, EJO SCHRAMA AND PNAM VISSER: An improved sampling rule for mapping geopotential functions of a planet from a near polar orbit. Journal of Geodesy 87, pp 127-142, DOI: 10.1007/s00190-012-0585-0

WEIGELT M, T VAN DAM, A JÄGGI, L PRANGE, W KELLER AND N SNEEUW: Time-variable gravity signal in Greenland revealed by high-low satellite-to-satellite tracking. Journal of Geophysical Research: Solid Earth 118, pp 3848-3859, DOI: 10.1002/jgrb.50283

Other Refereed Contributions

ROTH M, N SNEEUW and W KELLER: Euler Deconvolution of GOCE Gravity Gradiometry Data. In: Nagel W, D Kröner and M Resch (Eds.): High Performance Computing in Science and Engineering ’12, Springer-Verlag Berlin Heidelberg, pp 503-515, DOI: 10.1007/978-3-642-33374-3_36

Non-refereed Contributions

SNEEUW N, B DEVARAJU AND MJ TOURIAN: Die Vermessung der Welt aus dem All. Themenheft Forschung 9, Universität Stuttgart, 56-63

Poster presentations

ANTONI M, M WEIGELT, W KELLER AND T VAN DAM: Boundary elements for modelling gravitational signals observed by inter-satellite ranging. IAG Scientific Assembly, Potsdam, Germany (1.-6.9.)

BAUR O, H BOCK, P DITMAR, H HASHEMI FARAHANI, A JÄGGI, T MAYER-GÜRR, T REUBELT AND N ZEHENTNER: Comparison of GOCE-GPS gravity fields derived by different approaches. EGU General Assembly, Vienna, Austria (7.-12.4.)

BAUR O AND T REUBELT: Mass Change Detection from Swarm Time-Variable Gravity. Dragon III Symposium, Palermo, Italy (3.-7.6.)

CHEN Q, J ZHANG, B DEVARAJU AND N SNEEUW: Seasonal loading deformation from GPS and GRACE observations on the Tibetan Plateau. Dragon III Symposium, Palermo, Italy (3.-7.6.)

CHEN Q, J ZHANG, L WANG, T VAN DAM, M WEIGELT, B DEVARAJU AND N SNEEUW: Comparison of seasonal hydrological loading information from GPS and GRACE observations. IAG Scientific Assembly, Potsdam, Germany (1.-6.9.)

ELMI O, MJ TOURIAN and N SNEEUW: Monitoring of the hydrological cycle using remote sensing approaches. ESA Advanced Training Course in Land Remote Sensing, Athens, Greece

GRUBER TH, R PAIL, M MURBÖCK, N SNEEUW, T REUBELT, S IRAN POUR, J MÜLLER, J FLURY, P BRIEDEN, M NAEMI, K DANZMANN, G HEINZEL, B SHEARD, V MÜLLER, J KUSCHE, A LÖCHER, D FEILI, F FLECHTNER, JC RAIMONDO, B DOLL, X WANG AND M LANGEMANN: Next Generation Satellite Gravimetry Mission Study (NGGM-D). AGU Fall Meeting, San Francisco, USA (9.-13.12.)

IRAN POUR S, T REUBELT, M ELLMER AND N SNEEUW: Influence of Ground-Track Pattern Distribution of Double Inline Satellite Pair on Quality of the Gravity Solutions. ESA Living Planet Symposium, Edinburgh, UK (9.-13.9.)

MURBÖCK M, R PAIL, T REUBELT, N SNEEUW, T GRUBER AND I DARAS: On Reducing Temporal Aliasing with Multi-Satellite Formations. ESA Living Planet Symposium, Edinburgh, UK (9.-13.9.)

REUBELT T, O BAUR, M WEIGELT AND N SNEEUW: On the capability of SWARM for estimating time-variable gravity fields and mass variations. EGU General Assembly, Vienna, Austria (7.-12.4.)

ROOHI S and N SNEEUW: Analysis of sampling behavior of candidate SWOT satellite orbits. ESA Living Planet Symposium, Edinburgh, UK (9.-13.9.)

SHARIFI MA, N SNEEUW and K GHOBADI: Analysis of GOCE data based on the Rosborough method. Hotine-Marussi Symposium, Rome, Italy (17.-21.6.)

TOURIAN MJ, O ELMI AND N SNEEUW: A multi-sensor approach to monitor the desiccation of Lake Urmia in Iran. EGU General Assembly, Vienna, Austria (7.-12.4.)

VARGA P, FW KRUMM, EW GRAFAREND, N SNEEUW, F HORVATH AND AA SCHREIDER: Axial rotation and paleogeodynamics during Phaneorozoic. IAG Scientific Assembly, Potsdam, Germany (1.-6.9.)

WEIGELT M, T VAN DAM, A JÄGGI, L PRANGE, N SNEEUW AND W KELLER: Long-term mass changes over Greenland derived from high-low satellite-to-satellite tracking. EGU General Assembly, Vienna, Austria (7.-12.4.)

WU G, O ELMI, MJ TOURIAN AND N SNEEUW: Combined Measurements of Lake Level and Surface Extent Change. ESA Living Planet Symposium, Edinburgh, UK (9.-13.9.)

WU G, O ELMI, MJ TOURIAN AND N SNEEUW: Combined Measurement of Lake Levels and Surface Extent Change in the Yangtze River Basin. Dragon III Symposium, Palermo, Italy (3.-7.6.)

YE Z, N SNEEUW and L LIU: Computation of topographic and isostatic effect on GOCE in the frequency domain. IAG Scientific Assembly, Potsdam, Germany (1.-6.9.)

ZHANG Y, R WIDMER-SCHNIDRIG and N SNEEUW: Can SGs be used to validate GRACE Gravity Field Models ? - Coherency Analysis between SGs at BFO and Strasbourg. IAG Scientific Assembly, Potsdam, Germany (1.-6.9.)

Conference presentations

BAUR O, T REUBELT AND M WEIGELT: Bridging the gap between GRACE and GRACE follow-on: the potential of SWARM and SLR to detect time-variable gravity. ESA Living Planet Symposium, Edinburgh, UK (9.-13.9.)

CHEN Q, M WEIGELT, N SNEEUW AND T VAN DAM: On time-variable seasonal signals: comparison of SSA and Kalman filtering based approaches. Hotine-Marussi Symposium, Rome, Italy (17.-21.6.)

DAVOODIANIDALIKI M, A ABEDINI AND M SHANKAYI: Adaptive Edge Detection using Adjusted Ant Colony Optimization. International Archives of the Photogrammetry, Remote Sensing and Spatial Information Sciences, Volume XL-1/W3, 2013. SMPR 2013, Tehran, Iran (5.-8.10.)

DEVARAJU B and N SNEEUW: On the spatial resolution of filters on the sphere. Hotine-Marussi Symposium, Rome, Italy (17.-21.6.)

ELMI O, MJ TOURIAN AND N SNEEUW: A comparison between remote sensing approaches to water extent monitoring. EGU General Assembly, Vienna, Austria (7.-12.4.)

ELSAKA B, JC RAIMONDO, P BRIEDEN, T REUBELT, J KUSCHE, F FLECHTNER, N SNEEUW AND J MÜLLER: Full-scale numerical simulation scenarios using three-month observations of possible future satellite-gravimetric missions. Hotine-Marussi Symposium, Rome, Italy (17.-21.6.)

GRAFAREND E: Das duale Paar Moritz-Molodenskij: Geodätische Höhen und Höhensysteme. 80 Jahre Helmut Moritz, Leibniz-Sozietät der Wissenschaften, Berlin (15.11.)

GRAFAREND E: Space Gradiometry on the International Reference Ellipsoid. Hotine-Marussi Symposium, Rome, Italy (17.-21.6.)

GRAFAREND E: The Geometry of Kepler orbit/ perturbed Kepler orbit in Maupertuis Manifolds by minimizing the scalar of the Riemann Curvature Tensor, aspects of the Kustaanheimo-Stiefel elements in Satellite Geodesy. EGU General Assembly, Vienna, Austria (7.-12.4.)

GRIBOVSZKI K, G BOKELMANN, G SZEIDOVITZ, P VARGA, I PASKALEVA, L BRIMICH AND K KOVÁCS: Comprehensive investigation of intact, vulnerable stalagmites standing in Hungarian, Bulgarian, Slovakian and Austrian caves in order to estimate of an upper limit on prehistoric peak ground horizontal acceleration. Vienna Congress on Recent Advances in Earthquake Engineering and Structural Dynamics and 13. D-A-CH Tagung

GRIBOVSZKI K, L BRIMICH, P VARGA, K KOVÁCS, CC SHEN, S KELE, Á TÖRÖK AND A NOVÁK: Estimation of an upper limit on prehistoric horizontal peak ground acceleration using the parameters of intact stalagmites and the mechanical properties of broken stalagmites in Domica cave, Slovakia. Geophysical Research Abstracts 15, EGU2013-11541, 2013, EGU General Assembly, Vienna, Austria (7.-12.4.)

IRAN POUR S, T REUBELT AND N SNEEUW: Searching for the optimal dual pair gravity satellite missions. Geodätische Woche Essen (8.-10.10.)

KRUMM FW, G MENES AND P VARGA: Tidal friction and despinning of axial rotation of the Earth. Session VI: Tides and earth reology. Earth Tide Symposium, Warsaw, Poland (15.-19.4.)

LORENZ C, H KUNSTMANN, B DEVARAJU AND N SNEEUW: Assimilation of GRACE and hydro-meteorological information for improving large-scale total water storage changes. EGU General Assembly, Vienna, Austria (7.-12.4.)

MEYER U, A JÄGGI, H BOCK, G BEUTLER, C DAHLE and N SNEEUW: Orbit and gravity field: common versus sequential analysis. Hotine-Marussi Symposium, Rome, Italy (17.-21.6.)

REUBELT T, O BAUR, M WEIGELT, T MAYER-GÜRR, N SNEEUW, T VAN DAM AND MJ TOURIAN: On the capability of non-dedicated GPS-tracked satellite constellations for estimating mass variations: case study Swarm. IAG Scientific Assembly, Potsdam, Germany (1.-6.9.)

RIEGGER J AND MJ TOURIAN: Characterization of Runoff- Storage Relationships by Satellite-Gravimetry and Remote Sensing. EGU General Assembly, Vienna, Austria (7.-12.4.)

ROOHI S and N SNEEUW: Lake level variations from satellite radar altimetry with retracking of multi-leading edge. Geodätische Woche Essen (8.-10.10.)

ROOHI S and N SNEEUW: Monitoring drying up of Urmia lake with satellite altimetry. EGU General Assembly, Vienna, Austria (7.-12.4.)

SHARIFI MA, N SNEEUW, MR SEIF AND S FARZANEH: A semi-analytical formulation of the Earth's flattening on the satellite formation flying observables using the Lagrange coefficients. Hotine-Marussi Symposium, Rome, Italy (17.-21.6.)

SNEEUW N: Rosborough representation in satellite gravimetry. Hotine-Marussi Symposium, Rome, Italy (17.-21.6.)

SNEEUW N, R THOR AND MJ TOURIAN: River discharge from ungauged catchments by least-squares prediction. Geodätische Woche Essen (8.-10.10.)

THOR R, MJ TOURIAN AND N SNEEUW: Least squares prediction of discharge over ungauged basins. IAG Scientific Assembly, Potsdam, Germany (1.-6.9.)

TOURIAN MJ, C LORENZ, B DEVARAJU, J RIEGGER, H KUNSTMANN AND N SNEEUW: Estimating runoff using hydro-geodetic approaches; assessment and comparison. AGU Fall Meeting, San Francisco, USA (9.-13.12.)

TOURIAN MJ, R THOR, J RIEGGER AND N SNEEUW: Runoff estimation using satellite altimetry, GRACE and least squares prediction. Geodätische Woche Essen (8.-10.10.)

VAN DAM T, MJ TOURIAN, M WEIGELT, N SNEEUW, A JÄGGI AND L PRANGE: Hydrological mass changes inferred from high-low satellite-to-satellite tracking data. EGU General Assembly, Vienna, Austria (7.-12.4.)

VARGA P, FW KRUMM, EW GRAFAREND, N SNEEUW, F HORVATH AND AA SCHREIDER: Axial rotation and paleogeodynamics during Phaneorozoic. IAG Scientific Assembly, Potsdam, Germany (1.-6.9.), Theme 4, p 434

WANG L, T VAN DAM, M WEIGELT, Q CHEN, MJ TOURIAN AND N SNEEUW: An inversion approach for determining water storage change from 3-D GPS coordinates time series in Europe. IAG Scientific Assembly, Potsdam, Germany (1.-6.9.)

WEIGELT M, T VAN DAM, T BANDIKOVA, J FLURY AND N SNEEUW: A variant of the differential gravimetry approach for low-low satellite-to-satellite tracking based on angular velocities. IAG Scientific Assembly, Potsdam, Germany (1.-6.9.)

WU G, O ELMI, MJ TOURIAN AND N SNEEUW: Combined Measurements of Lake Levels and Surface Extent Change. Geodätische Woche Essen (8.-10.10.)

XU X, T REUBELT, O BAUR, X ZOU AND H WEI: A GOCE only gravity model from space-wise observables along the orbit based on the least-square method. IAG Scientific Assembly, Potsdam, Germany (1.-6.9.)

Books and Miscellaneous

FLECHTNER F, N SNEEUW AND W-D SCHUH (EDS.): Observation of the System Earth from Space - CHAMP, GRACE, GOCE and Future Missions. Geotechnologien Science Report No. 20, Springer Heidelberg New York

ROTH M: GOCEXML2ASCII - an XML to ASCII converter for GOCE level 2 EGG_NOM and SST_PSO data

Guest Lectures and Lectures on special occasions

KLUMPP K-H (Kretz + Klumpp Ingenieurgesellschaft mbH Pfinztal): Bahnprojekt Stuttgart 21 / Wendlingen-Ulm: Eine besondere Herausforderung an die Ingenieurvermessung (8.2.)

MOTAGH, M (Dept. of Geodesy and Remote Sensing, GFZ Potsdam): Emerging applications of InSAR Geodesy for geodynamics and engineering studies (11.7.)

TENZER, R (School of Geodesy and Geomatics, Wuhan University, China): Gravimetric forward and inverse modeling of crust structure in a frequency domain (16.7.)

TENZER, R (School of Geodesy and Geomatics, Wuhan University, China): Analysis of sea variations offshore New Zealand (16.7.)

Lectures at other universities

GRAFAREND E
System Dynamics of Polar Motion and Length-of-Day Variation, National Geodetic Research Institute, Masala, Helsinki (23.8.)
Satellite Gradiometry on the International Reference Ellipsoid, Université Paris 8, Diderot, Laboratoire LAREG, Paris, France (12.4.)

Research Stays

GRAFAREND E:
Finnish Geodetic Institute, Masala/Helsinki, Finland (13.8.-3.9.)

Lecture Notes

(http://www.uni-stuttgart.de/gi/education/MSC/lecturenotes.en.html
http://www.uni-stuttgart.de/gi/education/BSC/lecturenotes.en.html
http://www.uni-stuttgart.de/gi/geoengine/lecturenotes.html)

GRAFAREND E AND F KRUMM
Kartenprojektionen (Map Projections), 238 pages

KELLER W
Dynamic Satellite Geodesy, 90 pages Foundations of Satellite Geodesy, 51 pages Observation Techniques in Satellite Geodesy, 50 pages

KRUMM F AND SNEEUW N
Adjustment Theory, 155 pages

KRUMM F
Adjustment Theory, 104 pages
Map Projections and Geodetic Coordinate Systems, 177 pages
Mathematical Geodesy, 165 pages
Reference Systems, 174 pages

SNEEUW N
Dynamic Satellite Geodesy (draft), 90 pages
Introduction to Geodesy and Geodynamics, Part Geodesy, 31 pages
History of Geodesy, 38 pages
Physical Geodesy, 137 pages

SNEEUW N AND WEIGELT M
Analytic Orbit Computation of Artificial Satellites, a historical introduction, 36 pages

WOLF D
Continuum Mechanics in Geophysics and Geodesy: Fundamental Principles, 100 pages

Participation in Conferences, Meetings and Workshops

ANTONI M
- IAG Scientific Assembly, Potsdam, Germany (1.-6.9.)

GRAFAREND E
- European Geosciences Union (EGU), General Assembly 2013, Vienna, Austria (7.-12.4.)
- VIII. Hotine-Marussi Symposium 2013, Rom, Italy (17.-21.6.)
- 80 Jahre Helmut Moritz, Leibniz Societät der Wissenschaften, Berlin (15.11.)

REUBELT T
- EGU General Assembly, Vienna, Austria (7.-12.4.)
- IAG Scientific Assembly, Potsdam, Germany (1.-6.9.)

ROOHI S
- European Geosciences Union (EGU), General Assembly 2013, Vienna, Austria (7.-12.4.)
- Geodetic Week, Essen, Germany (8.-10.10.)

SCHLESINGER R
- Erfahrungsaustausch der Anwender des Relativgravimeters Scintrex CG-5, Landesamt für Vermessung und Geoinformation Rheinland-Pfalz, Koblenz (19.-20.2.)

SNEEUW N
- European Geosciences Union (EGU), General Assembly 2013, Vienna, Austria (7.-12.4.)
- Dragon 3 - 2013 Palermo Symposium / ESA Cooperation Programme, Palermo, Italy (3.-7.6.)
- VIII. Hotine-Marussi Symposium 2013, Rom, Italy (17.-21.6.)
- IAG Scientific Assembly, Potsdam, Germany (1.-6.9.)
- Geodetic Week, Essen, Germany (8.-10.10.)

TOURIAN M
- CryoSat Third User Workshop, Dresden, Germany (12.-14.3.)
- European Geosciences Union (EGU), General Assembly 2013, Vienna, Austria (7.-12.4.)
- Geodetic Week, Essen, Germany (8.-10.10.)

University Service

Grafarend E
- Member Faculty of Aerospace Engineering and Geodesy
- Member Faculty of Civil- and Environmental Engineering
- Member Faculty of Mathematics and Physics

KELLER W
- Associated Dean (Academic)

ROTH M
- Member of the PR-committee Geodesy and Geoinformatics

SNEEUW N
- Search Committee Satellitentechnik
- Stand-by Member Senate Committee for Structural Development and Research, Stuttgart

Professional Service (National)

GRAFAREND E
- Emeritus Member German Geodetic Commission (DGK)

SNEEUW N
- Full Member Deutsche Geodätische Kommission (DGK)
- Chair DGK section „Erdmessung“
- Member Scientific Board of DGK
- Member Scientific Advisory Committee of DGFI
- Chair AK7 (Working Group 7), „Experimentelle, Angewandte und Theoretische Geodäsie“, within DVW (Gesellschaft für Geodäsie, GeoInformation und LandManagement)
- Search Committee Geodätische Erdsystemforschung, TU Dresden

Professional Service (International)

GRAFAREND E
- Elected Member of the Finnish Academy of Sciences and Letters, Finland
- Elected Member of the Hungarian Academy of Sciences, Hungary
- Member Royal Astronomical Society, Great Britain
- Corresponding Member Österreichische Geodätische Kommission (ÖGK)
- Member Flat Earth Society
- Elected Member Leibniz-Sozietät, Berlin
- Fellow International Association of Geodesy (IAG)

SNEEUW N
- Member Editorial Board of Studia Geophysica et Geodaetica
- Member Editorial Board of Journal of Geodesy and Geoinformation
- President IAG InterCommission Committee on Theory (ICCT)
- Member of IAG GGOS Working Group Satellite Missions
- Fellow International Association of Geodesy (IAG)

Courses - Lecture/Lab/Seminar

Advanced Mathematics (Keller, Antoni, Roth)	3/2/0
Aktuelle Geodätische Satellitenmissionen (Sneeuw, Antoni)	2/2/0
Amtliche Geoinformation (Heß)	2/0/0
Amtliches Vermessungswesen und Liegenschaftskataster (Steudle)	2/0/0
Ausgewählte Kapitel der Parameterschätzung (Krumm)	2/2/0

Ausgleichungsrechnung I (Krumm, Roth)	1/1/0
Dynamische Erdmodelle (Engels)	1/1/0
Dynamische Satellitengeodäsie (Keller, Sneeuw, Tourian)	1/0.5/0
Einführung Geodäsie und Geoinformatik (Sneeuw)	0.5/0.5/0
Fernerkundung in der Hydrologie und Wasserwirtschaft (Tourian)	0.5/0.5/0
Grundstücksbewertung (Bolenz)	1/0/0
Integrated Field Work Geodesy and Geoinformatics (Keller, Sneeuw et al.)	10 days
Koordinaten- und Zeitsysteme in der Geodäsie, Luft- und Raumfahrt (Sneeuw)	2/0/0
Landesvermessung (Krumm, Roth)	2/2/0
Map Projections and Geodetic Coordinate Systems (Krumm, Roth)	4/2/0
Physical Geodesy (Sneeuw, Reubelt)	2/1/0
Physikalische Geodäsie (B.Sc.) (Sneeuw, Reubelt)	2/2/0
Physikalische Geodäsie (M.Sc.) (Engels, Reubelt)	2/2/0
Referenzsysteme (Krumm)	2/2/0
Satellite Geodesy (Keller)	2/1/0
Satellite Geodesy Observation Techniques (Antoni)	1/1/0
Satellitengeodäsie (B.Sc.) (Sneeuw, Reubelt)	1/1/0
Satellitengeodäsie (M.Sc.) (Keller, Sneeuw, Tourian)	2/0.5/0
Schwerefeldmodellierung (Keller)	2/2/0
Statistical Inference (Krumm, Roth)	2/1/0
Wertermittlung (Bolenz)	2/0/0

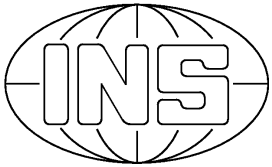

Institute of Navigation

Breitscheidstrasse 2, D-70174 Stuttgart,
Tel.: +49 711 685 83400, Fax: +49 711 685 82755
e-mail: ins@nav.uni-stuttgart.de
homepage: http://www.nav.uni-stuttgart.de

Head of Institute

Prof. Dr.-Ing. A. K l e u s b e r g

Deputy: Dr.-Ing. Aloysius W e h r
Secretary: Helga M e h r b r o d t

Staff

Dipl.-Ing. Doris B e c k e r	Navigation Systems
Dipl.-Ing. Michael G ä b	Navigation Systems
Dipl.-Geogr. Thomas G a u g e r	GIS Modelling and Mapping
Dipl.-Ing. René P a s t e r n a k	Remote Sensing
Dipl.-Ing. Bernhardt S c h ä f e r	Navigation Systems
M. Sc. Hendy S u h a n d r i	Navigation Systems
Dipl.-Ing. (FH) Martin T h o m a s	Laser Systems
Dr.-Ing. Aloysius W e h r	Laser Systems
Dr. Ing. Franziska W i l d - P f e i f f e r	Navigation Systems

EDP and Networking

Regine S c h l o t h a n

Laboratory and Technical Shop (ZLW)

Dr.-Ing. Aloysius W e h r (Head of ZLW)
Technician Peter S e l i g - E d e r
Electrician Sebastian S c h n e i d e r
Mechanician Master Michael P f e i f f e r

External teaching staff

Hon. Prof. Dr.-Ing. Volker L i e b i g - Directorate ESA
Hon. Prof. Dr.-Ing. B r a u n - RST Raumfahrt Systemtechnik AG, St.Gallen

Research Projects

Design and production of inertial measurement units from MEMS components for body mounted usage

MEMS inertial sensors, which meet the requirements in terms of sensor range, are identified and chosen for the application pedestrian navigation. Several prototypes of low cost sensors for pedestrian navigation research (LOPSTRE) have been designed and produced at the Institute of Navigation in 2013 (Fig 1 and 2).

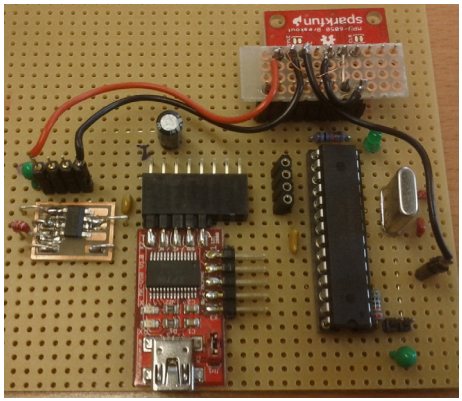

Figure 1 Prototype configuration incorporating MPU6050 on a protoboard (LOPSTRE 3).

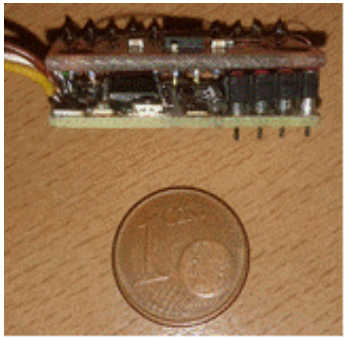

Figure 2 Prototype configuration incorporating small microcontroller printed circuit board and MPU9150 board (version 5).

The size of the prototypes could be reduced to 19 mm x 19 mm (Fig 3). IMUs of the version 5 and 6 are mounted in casings which make them useable in experiments like static calibrations and foot mounted navigation. Additionally the firmware running on the IMU could be improved in terms of stability, usability and performance.

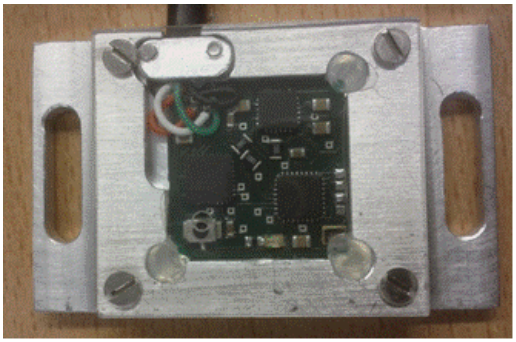

Figure 3 Prototype configuration incorporating only one printed circuit board with casing (version 6).

Microcontroller boards for students' exercises

For exercises of the MSc course „MEMS technology" new microcontroller evaluation boards were designed and assembled at the Institute of Navigation (Fig 4). They use a very common micro-controller from ATMEL and share some design features with the commonly used Arduino boards, but offer more functionalities.

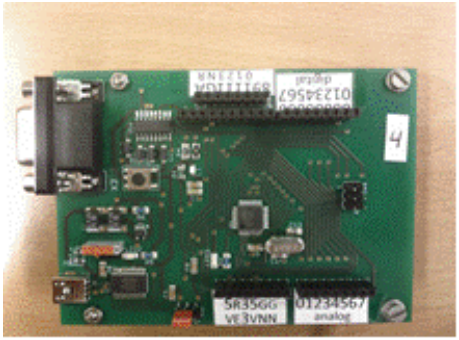

Figure 4 INS microcontroller evaluation board.

Students are learning how to programme a microcontroller, controlling simple digital and analogue outputs and communicating with a PC via an USB interface. Exercises include reading out, save, visualize and analyse simple analogue sensor readings. In a more sophisticated exercise students learn how to program the microcontroller to read out data from a digital inertial sensor like the BOSCH BMI055 using the two wire interface I2C (Fig. 5).

Figure 5 INS microcontroller evaluation board with BOSCH BMI055 and Bluetooth module

Analysis of Data sets of Nitrogen Deposition in Baden-Württemberg Contributing to a Country Specific Nitrogen Balance

On behalf and on the account of Baden-Württemberg the project „Application of modelled nitrogen deposition 2007/2009 for ecosystems in Baden-Württemberg“ is carried out. The results of the research BMU/UBA project „Assessment, Prognosis, and Review of Deposition Loads and Effects in Germany“ (BMU/UBA FE-No 3707 64 200), finalised in 2011, and of its follow-up project PINETI (Pollutant Input and EcosysTem Impact; BMU/UBA FE-No 3710 63 246), are compiled and analysed within this project.

The modelled data of previous BMU/UBA modelling and mapping projects are of interest for the federate states of Germany, because these data are supporting EU and national regulations on air pollution control and emission abatement (EU NEC directive, BImSchG, TA-Luft), which have to be implemented on the sub-national level. Moreover scientific interest is supported by these data, e.g. when setting up flux assessment studies for certain ecosystems.

Within the project national maps of deposition loads are used to derive ecosystem specific nitrogen deposition fluxes at the locations of interest (see Figure 1). The resulting data of this project are delivered as data base for further calculation of a comprehensive nitrogen balance for Baden-Württemberg. Those data will also be used for different administrative applications aiming at emission control and emission reduction.

From data of modelled high resolution maps of different deposition fluxes nitrogen loads are calculated using GIS technique. The dose, in terms of deposition loads of air pollutants causing acidification and eutrophication efffects in terrestrial ecosystems can be compared to ecosystem sensitivity given as modelled critical loads in order to provide an impact assessment for these ecosystems of interest. The trend of air pollutant input over time into the respective receptors on the regional and local scale can be identified.

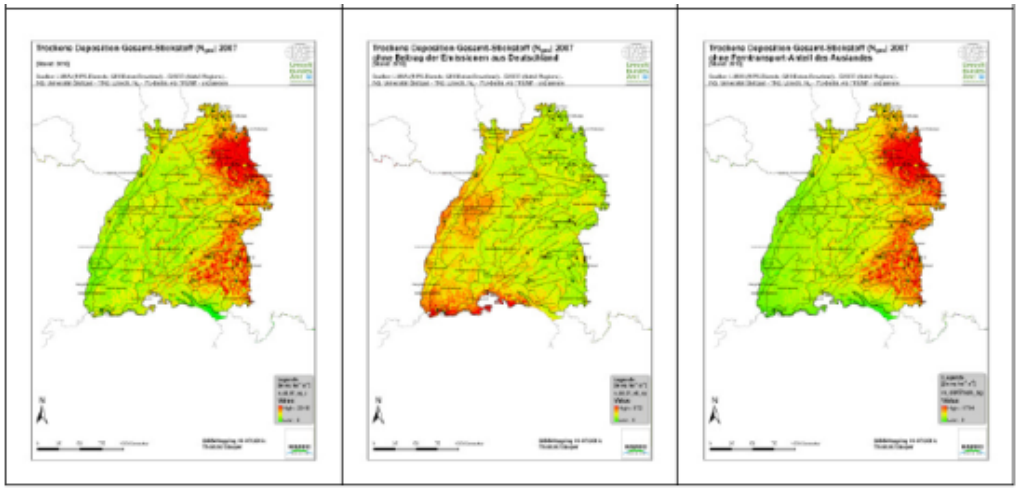

Fig. 1: Dry deposition of reactive nitrogen in Baden-Württemberg 2007 (left); without contribution of emission in Germany (center); and without contribution of emissions from abroad (right); note the different legend scale. Source: Gauger et al. 2010, re-calculated in 2013

Phenological Impact on a transferable classification concept for multitemporal TerraSAR-X-data (PI-X)

Microwaves have the possibility to penetrate into an object. A general rule is that for the same object with shorter wavelength the penetration depth decreases. The TerraSAR-X signal operated at a center frequency of 9.65 GHz has a penetration depth of some centimetres only. Therefor the canopy properties of a plant cover are most important for the backscatter. Surface influences can be neglected.

During plant growing every plant has same development steps: (seeding) → germination → growing-flowering → maturity → (harvest). Within large-scale snap-shots as satellites provide you find plants at different development steps. This is caused by climate- and weather-induced differences on a local level. On periodically observations year-by-year weather variations make image analysis for the same location more difficult. Depending on these variations the date at which a certain development step of a plant occurs varies, too.

The approach of PI-X is that the backscatter of a plant species will be the same when the plants reach the same development step. Due to mentioned climate - and weather variations the expected backscatter is time shifted. If it is possible to forecast the plant development the image analysis can be facilitated and the acquisition of satellite images can be scheduled.

Rate of development of plant depends on the temperature. Besides temperature as the most important controlling factor of the plant development, there are other factors such as water, light availability, and daylight length may modify this effects.

A method to get information about the plant stage is the measurement and accumulation of daily averaged temperature. The accumulation of heat or temperature units above a threshold or base temperature is strongly related to certain development steps. The accumulation of heat is measured as Growing Degree Days (GDD). GDD are calculated by adding the daily values for the average of the daily maximum and minimum temperatures compared to a base temperature, below which little or no growth occurs.

Stage Description	Barley		Wheat	
	GDD Required	Accumulated GDD Req	GDD Required	Accumulated GDD Req
Planting Date	0	0	0	0
Emergence Date	176	176	180	180
Leaf 1 (Fully Extended)	69	245	72	252
Leaf 2 (Fully Extended)	139	384	143	395
Leaf 3 (Tillers Begin To Emerge)	139	523	143	538
Leaf 4 (Fully Extended)	139	662	143	681
Leaf 5 (Tillering Ends)	139	801	143	824
Leaf 6 (Fully Extended)	139	940	143	967
Leaf 7 (Fully Extended)	139	1079	143	1110
Flag Leaf Emerged (Collar Visible)	139	1218	71	1181
Boot Swelling Begins (Flag leaf stem elongated) (Awns just peeking out of boot)	139	1357	72	1255
Mid-Boot (Head half emerged)	69	1426	143	1396
Head Emerged (Boot Complete) (Flowering Complete)	70	1496	143	1539
Heading Complete	139	1635	28	1567
Kernel Watery Ripe	110	1745	115	1682

Table 1: Needed GDD values at different development steps for Barley and Wheat. Source: http://ndawn.ndsu.nodak.edu/ (last access on 02/14/14).

The test sides are located north and south of Stuttgart. The direct North-South-distance (as the crow flies) is 95km between them and their altitude difference is about 650m Compared with test side data of 2011 for Winter Barley, seeded in autumn 2010, and Spring Barley, seeded in spring 2011, you see that lowest backscatter occurred in May and in June respectively of that year. During that period Winter Barley's inflorescence emerged and swelling of boots of Spring Barley began. Before and later the backscatter values are higher. It is evident from these figures that the time shifted development of barley is related to the backscatter values.

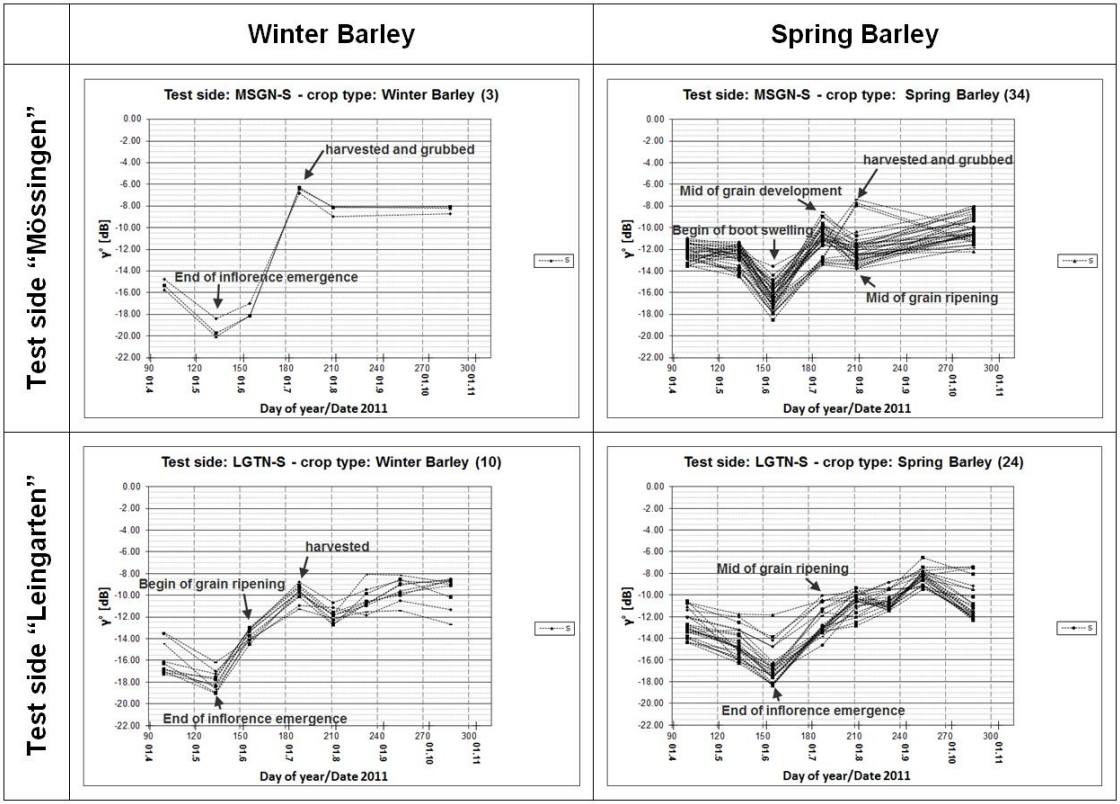

Figure 1: Backscatter values for Winter - and Spring Barley of two test sides in 2011

The next step is to investigate the relation between GDD, plant development steps, and the backscatter values with the help of data from the German Weather Service (DWD).

Geodetic excursion 04/08/13 - 04/12/13

On 8th April 2013 students of the Master course „Geodesy and Geoinformatic“ and 2 assistants started an international excursion. Stopping point were

- Illwerke, Partenen (Austria)
- Ceneri Base Tunel, Sigirino (Switzerland)
- Joint Research Centre JRC, Ispra (Italy)
- MOSE-Project, Venice (Italy)
- Geodetic Institute of the University of the German Federal Armed Forces, Munich

Since 2009 the company **Illwerke** has operated a modern pumped-storage power plant named Kopswerk II. Mining galleries for the water and the caverns for the power plant are located within the mountain, to some extend up to 200m.

Measurements problems during the construction phase were discussed and explained with a guided tour inside of of the power plant.

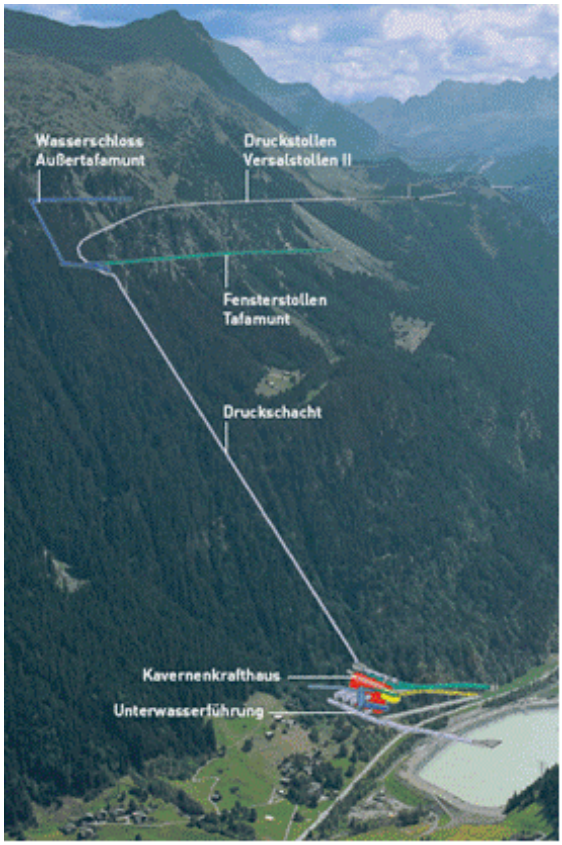

The **Ceneri Base Tunnel** is a railway tunnel with a length of 15.4 km. It is part of the AlpTransit project. Together with the Gotthard Base Tunnel the journey time will be shortened up to an hour travelling time Zurich-Milan will be reduced of 1h.

It was explained how a basic primary network of survey control points was build up and refined in front of the tunnel portals. Project and daily problems for a survey engineer were discussed. Finally it was possible to visit the inner construction site

After general information about the **Joint Research Centre** the focus of this stop was on the investigation on remote sensing data. Methods of detecting forest changes in the tropical area of South America and forest mapping in Europe were explained.

Visiting the European Crisis Management Laboratory it was shown how different information retrieved from sensor networks, satellites, and even social networks can help to make the right decisions in case of an environmental catastrophe.

The goal of the **MOSE-project** is to prevent the historical City of Venice from flooding („Acqua alta“). At the end the Venetian Lagoon will be separated from the Mediterranean Sea then. 78 mobile gates will close the 3 inlets in case of high waters. Because an inspection of the construction sites was not possible the visitor centre including a scientific lecture about the project was visited.

The **Institute of Geodesy of the University of the German Federal Armed Forces** investigates and monitors landslides in the Eastern part of the Bavarian Prealps. The fixed monitoring system and the used instruments and methods were introduced. At the end of the stop the Institute itself and its infrastructure and equipment were shown. E.g. with the help of a track vehicle the position and the track geometry of the laid tracks within the Gotthard Base Tunnel can be measured.

Publications and Presentations

Wild-Pfeiffer, F.: „MEMS-Sensoren und ihre Anwendungen in der Geodäsie und Navigation“, Geodätisches Kolloquium der HCU-Geomatik, 31.01.2013, Hamburg.

Diploma Thesis

Mayer, H.: Untersuchung der Integrierbarkeit von low-cost 3D-Sensoren für die Analyse komplexer menschlicher Bewegungen (Wild-Pfeiffer)

Zhang, J.: Untersuchung der visuell-gestützten Eigenbewegungsschätzung für Fahrerassistenzsysteme (Wild-Pfeiffer)

Master Thesis

Mehmood, Anser: Classification of arable land using multi-temporal TerraSAR-X data (Pasternak)

Mohammadi, Neda: Large-scale characterization of human settlement patterns using binary settlement masks derived from globally available TerraSAR-X data (Pasternak)

Study Thesis

Ganzhorn, Peter: „Datenerfassung und Kalibrierung einer low-cost MEMS IMU“, Bachelorarbeit, Institute of Navigation; University of Stuttgart; Nov 2013; (Schäfer).

Schmidt, Matthias: „Evaluierung verschiedener Schritterkennungsalgorithmen“, Studienarbeit, Institute of Navigation; University of Stuttgart; Feb 2013; (Schäfer).

Zhou, Ye: „Quality analysis of UAV Trajectory“; Diplomarbeit, Institute of Navigation; University of Stuttgart; July 2013; (Schäfer).

Efinger, B.: Anwendungen von MEMS-Sensoren in der Geodäsie und Navigation (Wild-Pfeiffer)

Ren, L.: Grundprinzipien bei MEMS-Aktoren (Wild-Pfeiffer)

Guest Lectures

Hafner, V.V. (Institut für Informatik, Humboldt-Universität zu Berlin): „Bio-inspirierte Navigationsstrategien in der Robotik “, 24.01.2013.

Weidner, U. (Institute of Photogrammetry and Remote Sensing, Karlsruhe Institute of Remote Sensing): „Hyperspektrale Fernerkundung“, 20.11.2013.

Activities in National and International Organization

Alfred Kleusberg:

Fellow of the International Association of the Geodesy
Member of the Institute of Navigation (U.S.)
Member of the Royal Institute of Navigation
Member of the German Institute of Navigation

Education (Lecture / Practice / Training / Seminar)

Introduction of Geodesy and Geoinformatic (BSc) (Kleusberg, Schäfer)	2/2/0/0
Electronics and Electrical Engineering (Wehr)	2/1/0/0
Satellite Measurement Engineering (Wehr)	2/1/0/0
Parameter Estimation in Dynamic Systems (Kleusberg)	2/1/0/0
Navigation I (Kleusberg, Gäb)	2/2/0/0
Inertial Navigation (Kleusberg,Schäfer)	2/2/0/0
Remote Sensing I (Wild-Pfeiffer, Pasternak)	2/2/0/0
Remote Sensing I (BSc) (Wild-Pfeiffer, Pasternak)	2/1/0/0
Remote Sensing II (Wild-Pfeiffer, Pasternak)	1/1/0/0
MEMS-Technologie (MSc) (Wild-Pfeiffer)	1/1/0/0
Satellite Programs in Remote Sensing, Communication and Navigation I (Liebig)	2/0/0/0

Satellite Programs in Remote Sensing, Communication and Navigation II (Liebig)	2/0/0/0
Radar Measurement Methods I (Braun)	2/0/0/0
Radar Measurement Methods II (Braun)	2/1/0/0
Dynamic System Estimation (Kleusberg, Suhandri)	2/1/0/0
Integrated Positioning and Navigation (Kleusberg, Suhandri)	2/1/0/0
Satellite Navigation (Kleusberg, Suhandri)	2/1/0/0
Interplanetary Trajectories (Becker)	1/1/0/0
Geodetic Seminar I, II (Fritsch, Sneeuw, Keller, Kleusberg, Möhlenbrink)	0/0/0/4
Integrated Fieldwork (Schäfer)	(SS 2012)

Institute for Photogrammetry

Geschwister-Scholl-Str. 24D, D-70174 Stuttgart
Tel.: +49 711 685 83386, Fax: +49 711 685 83297
e-mail: firstname.secondname@ifp.uni-stuttgart.de
url: http://www.ifp.uni-stuttgart.de

Head of Institute

Director: Prof. Dr.-Ing. Dieter Fritsch
Deputy: apl. Prof. Dr.-Ing. Norbert Haala
Personal Assistant: Martina Kroma

Professor Emeritus: Prof. i.R. Dr. mult. Fritz Ackermann

Research Groups at the ifp:

Geoinformatics

Chair: Prof. Dr.-Ing. Dieter Fritsch	
Deputy: Dr.-Ing. Volker Walter	Geographic Information Systems
Dr.-Ing. Susanne Becker	Point Cloud Interpretation and Hybrid GIS

Photogrammetry and Computer Vision

Chair: Prof. Dr.-Ing. Dieter Fritsch	
Deputy: Dr.-Ing. Michael Cramer	Digital Airborne Sensors
Dipl.-Ing. Alessandro Cefalu	Photogrammetric Calibration and Object Recognition
Dipl.-Ing.(FH) Markus Englich	Sensor Laboratory, Computing Facilities
M.Sc. Eng. Ali Mohammed Khosravani	Indoor Modeling and Positioning
M.Sc. Eng. Wassim Moussa	Terrestrial Laser Scanning and Sensor Fusion
M.Sc. Eng. Mohammed Othman	Image Orientation by Structure-from-Motion
Dipl.-Ing. Michael Peter	Indoor Positioning
Dipl.-Ing. Konrad Wenzel	Dense Image Matching in Close Range Applications

Photogrammetric Image Processing

Chair: apl. Prof. Dr.-Ing. Norbert Haala	
Dipl.-Ing. Mathias Rothermel	Semi-Global Matching
Dipl.-Ing. Patrick Tutzauer	Façade Reconstruction, Interpretation and Modelling

External Teaching Staff

Dipl.-Ing. Stefan Dvorak, Amt für Stadtentwicklung und Vermessung, Reutlingen

Research Projects

Geoinformatics

Automatic Map Interpretation

The internet contains huge amounts of maps representing almost every part of the Earth of different scales and map types. However, this enormous quantity of information is completely unstructured and it is very difficult to find a map of a specific area and with certain content, because the map content is not accessible by search engines in the same way as web pages. However, searching with search engines is at the moment the most effective way to retrieve information in the internet and without search engines most information would not be detected. In order to overcome this problem, methods are needed to make the implicit information of maps explicit so that it can be processed by machines. In this research we investigate how the type of maps can be interpreted automatically.

For the interpretation we use a Kohonen Feature Map which is a special type of Artificial Neural Networks. Objects, that should be interpreted with a Kohonen Feature Map, must be represented with a feature vector which describes the object characteristics. This feature vector is the input for the Kohonen Feature Map. The output is a classification of the objects into different object classes.

We tested the classification approach on 127 maps. Figure 1 shows typical examples of six different map types that should be interpreted. Figure 1 a) shows an example of a map that contains a grid that represents map sections. The sections are represented with a rectangular grid. Figure 1 b) shows an example of a map with building footprints. Figure 1 c) shows a map that represents footprints of Landsat TM images. The footprints are overlapping and are organized in a non-rectangular grid with grid cells that have a uniform size. This structure is also typical for other satellite images footprints. Figure 1 d) shows an example of a map that contains lakes. Figure 1 e) represents a map with regions. The characteristics of regions are that they are connected and not overlapping and have irregular shapes. Figure 1 f) shows a map that represents a city plan. City plans are similar to region maps with the difference that they contain more rectangular structures.

The characteristics of the different map types have to be defined with a vector consisting of 0 and 1 values. Altogether nine characteristics are used (see Table 1) which results in an input vector with the dimension 9. The selection of appropriate object characteristics is the most important

part of the definition of a Kohonen Feature Map. Typically, a good configuration can only be found by testing and optimizing different combinations of possible characteristics. In the next step, the numbers of neurons of the Kohonen Feature Map have to be defined. The number of neurons of the input layer corresponds to the number of different object characteristics. The optimum number of neurons of the output layer was estimated by testing. Based on an evaluation of different configurations, we use 30*30 neurons in the output layer.

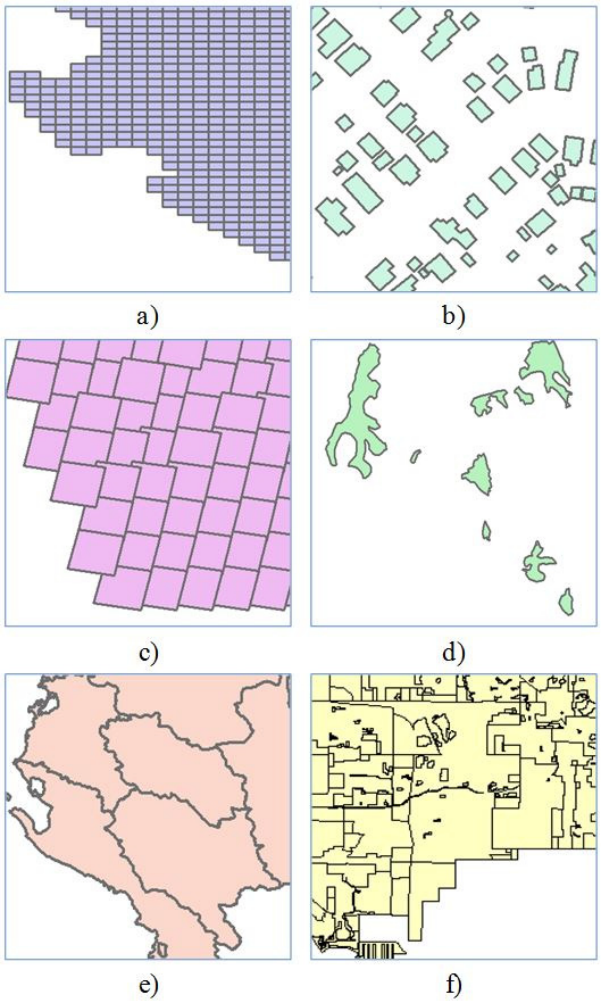

Figure 1: Different map types which can be classified with the approach.

Object characteristics	Map grids	Buildings	Satellite images	Lakes	Regions	City maps
Regular area size	1	1	1	0	0	0
Irregular area size	0	0	0	1	1	1
Area size < 10.000 m²	1	1	1	0	0	1
Area size > 10.000 m²	0	0	0	1	1	0
With perpendicularity	1	1	0	0	0	1
Without perpendicularity	0	0	1	1	0	0
Neighbored polygons	1	0	1	0	1	1
Non-neighbored polygons	0	1	0	1	0	0
Surrounding polygons	0	0	0	0	0	1

Table 1: Characteristics for different map types.

The final results of the interpretation using this trained Kohonen Feature Map are shown in Table 2. The results of the automatic interpretation of the map type are very good. The main reason for this is that the different map types have clear distinguishable characteristics. If we use more different map types, the definition of the object characteristics will be more overlapping and the number of wrong classified map types will presumably be higher. We will make more comprehensive tests to examine this situation.

	Map grids	Buildings	Satellite images	Lakes	Regions	City maps
Number of maps	7	7	6	70	29	8
Correct interpreted	7	7	6	60	24	8

Table 2: Results of the map type interpretation.

Grammar-supported Indoor Modeling

Digital representations of building interiors can support daily life in many fields. Beside the support of indoor navigation and positioning, possible applications are emergency services, crowd management, architectural planning, simulations etc. Building interiors are subject to numerous geometric and topological conditions: inner walls are often rectangular or parallel to outer walls; rooms can be adjacent but not overlapping etc. These conditions can be used to support the reconstruction of interiors. Obviously, formal grammars are powerful tools to facilitate this fact. The huge potential of formal grammars lies in the compact rule-based description of object knowledge, and the generative part which allows for efficient procedural modeling approaches.

We are striving for a fully automatic approach for grammar-supported indoor modeling based on observation data from low-cost sensors. For this purpose, we developed a formal grammar which is able to store geometric, topological and semantic information on building interiors. The grammar is flexible as it is designed in such way that it can be automatically derived from observations. This enables the grammar to be integrated in a continuous update and enhancement loop: An initial grammar derived from currently available observations is used to generate hypotheses about possible indoor geometries. As soon as new observations are available, the previously generated hypotheses can be checked against them, and the new observations can be used to automatically update the initial grammar. Continuing this loop finally results in a high-level grammar which is able to generate indoor geometries of high reliability.

Typically, the geometric structure of building interiors is organized through a horizontal partitioning of the building's body into floors, and a vertical partitioning of each floor into rooms. While the arrangement of floors is linear showing a one-dimensional topology, the topology of room configurations within a floor is two-dimensional and, therefore, much more complex. However, such arrangements are not the result of establishing walls in a floor randomly, but instead follow architectural principles and are subject to functional restrictions. In order to provide as much support as possible to indoor modeling, our grammar is designed to reflect such knowledge. The following properties of building interiors are crucial for our grammar design: (1) To ensure convenient access to the rooms, buildings are usually traversed by a system of hallways. (2) The system of hallways divides each floor into hallway-spaces and non-hallway-spaces. Non-hallway-spaces can be further divided into smaller room units which are mostly arranged in a linear sequence parallel to the adjacent hallway.

Properties 1 and 2 give reasons for pursuing two different modeling strategies: The course of the hallways, on the one hand, reminds of a network-like propagation of linear structures and thus is described using a specially designed L-system. The layout of the rooms, on the other hand, can be efficiently generated by a spatial partitioning applied to the interspaces of the hallway network. For the modeling of room layouts we develop a separate grammar which is mainly based on split operations.

To explore the power of our grammar-based concept for indoor modeling, we applied it in a real world scenario: We used erroneous and incomplete trace data originating from foot-mounted MEMS IMU positioning systems (see Figure 2a). From these traces hypotheses about indoor geometries for the complete floor using grammar support were automatically generated. The existing hallway system is augmented by hypotheses about further hallways (red polygons in Figure 2b); the hypothesized rooms, which result from applying the split grammar to the previously generated non-hallway spaces, can be seen in Figure 2c, while the ground truth is given in Figure 2d.

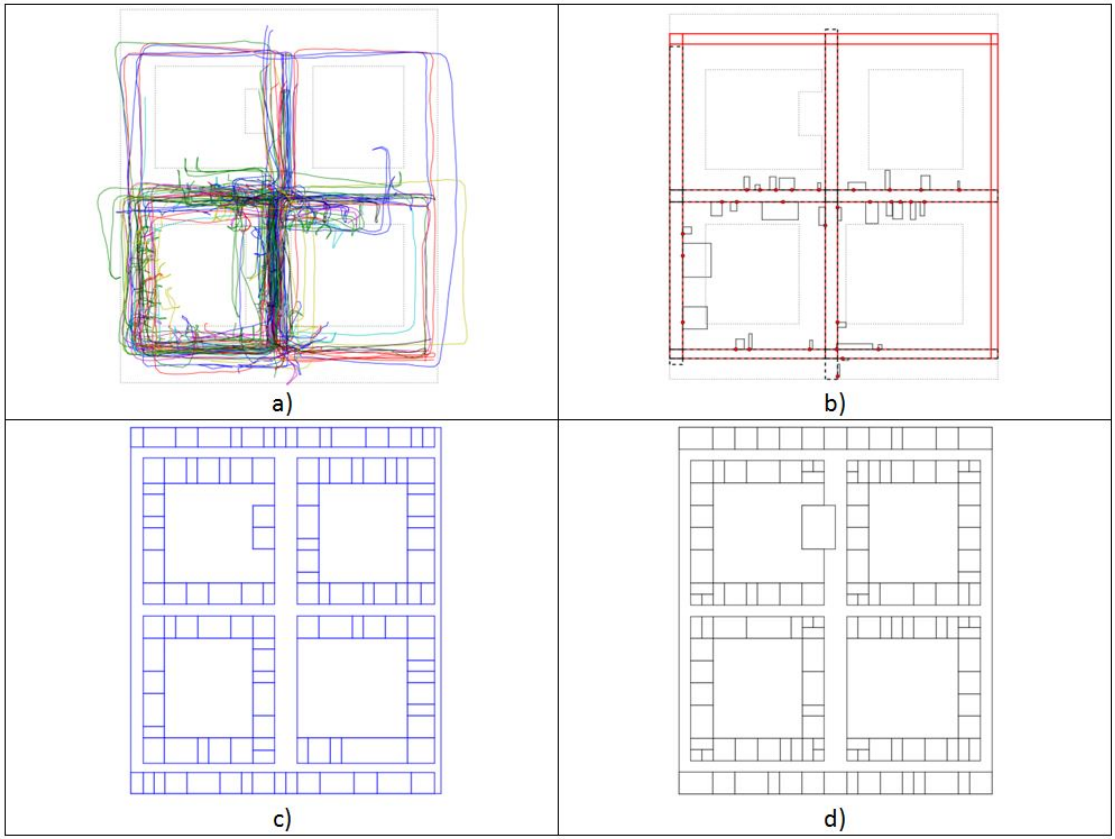

Figure 2: a) Traces acquired in the 2nd floor of a university building; b) hallways (dotted polygons) and rooms with door positions (small polygons) derived from traces, hypothesized hallways (red solid polygons); c) complete model with hypothesized rooms; d) ground truth.

Photogrammetry and Computer Vision

Indoor reconstruction using low cost sensor systems

In (Khosravani et al., 2012) we compared methods for the alignment of point clouds collected by the range camera Microsoft Kinect as an affordable and accessible sensor system. The methods are based on image space (for Structure from Motion approaches) and 3D object space observations (for sequential Iterative Closest Points algorithm). They might fail in scenarios where neither enough image features for a successful Structure from Motion approach can be found, nor the Iterative Closest Points algorithm can fix the sensor's pose 6 degrees of freedom (e.g. hallways).

Therefore, as a complementary method, we took advantage of the user's track to directly align the point clouds collected from different viewpoints (see Figure 3). The user's track is derived from an indoor positioning approach based on a foot mounted MEMS IMU with zero velocity updates. The accuracy of this method for the point cloud alignment is directly related to the accuracy of the positioning approach, which was estimated around 10cm in our study case.

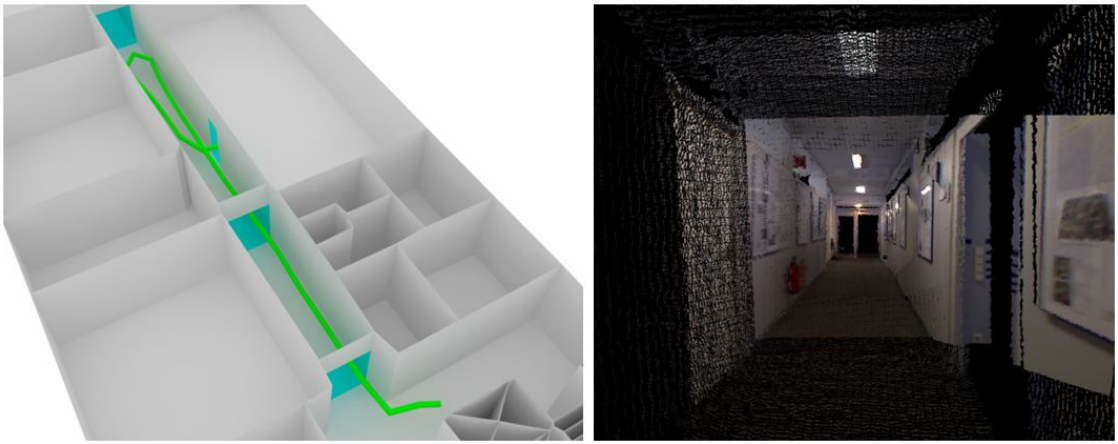

Figure 3: Alignment of a hallway point clouds captured by MS Kinect.

The aligned point clouds of building interiors enable the update and refinement of available coarse indoor models which can be automatically generated from photographed evacuation plans. The coarse model is refined by adding the door locations and details missing in the evacuation plans due to the generalization process or recent changes in the building interiors (e.g. new walls and cupboards). This is achieved by the fusion of a model with higher levels of detail to the available coarse model. For this purpose, the CAD models of individual entities (rooms and hallways) are first automatically reconstructed from the collected point clouds, and then fused with the coarse model.

For the reconstruction of the CAD models, the furniture is removed and the point cloud is levelled in the horizontal plan. In the next step, a ground plan histogram is generated and the walls are estimated using a Hough transformation. The results are then topologically corrected for a robust and consistent reconstruction.

The user's track derived from the MEMS IMU positioning approach is used for the initial registration of the detailed models to the coarse model (Figure 4a). The registration is further improved by the best fitting of individual entities to the corresponding rooms in the coarse model (Figure 4b and c).

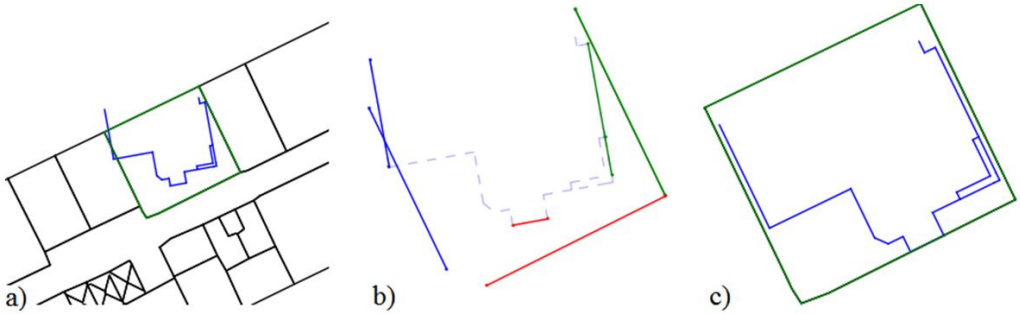

Figure 4: Initial registration to the coarse model (a); corresponding lines in the detailed and coarse models (b); best fitting of the detailed and coarse models (c).

Finally, in a follow-up fusion process, existing gaps in the detailed models (caused by occlusions in the point clouds) are automatically reconstructed using the information extracted from the coarse model (Figure 5), and the resulting models are merged with the coarse model.

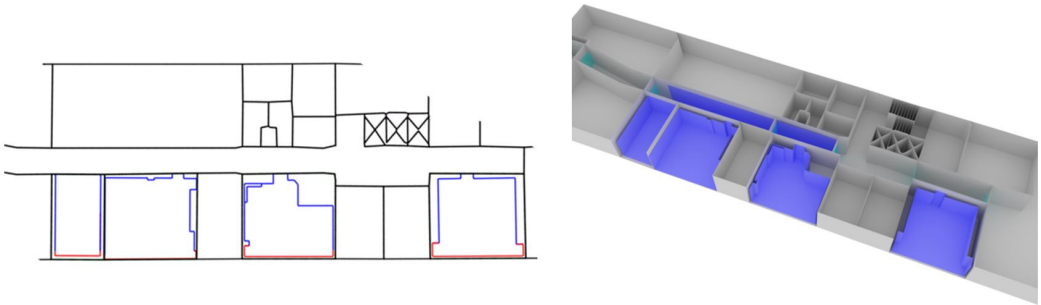

Figure 5: Refinement of a coarse model by the fusion of detailed models of some exemplary rooms and a hallway (front walls of the detailed models are removed for visibility purposes).

Automatic Registration of non-overlapping laser scans

We developed an automatic methodology capable of registering non-overlapping laser scans based on a bundle block adjustment for the orientation estimation of synthetic images generated from 3D laser data and camera images by means of a Structure-from-Motion (SfM) reconstruction method. Adding camera images to the registration of generated images from the laser data can improve the block geometry by providing sufficient overlapping geometry in between and they can match with the surrounding scans as well. This holds particularly in case of completely non-overlapping laser scans. The synthetic images are derived from reflectance or RGB values obtained from the laser scanner's embedded camera by reprojecting each single laser scanner point cloud onto a virtual image plane using the collinearity equations. To integrate the synthetic images in the SfM method, virtual cameras are assumed to be calibrated except the principle point must be shifted to the projected point of the laser scanner's center point onto the synthetic image plane.

Employing both input images in one SfM process provides accurate image orientations and sparse point clouds, initially in an arbitrary model space. Each synthetic image involved in the SfM process stores 2D-to-3D correspondences between each image pixel or feature and the 3D laser data. This allows an implicit determination of the 3D-to-3D correspondences between the sparse point clouds and the laser data. Using these 3D correspondences, a Helmert transformation is introduced and its parameters are computed. This provides absolute oriented images in relation to the laser data by introducing the scale information to the bundle. An alternative method that can increase measurement redundancy is by reprojecting the sparse point clouds onto a synthetic image using the collinearity equations. Then, the 3D-to-3D correspondences between the sparse point clouds and the laser data can be determined using the 2D-to-3D correspondences between the latter projected sparse point clouds and the laser data stored in the synthetic image. For the reason that some points will be reprojected from object surfaces that are not covered in the synthetic image, the geometric relationship of the 3D-to-3D correspondences should be evaluated to remove these wrong points. This can be done using a RANSAC filtering scheme based on seven-parameter transformation. Furthermore, an outlier removal process can be applied on the reprojection errors in object space. This results in registering the non-overlapping laser scans, since the relative orientations between the synthetic images are determined at the SfM step and transformed to the absolute coordinate system automatically (see Figure 6).

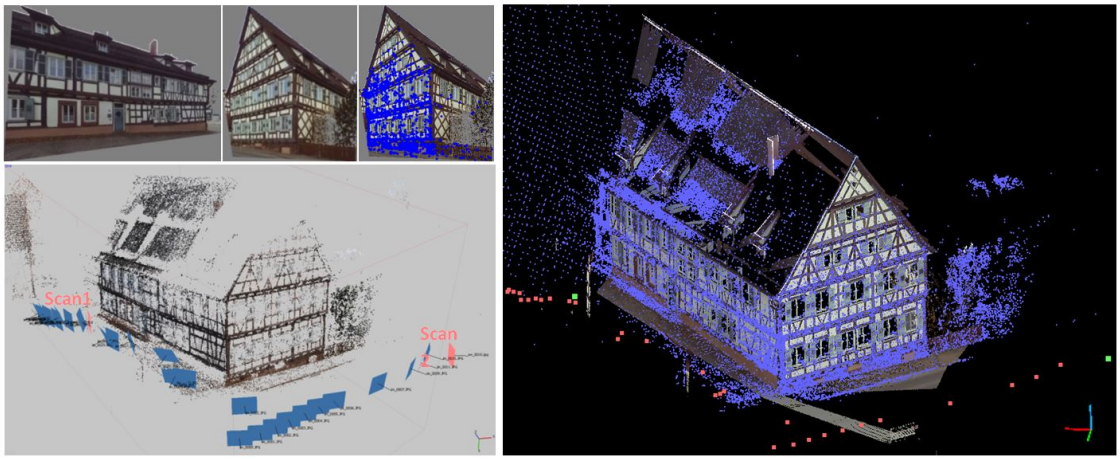

Figure 6: The Hirsau Abbey dataset. Left 1^{st} row: Generated RGB images from two non-overlapping laser scans acquired by the Faro Focus3D (at approximate point sampling distance of about 7mm at 10m distance); Scan1 left and Scan2 middle, 3D correspondences (2104 keypoints) between the sparse point clouds and the laser data (of Scan2) which are used for the calculation of the seven-parameters, depicted on the corresponding RGB image (right). Left 2^{nd} row: SfM output: sparse point clouds (colored), 30 camera positions (blue image planes) and 2 scan stations (pink image planes) aligned in one local coordinate system. Right: The latter sparse point clouds (blue), 30 camera positions (red dots) and 2 scan stations (green dots) aligned in one coordinate system with laser point clouds (colored) from both scan stations.

Multivariate Kernel Density Estimation for Filtering of Point Correspondences

Within Structure-from-Motion applications, efficiency of stereo orientation is still a noteworthy obstacle. The set of putative correspondences of an image pair is often contaminated by a large amount of outliers. This gives rise to the necessity of using very robust methods as RANSAC. Although RANSAC is capable of finding a valid solution in such situations, its' efficiency remains an exponential function of the outlier ratio. We developed a method for filtering of outlier correspondences, which can be used in advance of the RANSAC procedure. It is based on kernel density estimation and makes use of the systematic characteristics of correct correspondences and chaotic behavior of outlier respectively.

Often, the descriptor distance is used as an indicator for the correctness of a correspondence. As Figure 7 shows, this assumption loses validity when the image similarity decreases. On the other hand other characteristics as the horizontal and vertical parallaxes px and py keep their systematic effects. In addition we use the relative rotation of the descriptors, which we call rotational parallax pr.

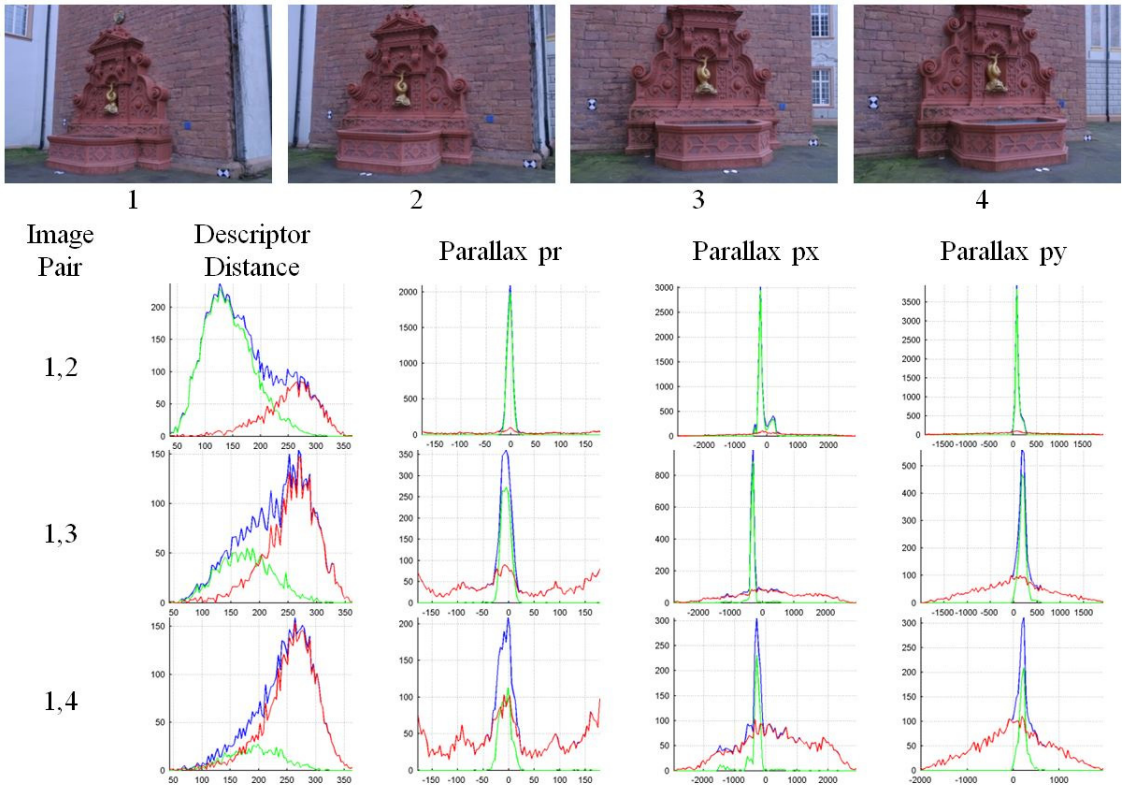

Figure 7: Top: Four images of the FountainP11 dataset. SIFT-points of the first image were matched to the other images. Below: The graphs depict the histograms of descriptor distances and the parallaxes pr, px and py. The histogram over all correspondences is colored blue. Inliers are colored green, outliers red. It gets clear, that the descriptor distance loses significance, with decreasing image similarity. In contrast, systematic effects in the parallaxes remain preserved.

In order to classify inliers and outliers we perform a 3D kernel density estimation in the space of the parallaxes, using the Gauß-kernel with a bandwidth of h = 1/175 and scaling the parallax space to unity with the matrix S. We then apply a dynamic threshold T to the estimated density by analyzing the loss of data with varying threshold. Using the ratio of the number of correspondences before filtering and after (nb and na) as well as the ratio between the threshold T and the maximal density value, we obtain a measure sim for the similarity of the images.

Figure 8: Four images of the CastleP30 dataset.

Table 3 shows some classification results for six image pairs built from four images (Figure 8). The inlier ratio could be increased significantly. The last four columns indicate the number of iterations needed for the RANSAC orientations process when the 5-Point-Algorithm (5PA) or the 7-Point-Algorithm (7PA) is used. Using the proposed pre-filtering method significantly reduces the amount out RANSAC iterations needed.

Pair	Image similarity %	Inlier before %	Inlier after %	Iterations before 5PA	Iterations after 5PA	Iterations before 7PA	Iterations after 7PA
1,2	46,80	47,98	96,70	269	4	1177	5
1,3	30,56	31,84	96,35	2109	4	20837	5
1,4	10,92	8,36	58,77	1687110	96	241138760	282
2,3	65,94	66,18	95,47	51	5	121	6
2,4	41,33	36,82	83,77	1018	13	7531	21
3,4	54,83	57,86	95,17	104	5	315	6

Table 3: Parameters of the filtering of the images in Figure 8.

Developments in Façade Reconstruction and Modelling

Previously developed algorithms at the Institute for Photogrammetry for façade reconstruction and modelling have been modified and extended. The original algorithms use a point cloud of a single façade and its corresponding building model as input. Based on the given data, a reconstruction is performed and a façade grammar derived. If there is no measurement available for the remaining façades of a building, the façade grammar can be propagated onto these.

These algorithms have been extended to handle large amounts of data. Sequential processing of data given for a complete district or city shall be possible in the future. New input data consists of 3D point clouds of complete districts or cities and a corresponding CityGML model in LoD2. The task is to reconstruct safety and navigational relevant features like doors, windows and protrusions from the point cloud to enrich the CityGML model to LoD3. Problems that have to be handled are:

- Inconsistent point distribution and density
- Misalignments of the CityGML model and point cloud
- Differences in handling of point cloud data stemming from the source of 3D data production

Latter means that the point cloud data might look differently in key regions like windows. Laser scanner data contains holes in window areas due to the loss of beam reflectance, whereas point clouds produced by dense stereo matching might represent a window pane correctly.

Furthermore, new approaches to efficiently segment (façade) point clouds generated from dense image matching and therefore offering RGB information, are investigated.

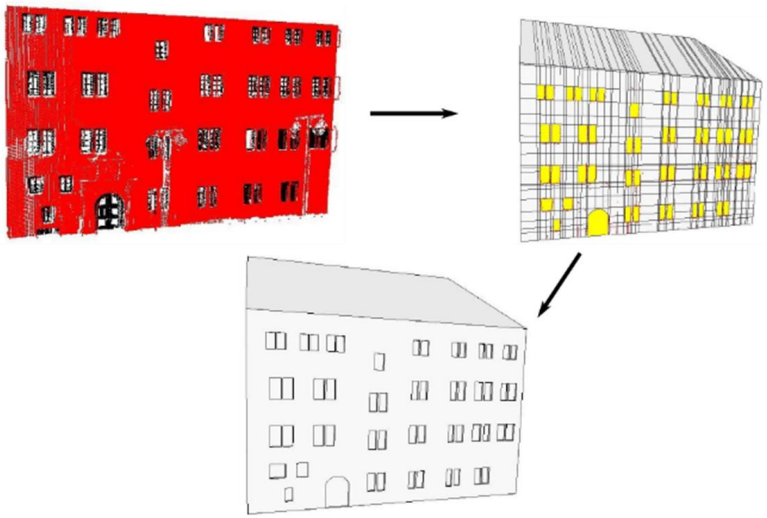

Figure 9: From a point cloud to an enriched building model.

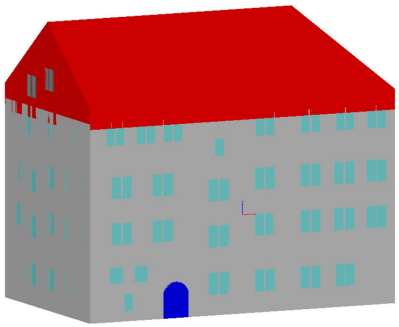

Figure 10: Corresponding CityGML LoD3 Model.

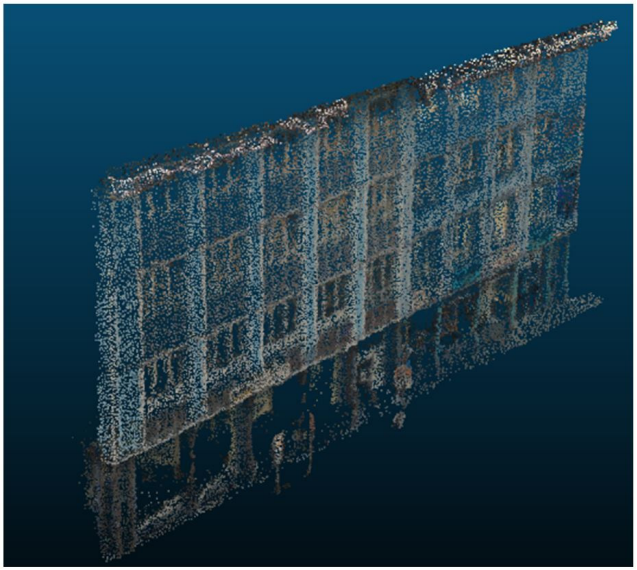

Figure 11: RGB façade point cloud.

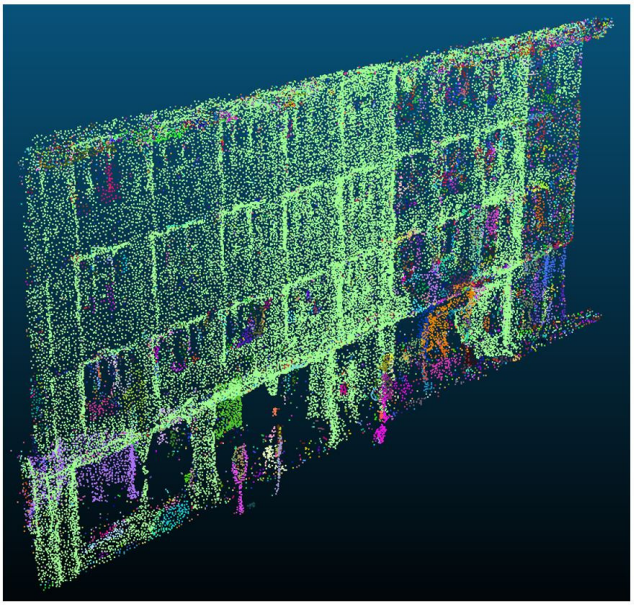

Figure 12: Segmented façade using region growing.

The European Union 4D CH Project - Four-dimensional Cultural Heritage World

The 4D-CH-World project aims to analyze, design, research, develop and validate an innovative system integrating the latest advances in computer vision and learning, as well as 3D modeling and virtual reality for the rapid and cost-effective 4D maps reconstruction in the wild for personal use, and support the aim of our European Commons and the digital libraries EUROPEANA and UNESCO Memory of the World (MoW) to build a sense of a shared European cultural history and identity.

The main goal of the 4D-CH-World is to enable historians, architects, archaeologists, urban planners, or any other affiliated scientists to reconstruct from available data on repositories, study, understand, preserve or document urban environments, as well as organizing collections of thousands of images (spatially and temporally) in generating novel views of historical scenes by interacting with the time-varying model itself. The evolving steps depiction helps understanding the cultural trends, performing behavioral analysis, exploiting the impact of the available raw resources in building development, further analyzing the urban economy factors, and simulating a future urban growth in order to understand the future demands, and satisfy in time the people's concrete needs. Education systems will have the opportunity to exploit this innovative system to motivate students and help them better understand many things in an amusing way. Finally, pupils, university students, tourists, communes, future mechanics and economists, will observe urban environment changes through time, not just read it, and therefore understand it, so as, future plans of action, regarding urban renewal or sustainable development would be less likely to fail.

The huge amount of data collected through photographs over the past decades provide a base for the three-dimensional digitalisation of existing monuments and sites using all kind of imagery available at online archives as well as in-situ data collections. These sources allow for achieving time dependent morphological 3D models to enable historians, architects, archaeologists, urban planners, or any other affiliated scientists to study, compare and share their conclusions with a broader public. Additionally, the resulting material can be used for various multi-media formats such as immersive virtual reality or augmented reality applications supporting cultural heritage service providers and educational programs.

One of the main testbeds chosen for this study is the historic Market Square in Calw, a city located 40 km southwest of Stuttgart, Germany. The on-going data collection using terrestrial laser scanning, close-range photographs and aerial imagery and its resulting 3D modeling is serving not only the interests of the researchers of the 4D-CH-World project, but also the public, as this city has thousands of visitors every year.

As an example for a photorealistic 3D reconstruction photos of the famous "Nikolausbruecke" (Santa Claus Bridge) have been downloaded „from the wild" and used in a manual reconstruction process, in cooperation between the Institute for Photogrammetry and 7reasons GmbH, Vienna.

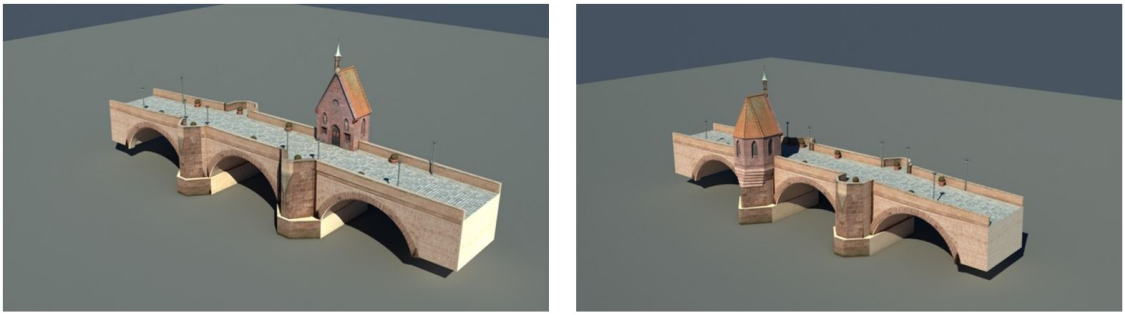

Figure 13: Photorealistic 3D reconstruction of the Nikolausbruecke in Calw, Germany.

UAS in teaching

As it was clearly proven in last year's conferences and fairs, Remotely Piloted Aircraft Systems (RPAS) - as one group of Unmanned Airborne Systems (UAS) - are going operational. This is why the four institutes responsible for the education of Geodesy & Geoinformatics Bachelor and Master Students have decided to invest into an Octocopter UAS and to integrate this as one new type of sensor platform within their lectures and labs. The first project where this Octocopter was used was to model some parts of a farm, which also was surveyed as part of the Integrated Field Work 2013. In order to prepare this project, students attending one of the elective Master modules offered by the Institute for Photogrammetry did a first evaluation test before the start of integrated field work. After successful completion of this system evaluation the Octocopter project became official part of this year's Integrated Field Work. During the two weeks outside on the Swabian Alb nearby Eningen/Achalm, RPAS data acquisition and processing was deeply shown and also investigated by students. The flights were done with the support of the colleagues from the Institute of Flight Mechanics and Control from Aerospace Engineering just to make sure, that an experienced pilot is available to control the RPAS during landing and starting phase and to take over remote control in case any problem occurs during the automatic flight phase.

Figure 14 shows the flown trajectory, where the real positions are compared to the nominal way-points from flight planning. As one can see, the Octocopter is able to almost perfectly realize the given flight path during automatic flying. During the flight images were taken with a 12Mpix Canon IXUS 100 digital camera, which have been georeferenced using structure-from-motion procedures and some ground control. The oriented images then were used to derive dense surface models as shown in Figure 15. The dense matching was done by the SURE software. As the nominal ground sampling distance (GSD) was about 1.3cm for these flights, the dense surface model was derived with a grid width of 2cm. With other words, each 2cm a 3D point was derived from the photogrammetric dense surface reconstruction. The quality of the point clouds was checked by comparing to defined planar surfaces, like street segments. The standard deviation (noise) was proven to be in the range of 1 pixel.

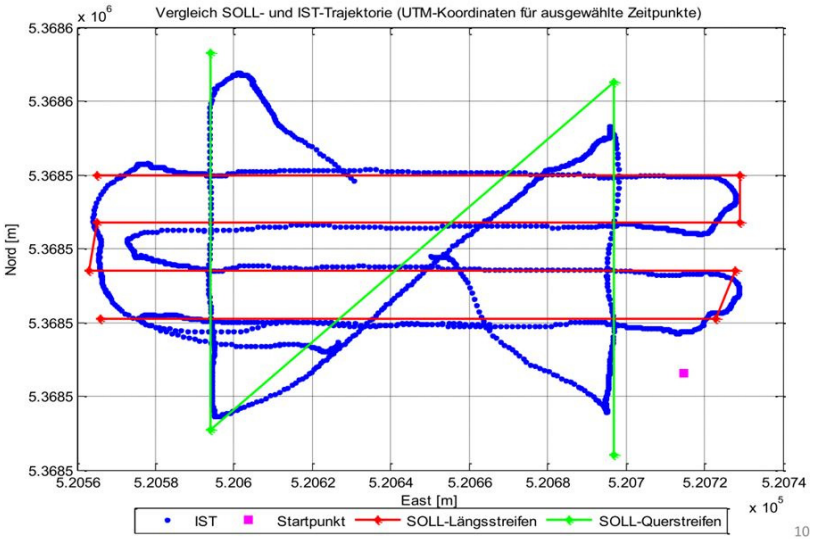

Figure 14: Octocopter trajectory as flown during one of the flights. The flown trajectory is compared to the planned trajectory between pre-defined waypoints.

Figure 15: Dense point cloud of visible surface derived from SURE software. The farm buildings are completed modeled, parts of vegetation can also be seen.

As one can clearly see from Figure 16, students were really satisfied in learning to use this most recent technology for data acquisition and 3D mapping.

Figure 16: Students during UAS data acquisition at Integrated Field Work on Swabian Alb - obviously students were quite satisfied and happy with this new type of data acquisition platform.

Disaster mapping by use of RPAS

In last summer several landslides happened at the Swabian Alb close to Mössingen/Talheim. This was due to the heavy rain periods in June 2013, where large volumes of soil at the Swabian Alb sliped down to the valley region. This mostly happened in forest regions, but in one case also parts of a built-up area were affected. This already was mentioned in the news. The characteristic of each of the slides is that they happen in a quite small region only, with an approximate size of around 1 km^2 or even less. The national mapping agency is responsible to provide 3D models of the surface, thus changes in the surface have to be continuously updated. This also is true for landslides, as they quite impressively have changed the surface as it can be seen from Figure 17.

Thus the „Landesamt für Geoinformation und Landentwicklung Baden-Württemberg“ (LGL), the national mapping agency (NMA) of Baden-Württemberg, decided to fly one of the landslides using RPAS technology. Actually this type of airborne data acquisition is one of the only options, as long only small areas of interest should be mapped in a flexible way. The decision to use RPAS was also emphasized by the good experiences that have been made in the first RPAS pilot project in year 2012 - as cooperation between LGL and the Institute for Photogrammetry. Different to the pilot project, the flights in the Talheim project were done using the commercial RPAS fixed wing system eBee by senseFly (Switzerland) as it is shown in Figure 18. As the images had to be collected during leaves off period, the flights have been done in November 2013. It were very demanding flight conditions, not only because of sun light conditions (very low sun-angle, large contrasts as most parts of the slide were in shadow area only, whereas other parts of the area were fully exposed to the sun) and quite heavy wind gusts, which affected the very lightweight

RPAS and the image data acquisition. The images were taken with about 8cm ground sampling distance. As the terrain height differences are quite big (around 200m height difference) the flying height of each flight line was adopted to the mean terrain height, just to make sure, that almost all parts of the area of interest are flown with the same flying height above ground as this will affect the GSD. Figure 19 shows the individual camera positions after the orientation of the image block. Altogether 312 images have been collected within about 35min of flight time. The block geometry, where the flying heights above ground have to be strip-wise adopted, can be noticed. A first sparse point cloud already indicates the reconstructed surface.

Figure 17: The landslide Talheim-West at Swabian Alb in summer 2013. This area was later mapped with RPAS technology.

Figure 18: Preparing the sensFly eBee RPAS for the Talheim flight mission.

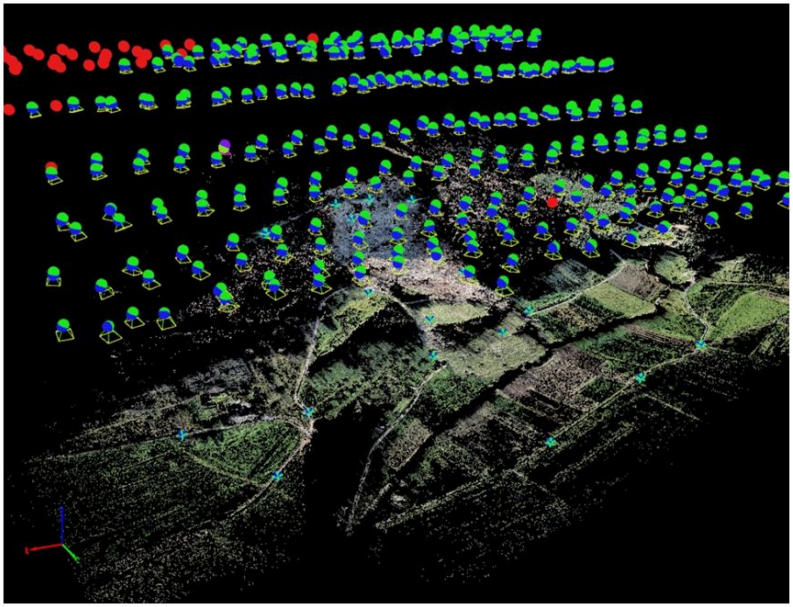

Figure 19: The photogrammetric block of Talheim GSD 8cm. The strip-wise flying heights above ground are adopted to the individual terrain heights to avoid large variations in GSD values.

In order to evaluate the performance of 3D surface reconstruction from dense matching (again the SURE software was used) height differences at 19 reference points from GNSS-measurements have been computed. Based on this the photogrammetrically derived surface model has an accuracy of 5cm (RMS) which is below 1 pixel.

The RPAS DSM later was compared to the reference terrain model from airborne laser scanning. The differences are within 10cm for the area which is surrounded by control points, but might increase to the border of the blocks. This is what should be expected from photogrammetric block configuration also. Again, this accuracy is fully sufficient to update the current 3D surface model.

Finally the DSM from dense surface matching was compared to reference 3D model from terrestrial laser scanning. One building in the test site was scanned by terrestrial scanning. This very dense point cloud is compared to the surface model from the RPAS images as seen in Figure 19. As one can see, the 3D point cloud matches well the roof planes, again the noise is around 1 GSD. The roof break lines show little large differences which is influenced due to less radiometric information in the original images. Due to the bright illumination these parts of the images were close to overexposure which negatively affects the quality of point matching.

Figure 20: Comparing of the 3D point cloud from airborne images derived from dense surface matching to a terrestrial point cloud from terrestrial laser scanning. The building walls from terrestrial scanning are clearly seen in the given profile. The airborne DSM nicely fits the roof shape of the building.

Photogrammetric Image Processing

Image based 3D surface reconstruction

Dense image matching methods enable efficient 3D data acquisition. Digital cameras are available at high resolution, high geometric and radiometric quality and high image repetition rate. They can be used to acquire imagery for photogrammetric purposes in short time. Accuracy and resolution can be chosen freely with the selection of the camera and the image stations.

Photogrammetric image processing methods can be used to derive 3D information automatically. For example, *Structure-from-Motion (SFM)* reconstruction methods can be used to derive orientations and sparse surface information. In order to retrieve complete surfaces with high density, *dense image matching methods* can be applied subsequently.

At the Institute for Photogrammetry, a software solution for dense image matching with the name SURE has been implemented. It was released online in early 2013 and is since then in constant maintenance and improvement. We have been in touch with many users around the globe, which use SURE for research purposes - such as glacier surface estimation as shown in Figure 21.

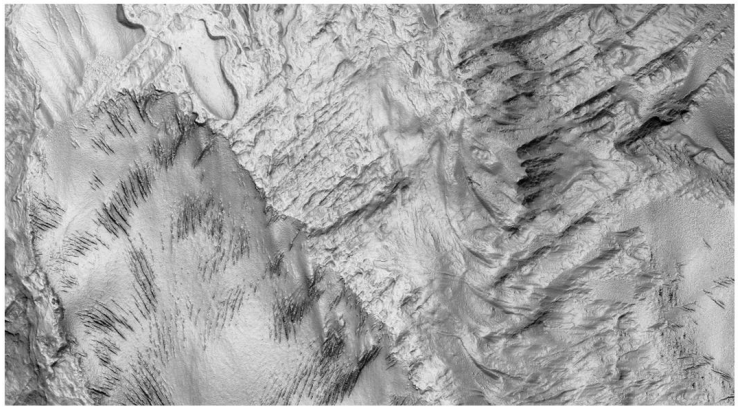

Figure 21: surface derived from 3 airborne images of a glacier using SURE (shaded mesh).

Strategies for Terrestrial Data Collection

Furthermore, we proposed a strategy for image acquisition in close range applications. The acquisition of images in such applications is often a challenge, since high overlap is required while gaps occur easily due to uncovered areas. The proposed method "One panorama each step" is a simplified approach of taking images for 3D reconstruction, in order to ensure complete coverage and sufficient data density within a straight forward acquisition process (Figure 22). Beside the acquisition process, a precision estimation as well as a strategy for the adjustment of camera settings has been presented.

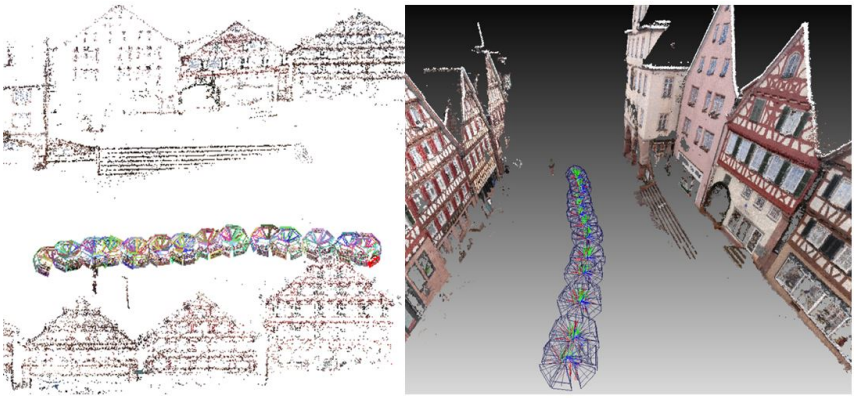

Figure 22: Simplified acquisition method for multi-view stereo "One panorama each step". Example: Calw city - left: result from Structure from Motion, right: result from dense image matching.

2.5D Surface Reconstruction from Urban UAV Image Sequences

Surface reconstruction using aerial imagery has been a vivid research area for decades. Although a large variety of large scale reconstruction algorithms were proposed in recent years SGM based techniques gained a lot of attention. Key features are density of results and the preservation of abrupt depth changes, as roof edges, particularly beneficial for reliable model generation. For moderate-sized reconstructions, UAVs equipped with imaging sensors represent an efficient alternative. Low flying altitudes and velocities allow for redundant data collection providing high detailed surface observations. In comparison to traditional aerial imagery however, signal-to-noise ratios are worse and images are frequently blurred due to minor flight stability of the small platforms. As a result image-based reconstruction techniques comprising Structure from Motion (SfM), Bundle Adjustment (BA) and dense matching get challenging. Typical issues range from increased noise levels of extracted surfaces over large number of blunders to incomplete reconstructions. Therefore, a module for exploiting redundancy contained in stereo models derived from high redundant imagery was implemented within the reconstruction framework SURE. Beside the improvement of surface precision, blunders can be reliably detected in the process „surface generation“ from high redundant imagery using the implemented multiview approch. An exempary reconstruction is shown in Figure 23.

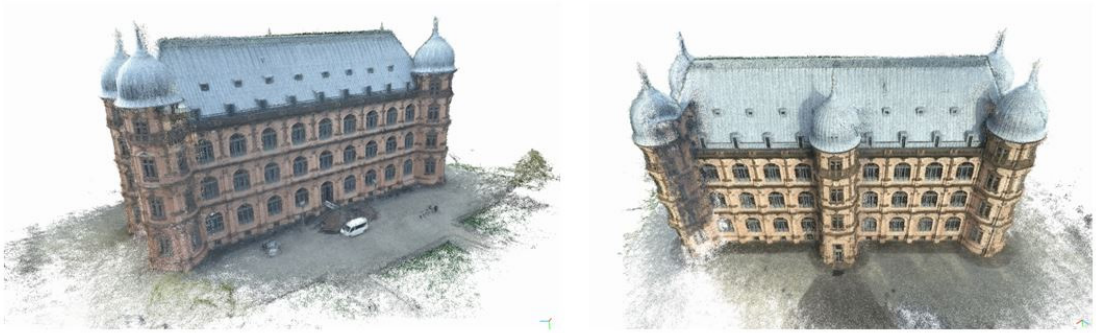

Figure 23: Reconstructed point cloud of Schloss Gottesaue. The utilized imagery was extracted from a video stream provided by Fraunhofer IOSB.

Usage of wide angle cameras enables reconstruction of surfaces containing real 3D structure as façades. However, in wide range of applications a 2.5D representation of the surface is required. Therefore points representing 3D entities must be detected and excluded from the generated point clouds. For this task algorithms based on point cloud gridding and subsequent grid analysis and filtering were investigated. Figure 24 shows benefits of the developed multi-view approach and examplary results of the 3D to 2.5D conversion.

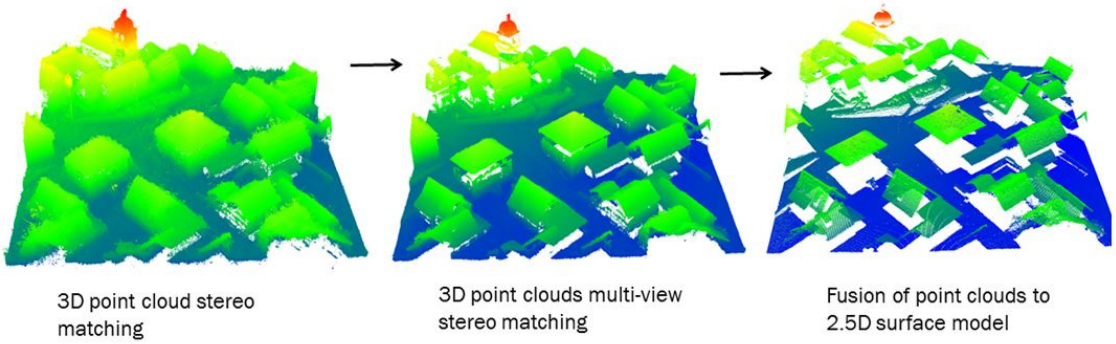

Figure 24: Visualization of precision improvement using the multi-view approch and subsequent DSM generation.

EuroSDR Project: Benchmarking of Image Matching Approaches for DSM Computation

Both, improvements in camera technology and new pixel-wise matching approaches triggered the development of new software tools for image based 3D reconstruction. Meanwhile research groups as well as commercial vendors provide photogrammetric software to generate dense, reliable and accurate 3D point clouds and Digital Surface Models (DSM) from highly overlapping aerial images. In view of the rapid progress in software technology, the European Spatial Data Research Organisation (EuroSDR) initiated a benchmark on image based generation of Digital Surface Models (DSM).

To limit the efforts required by potential participants for data processing the test was restricted to subsets of aerial image flights. Thus, two representative data sets consisting of two aerial image sub-blocks with different land cover and block geometry were prepared. The first data set, Vaihingen/Enz is representative for data usually collected during state-wide DSM generation at areas with varying land cover. The second test data set is more typical for applications in densely built-up urban areas. There images are usually collected at a higher overlap and resolution.

To enable a larger number of participants with varying background, the test was designed to be simple to implement while providing a basis for generating comparable data sets. All participants had to use the orientation parameters made available for the image blocks without modification. No 3D point clouds were taken into account, the evaluation was limited to a DSM raster in predefined size and resolution. Software systems investigated were SocetSet 5.6 (NGATE) from BAE Systems, Microsoft's UltraMap V3.1, Match-T DSM 5.5 from Trimble/inpho, ImageStation ISAE-Ext from GeoSystems, Pixel Factory from Astrium, the DSM Tool from the Royal Military Academy (RMA) of Brussels, the Remote Sensing software package from Joanneum Research, MicMac developed at IGN, SURE from the Institute for Photogrammetry (ifp), University of Stuttgart and the FPGA implementation of the SGM algorithm from the German Aerospace Center (DLR).

Figure 25: Vaihingen/Enz block, orthophoto, GSD is 20cm.

Ideally, a reference surface of superior quality should be available to evaluate the DSMs provided during the benchmark. Such quality is difficult to retrieve from independent measurements. Instead, the results from the participants were used to generate a median DSM. Of course this median cannot be regarded as independent ground truth. However, differences between the respective solutions are very well documented.

Figure 26 shows an orthoimage of a subset and a shaded relief representation of this median DSM for a part of the Vaihingen/Enz test area. A color coded representation of the root mean square differences of all DSMs with respect to this median is overlaid additionally. As it is also visible from the corresponding orthoimage in Figure 26 (right), larger differences occur in the shaded area of the quarry, in the river area, in the vicinity of patches of trees and in the area of the vineyards.

Figure 26: Ortho (left) and median DSM with RMS differences (right) for all solutions for a Vaihingen/Enz subsection.

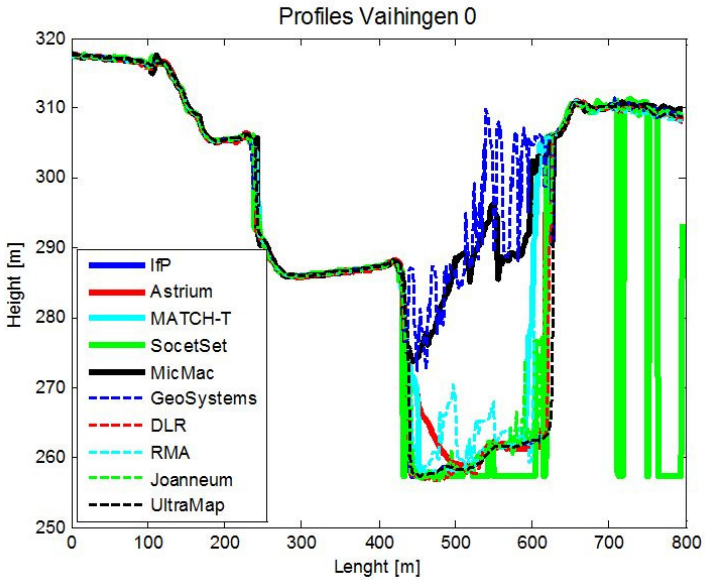

Figure 27: DSM profiles Vaihingen/Enz.

For a quantitative analysis, elevation profiles were additionally extracted for the different solutions. These lines are overlaid to the orthoimage in Figure 26 (left). The elevation profiles for line 0 are depicted in Figure 27. While all elevations are very similar for the well illuminated area of the quarry, larger differences for some solutions at the area subject to cast shadow. At object surfaces not subject to problems of image matching, differences between almost all solutions are in the order of 20cm, i.e. in this case equal to the GSD.

Results for the test area Munich are presented in Figure 28. Differences between the respective solutions are mainly visible at small details and steep edges which occur in the vicinity of building borders. Furthermore, cast shadows seem to result in larger differences and increasing noise for the reconstructed surfaces. The potential quality of the 3D data capture with the ifp software SURE is shown in Figure 29.

The EuroSDR benchmark shows that a growing number of software tools for detailed and reliable image based DSM generation is available. Processing not only benefits from improved algorithms but takes advantage from large image overlaps in order to efficiently eliminate erroneous matches. This provides a considerable reliability of DSM at vertical accuracy close to the sub-pixel level. Still, some scenarios can cause problems during image based surface reconstruction. A few solutions showed decreasing accuracies at cast shadows. Differences between the respective results also increased at fine object structures close to the resolution of the available images.

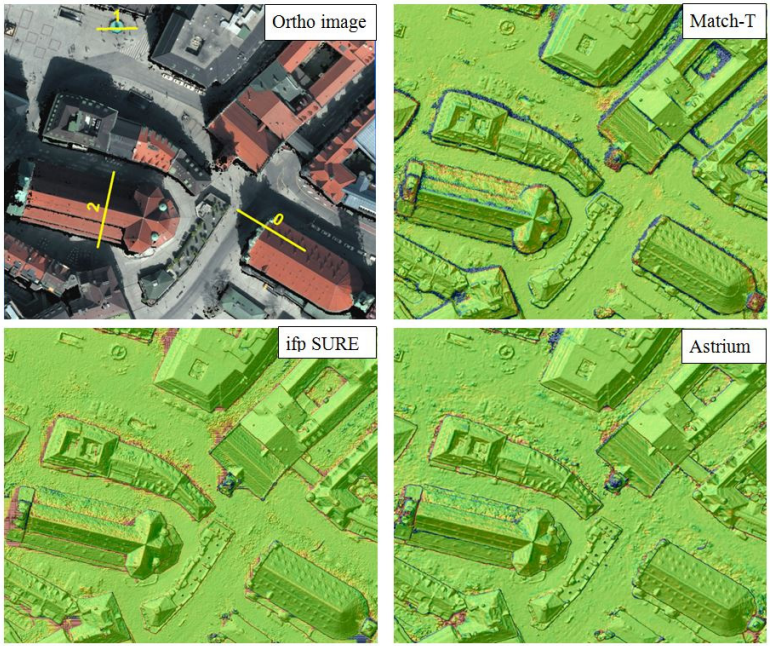

Figure 28: DSM differences to Median surface Munich.

Figure 29: 3D Visualisation München based on ifp SURE.

Current software development for image matching is subject to a considerable momentum. Thus, the major aim is not to rank the systems, but to demonstrate their capacity for area covering quality data collection. Furthermore, continuous improvements can be expected both for matching accuracy and computational performance. Thus the benchmark will be continued for future updates.

References 2013

Ahmadabadian, A.H., Robson, S., Boehm, J., Shortis, M., Wenzel, K., Fritsch, D.: A comparison of dense matching algorithms for scaled surface reconstruction using stereo camera rigs. ISPRS Journal of Photogrammetry and Remote Sensing 78, 157-167.

Becker, S., Peter, M., Fritsch, D., Phili, D., Baier, P., Dibak, C.: Combined Grammar for the Modeling of Building Interiors, ISPRS Annals of the Photogrammetry, Remote Sensing and Spatial Information Sciences, II-4/W1, 1-6.

Blanco-Vogt, A., Haala, N., Schanze, J.: Building extraction from remote sensing data for parameterizing a building typology: a contribution to flood vulnerability assessment. In: Proceedings JURSE Conference, Sao Paulo, April 21-23,147-150.

Budroni, A., Fritsch, D.: An Automatic Method to 3D Model Generation from Point Clouds. In: Terrestrisches Laserscanning - TLS. Schriftenreihe Band 72, DVW e.V. - Gesellschaft für Geodäsie, Geoinformation und Landmanagement, 15 S.

Cefalu A., Abdel-Wahab M., Peter M., Wenzel K., Fritsch, D.: Image based 3D Reconstruction in Cultural Heritage Preservation. In: Proceedings of the 10th International Conference on Informatics in Control, Automation and Robotics, 201-205.

Cramer, M.: The UAV@LGL BW Project - A NMCA Case Study. In: Fritsch, D. (Ed.): Photogrammetric Week '13, Wichmann, Berlin/Offenbach, 165-179.

Cramer, M., Bovet, S., Gültlinger, M., Honkavaara, E., McGill, A., Rijsdijk, M., Tabor, M., Tournadre, V.: On the Use of RPAS in National Mapping - EuroSDR UAV-g, 6. September, Rostock, Germany, Int. Arch. Photogramm. Remote Sens. Spatial Inf. Sci., XL-1/W2, 93-99.

Cramer, M., Haala, N., Rothermel, M., Leinss, B., Fritsch, D.: UAV@LGL - Pilotstudie zum Einsatz von UAV im Rahmen der Landesvermessung in Deutschland. Photogrammetrie - Fernerkundung - Geoinformation (PFG), Heft 5, 495-509.

Cramer, M., Haala, N., Rothermel, M., Leinss, B., Fritsch, D.: UAV-gestützte Datenerfassung für Anwendungen der Landesvermessung - das Hessigheim-Projekt. Tagungsband Vorträge 33. Wissenschaftlich-technische Jahrestagung DGPF, Publikationen der Deutschen Gesellschaft für Photogrammetrie, Fernerkundung und Geoinformation (DGPF) e.V., Band 22, 450-469.

Cramer, M., Schwieger, V., Fritsch, D., Keller, W., Kleusberg, A., Sneeuw, N.: GEOENGINE - The University of Stuttgart International Master's Program with more than 6 Years of Experience. In: Proceedings of FIG Working Week, Abuja, Nigeria, 6-10 May, 19 p.

Doulamis, A., Ioannides, M., Doulamis, N, Hadjiprocopis, A., Fritsch, D., Balet, O., Julien, M., Protopapadakis, E., Makantasis, K., Weinlinger, G., Johnsons, P.S., Klein, M., Fellner, Stork, A., Santos, P.: 4D Reconstruction of the Past. Pres. Paper 1st International Conference on Remote Sensing and Geoinformation of Environment, Paphos, Cyprus, 4p.

Fritsch, D.: The Future of EduServ. White Paper EuroSDR, EuroSDR Web access: www.eurosdr.net, 10p.

Fritsch, D. (Ed.): Photogrammetric Week ’13. Wichmann, Berlin/Offenbach, 352p.

Fritsch, D., Madden, M., Trinder. J.: Annual Report 2012, The ISPRS Foundation, www.isprs.org/foundation, 28p.

Fritsch, D.: Management of EuroSDR Workshops and Projects. White Paper EuroSDR, www.eurosdr.net, 11p.

Fritsch, D., Cramer, M.: The Relevance of RPAS for National Maping and Cadastre Agencies in Europe. In: RPAS Remotely Piloted Aircraft Systems - The Global Perspective 2014, Blyneburgh & Co., Paris, 115-118.

Fritsch, D., Grimm, A., Kremer, J., Rothermel, M., Wenzel, K.: Bilddatenerfassung mit einem Gyrocopter - Erste Erfahrungen zur „Photogrammetrie nach Bedarf“. Tagungsband Vorträge 33. Wissenschaftlich-technische Jahrestagung DGPF, Publikationen der Deutschen Gesellschaft für Photogrammetrie, Fernerkundung und Geoinformation (DGPF) e.V., Band 22, 470-480.

Fritsch, D., Pfeifer, N., Franzen, M. (Eds.): 2nd High Density Image Matching for DSM Computation Workshop. EuroSDR Workshop Proceedings, EuroSDR Publication No. 63, ISSN 0257-0505, ISBN 9789051798032 (CD-ROM).

Fritsch, D., Rothermel, M.: Oblique Image Data Processing - Potential, Experiences and Recommendations. In: Fritsch, D. (Ed.): Photogrammetric Week ’13, Wichmann, Berlin/Offenbach, 73-88.

Fritsch, D., Becker, S., Rothermel, M.: Modeling Facade Structures Using Point Clouds from Dense Image Matching. Proceedings Intl. Conf. Advances in Civil, Structural and Mechanical Engineering, Inst. Research Eng. and Doctors. August 3-4, Hongkong, 57-64.

Fritsch, D., Rothermel, M., Wenzel, K., Walter, V., Becker, S., Cramer, M., Haala, N.: All About 3D Modelling - From 2.5D Meshes to 3D Virtual Reality Models. Lecture Notes, Tutorial PhoWo. Institute for Photogrammetry, Univ. Stuttgart, 600p.

Haala, N.: The Landscape of Dense Image Matching Algorithms. In: Fritsch, D. (Ed.): Photogrammetric Week ’13, Wichmann, Berlin/Offenbach, 271-284.

Haala, N., Cramer, M., Rothermel, M.: Quality of 3D Point clouds from highly overlapping UAV Imagery. Int. Arch. Photogramm. Remote Sens. Spatial Inf. Sci., XL-1/W2, 183-188.

Haala, N., Rothermel, M., Pfeifer, N.: Benchmarking Image-based DSM generation. GIM International. Volume 27, Issue 12, 27-29.

Ioannides, M., Hadjiprocopi, A., Doulamis, N., Doulamis, A., Protopapadakis, E., Makantasis, K., Santos, P., Fellner, D., Stork, A., Balet, O., Julien, M., Weinlinger, G., Johnsons, P.S., Klein,

M., Fritsch, D.: 4D Reconstruction Using Multi-Images Under Open Access. XXIV. CIPA Symposium, ISPRS Ann. Photogramm. Remote Sens. Spatial Inf. Sci., II-5/W1, 169-174.

Ivan, I., Longley, P., Horák, J., Fritsch, D., Cheshire, J., Inspektor, T. (Eds.): Geoinformatics for City Transformations. Proceedings 10. International Symposium Ostrava, Czech Republic, January, Technical University of Ostrava, 298 p.

Khosravani, A.M., Peter, M., Fritsch, D: Alignment of Range Image Data Based on MEMS IMU and 3D Coarse Models derived from Evacuation Plans. In SPIE Videometrics, Range Imaging, and Applications XII. Vol. 8791A, 1-6.

Moussa, W., Wenzel, K., Rothermel, M., Abdel-Wahab, M., Fritsch, D.: Complementing TLS Point Clouds by Dense Image Matching. Int. Journal of Heritage in the Digital Era, Vol. 2, No. 3, 453-470.

Peter, M., Becker, S., Fritsch, D.: Grammar Supported Indoor Mapping. In: Proceedings of the 26th International Cartographic Conference, 1-18.

Peter, M., Khosravani, A.M., Fritsch, D.: Refinement of Coarse Indoor Models Using Position Traces and a Low-Cost Range Camera. In: Proceedings of the 4th International Conference on Indoor Positioning and Indoor Navigation, 787-795.

Tang, R., Fritsch, D.: Correlation Analysis of Camera Self-Calibration in Close Range Photogrammetry. The Photogrammetric Record, Special Issue: DIAMOND JUBILEE ISSUE, Volume 28, Issue 141, 86-95.

Walter, V., Fritsch, D.: Results of the EuroSDR Survey: 3D Data Management in European National Mapping and Cadastral Agencies. INSPIRE Conference, Florence, Italy, Published online: http://inspire.jrc.ec.europa.eu/events/conferences/inspire_/schedule/submissions/20.html

Walter, V., Luo, F., Fritsch, D.: Automatic Map Retrieval and Map Interpretation in the Internet. In: Timpf, S., Laube, P.: Advances in Spatial Data Handling - Geospatial Dynamics, Geosimulation and Exploratory Visualisation, Springer, New York, 209-221.

Wenzel, K., Rothermel, M., Fritsch, D., Haala, N.: Image Acquisition and Model Selection for Multi-View Stereo, Int. Arch. Photogramm. Remote Sens. Spatial Inf. Sci., XL-5/W1, 251-258.

Wenzel, K., Rothermel, M., Haala, N., Fritsch, D.: SURE - The ifp Software for Dense Image Matching. In: Fritsch, D. (Ed.): Photogrammetric Week ’13, Wichmann, Berlin/Offenbach, 59-70.

Doctoral Theses

Budroni, A.: Automatic Model Reconstruction of Indoor Manhattan-World Scenes from Dense Laser Range Data. Deutsche Geodätische Kommission, Reihe C, Nr. 715, München, ISBN 978-3-7696-5127-0, 104 S.

Tang, R.: Mathematical Methods for Camera Self-Calibration in Photogrammetry and Computer Vision. Deutsche Geodätische Kommission, Reihe C, Nr. 703, München, ISBN 978-3-7696-5115-7, 111 S.

Diploma Theses / Master's Theses

Lingenfelder, M.: Qualifizierung des ShapeDrive 3D-Sensors integriert in die EVT-Bildverarbeitungs-Software für Prüfaufgaben in der automobilen Fertigung und Montage. Supervisors: Bürkle, H. (Daimler AG), Haala, N.

Morosan, R.: Digital Preservation of the Aurelius Church and the Hirsau Museum Complex by Means of HDS and Photogrammetric Texture Mapping. Supervisor: Fritsch, D.

Küver, M.: Descriptor-based Edge Feature Matching. Supervisors: Ohr, F. (Robert Bosch GmbH), Haala, N.

Liu, Z.: Conflation of National Mapping and Crowd-Sourced Data - a comparison of two different approaches. Supervisor: Walter, V.

Olaniyi, O.: Client/Server - based Indoor Positioning with WLAN. Supervisors: Walter, V., Peter, M.

Shi, R.: Development of a Mobile Campus Information System. Supervisor: Walter, V.

Li, J.: Digital Preservation of the Neighborhood of St. Peter & Paul by Means of Automated HDS and Photogrammetric Texture Mapping. Supervisor: Fritsch, D.

Dong, D.: Indoors and Outdoors Data Collection and Refinement - The Kentheim Project. Supervisor: Fritsch, D.

Bustamante T.A.: Digital Preservation of the Calw Market by Means of Automated HDS and Photogrammetric Texture Mapping. Supervisor: Fritsch, D.

Fu, H.: Dense Matching GPU Implementation. Supervisor: Rothermel, M., Haala, N.

Cheng, P.: Entwicklung eines Routenalgorithmus für Elektrofahrzeuge zur Energieversorgung unter Berücksichtigung von digitalen Geländemodellen. Supervisors: Walter, V., Warto, S. (Bertrandt Ingenieurbüro GmbH).

Cui, Y.: Radargrammetry by Semi-Global Matching with TerraSAR-X data over Trento, Italy. Supervisors: Balz, T. (Wuhan University), Haala, N.

Zwoelfer, T.: Face Recognition for a Mobile Service Robot. Supervisors: Haala, N., Bormann, R. (Fraunhofer IPA).

Tutzauer, P.: Grid-Based Road Surface Estimation for Active Suspension Systems. Supervisors: Haala, N., Wehking, T. (Robert Bosch GmbH).

Fang, Y.: Aufbau einer Innenraum-Ortung für ein bedarfsorientiertes Beleuchtungssystem (Developing an indoor-positioning system for a demand oriented lighting system). Supervisors:

Haala, N., Boer, J. (Fraunhofer Institut für Bauphysik), Aktuna, B. (Fraunhofer Institut für Bauphysik).

Cobalas, C.: Vergleich von Geodaten auf lokalen und internationalen Web-Portalen. Supervisors: Cramer, M., Gruber, M. (Microsoft/Vexcel Imaging GmbH).

Gao, Y: Optimisation of Service following in Automotive Radio by Applying a Reception Landscape Memory. Supervisors: Fritsch, D., Schmidt, A., Eireiner, T. (Daimler Research Ulm).

Study Theses / Bachelor Theses

Wenk, M.: Automatisierte Kamerakalibrierung. Supervisor: Wenzel, K.

Gaube, M.: Color Head-to-Head Image Registration using Correlation and Mutual Information. Supervisors: Haala, N., Hefele, J. (Hexagon Geosystems)

Fang, M.: Entwicklung eines Campus-Informationssystems mittels GIS Cloud. Supervisor: Walter, V.

Weimer, A.: Korrektur der chromatischen Aberration mittels radialsymmetrischer Verzeichnungsterme. Supervisor: Cefalu, A.

Lingenfelder, M.: Design and Evaluation of a Point Cloud Recording Device using Dense Image Matching and Registration in Object Space. Supervisor: Wenzel, K.

Xie, D.: Genauigkeitsanalyse dichter 3D Punktwolken aus UAV-Befliegungen. Supervisor: Rothermel. M.

Guo, Y.: 3D-Rekonstruktion des Klosters Hirsau mittels Terrestrischen Laserscanning und Nahbereichsphotogrammetrie. Supervisor: Fritsch, D.

Activities in National and International Organizations

Cramer, M.:
Co-Chair ISPRS ICWG III/I: Sensor Modeling for Integrated Orientation and Navigation

Englich, M.:
Webmaster ISPRS

Fritsch, D.:
Chairman Board of Trustees ‘The ISPRS Foundation’
Member CyberOne Award Commitee
Member Galileo/GMES Award Committee Baden-Württemberg
Member Jury Artur Fischer Invention Award
Member D21 Advisory Board
Member Board of Trustees German University in Cairo (GUC)
Member GUC Academic Advisory Committee

Memner GUC Academic Promotion Commitee
Member Apple's University Education Forum (UEF)
Vice-President Research EuroSDR

Haala, N.:
Chair ISPRS WG I/2 - LiDAR, SAR and Optical Sensors
Vorsitz DGPF Arbeitskreis Sensorik und Plattformen

Walter, V.:
Member of Editorial Advisory Board of the ISPRS Journal of Photogrammetry and Remote Sensing
Nationaler Berichterstatter für die ISPRS Kommission IV

Awards

Haala, N.: Carl Pulfrich Award 2013

Education - Lectures/Exercises/Training/Seminars

Bachelor „Geodäsie und Geoinformatik"

Adjustment Theory I (Fritsch, Sneeuw)	1/1/0/0
Adjustment Theory II (Fritsch, Sneeuw)	2/2/0/0
Geoinformatics I (Fritsch, Walter)	2/2/0/0
Geoinformatics II (Walter)	1/1/0/0
Image Processing (Haala)	2/1/0/0
Integrated Fieldworks (Fritsch, Sneeuw, Keller, Kleusberg)	0/0/4/0
Introduction into Geodesy and Geoinformatics (Cramer, Fritsch, Sneeuw, Keller, Kleusberg)	4/2/0/0
Photogrammetry (Cramer)	2/1/0/0
Signal Processing (Fritsch)	2/1/0/0
Urban Planning (Dvorak)	2/0/0/0

Master Course „Geodäsie und Geoinformatik"

Aerotriangulation (Cramer)	1/1/0/0
Close Range Photogrammetry and Machine Vision (Fritsch)	1/1/0/0
Computational Geometry (Walter)	1/1/0/0
Computer Vision for Image-based Acquisition of Geodata (Haala)	1/1/0/0
Databases and Geographical Information Systems (Walter)	1/1/0/0
Digital Terrain Models (Haala)	1/1/0/0
Fundamentals in Urban Planning (Dvorak)	2/0/0/0

Georeferencing of photogrammetrical Systems (Cramer)	1/1/0/0
Modelling and Visualisation (Haala)	1/1/0/0
Pattern Recognition and Image Understanding (Haala)	1/1/0/0
Scientific Presentation Seminar (Haala)	0/0/0/2
Terrestrial Laserscanning (Fritsch)	1/1/0/0
Topology and Optimisation (Becker)	1/1/0/0
Web-based GIS (Walter)	1/1/0/0

Master Course GEOENGINE

Airborne Data Acquisition (Fritsch, Cramer)	2/1/0/0
Geoinformatics (Fritsch, Walter)	2/1/0/0
Signal Processing (Fritsch)	2/1/0/0
Topology and Optimisation (Fritsch)	2/1/0/0
Integrated Fieldworks (Fritsch, Sneeuw, Keller, Kleusberg)	0/0/4/0

Master Courses „Infrastructure Planning“

Introduction to GIS (Walter)	2/0/0/0

Diplomstudiengang Luft- und Raumfahrttechnik

Image Processing (Haala)	2/1/0/0
Introduction into projective Geometry (Cramer)	2/0/0/0